Controlling Scaling in Groundwater Reverse Osmosis

Minimizing Antiscalant Consumption

Muhammad Nasir Mangal

CONTROLLING SCALING IN GROUNDWATER REVERSE OSMOSIS

MINIMIZING ANTISCALANT CONSUMPTION

Muhammad Nasir Mangal

CONTROLLING SCALING IN GROUNDWATER REVERSE OSMOSIS

MINIMIZING ANTISCALANT CONSUMPTION

DISSERTATION

to obtain
the degree of doctor at the University of Twente,
on the authority of the rector magnificus,
prof. dr. ir. A. Veldkamp,
on account of the decision of the Doctorate Board
to be publicly defended
on Wednesday 19 April 2023 at 14.45 hours

by

Muhammad Nasir Mangal

born on the 1st of August, 1989
in Paktia, Afghanistan

This dissertation has been approved by:

Supervisors

Prof. dr. ir. W.G.J. van der Meer

Prof. dr. M.D. Kennedy

Co-supervisors

Dr. ir. S.G. Salinas Rodríguez

Dr. ir. A.J.B. Kemperman

This research was conducted under the auspices of the Graduate School for Socio-Economic and Natural Sciences of the Environment (SENSE).

Cover page photo credit: Oasen Drinkwater
Printed by: Veenman, the Netherlands
ISBN (print): 978-90-365-5588-3
ISBN (digital): 978-90-365-5589-0
URL: https://doi.org/10.3990/1.9789036555890

Graduation Committee:

Chair / secretary:	Prof. dr. J.L. Herek (University of Twente)
Supervisors:	Prof. dr. ir. W.G.J. van der Meer (University of Twente)
	Prof. dr. M.D. Kennedy (Delft University of Technology/IHE Delft)
Co-supervisors:	Dr. ir. S.G. Salinas Rodríguez (IHE Delft)
	Dr. ir. A.J.B. Kemperman (University of Twente)
Committee Members:	Prof. dr. ir. N.E. Benes (University of Twente)
	Prof. dr. ir. E. Zondervan (University of Twente)
	Prof. dr. ir. E.R. Cornelissen (Ghent University)
	Prof. dr. P.A Davies (University of Birmingham)

ACKNOWLEDGMENTS

I would like to thank everyone who helped and encouraged me along the way of completing my PhD thesis.

I would like express my sincere gratitude to my promotors Prof. Maria D. Kennedy and Prof. Walter G.J. van der Meer, and to my supervisors Dr. Sergio G. Salinas Rodríguez and Dr. Antoine J.B. Kemperman for their continuous support, supervision, and encouragement throughout the research study. Special thanks to Prof. Em. Jan C. Schippers for his valuable input, suggestions and critical discussions during my progress meetings. I would also like to thank Dr. Bastiaan Blankert, ir. Jos Dusseldorp, and Dr. Victor A. Yangali Quintanilla for their contribution and valuable suggestions in finalizing my publications.

Many thanks to Oasen Drinking Water Company and for financing my PhD research, and for facilitating experimental setups for my research at the drinking water treatment plant. Deepest thanks to the IHE Delft laboratory staff (Fred Kruis, Frank Wiegman, Peter Heerings, Ferdi Battes, Berend Lolkema and Lyzette Robbemont) for their endless assistance during my laboratory experiments. Thank you, Berend and Peter, for your assistance with the assembly of the laboratory-scale reverse osmosis unit. Thanks to the IHE staff members (Bianca Wassenaar, Selvi Pransiska, Jolanda Boots, Floor Felix, Anique Karsten and others) for the administrative support. Many thanks to the MSc students (Madhuvi Kisoen and Chima Eke) for working with me in the laboratory. I want to thank Anniek van Veldhuizen for translating the thesis summary into Dutch.

I would like to thank all my Palestinians friends (Alaa Ouda, Karam Abu Shammala, Mohanad Abunada, Mohaned Sousi, Motasem Abushaban, and Yousef Albuhaisi) for all the good moments, pleasant memories, and (Ramadan) gatherings we've shared together. Thanks to my closest friend back home (Safiullah Nazari) for motivating me from distance. Many thanks to all of my friends and colleagues for the memorable times we had together at IHE Delft: Ahmed Mahmoud, Ahmed Elghandour, Aqeel Kakar, Eva Kocbek, Hesham Elmilady, Mary Barrios Hernandez, Nasir Majidi, Nazanin Moradi, Nirajan Dhakal, Prathna Chandrasekaran, and Taha Al-Washali.

Lastly and most importantly, I am grateful to my parents, my sister and brothers for their prayers and endless support in every aspect of my life. To my wife, thank you for your motivation, prayers, and continuous support.

SUMMARY

In reverse osmosis (RO) processes, it is essential to have the recovery (ratio of the permeate water to the feed water) of the system as high as possible in order to lower the total electrical consumption per unit volume of permeate, increase water production, decrease the volume of concentrate, and lower the use of pretreatment chemicals and their related costs. When treating seawater, the osmotic pressure limits the recovery of the RO system. However, in brackish water reverse osmosis (BWRO) processes, scaling is the main barrier to operating RO installations at high recoveries. Scaling is the precipitation of poorly soluble species (e.g., calcium carbonate, calcium sulphate, barium sulphate, calcium phosphate, etc.), which become oversaturated as the retained salts are concentrated in the RO system. Scaling results in decreased system performance, increased operating pressure, increased energy consumption, frequent chemical cleaning, increased salt passage, and undesirable system downtime.

To achieve high recoveries, many RO plants dose antiscalants to the feed water which prevents the precipitation of sparingly soluble salts on the membrane surface. It is well established that the scaling of calcium carbonate, calcium sulphate, barium sulphate can be effectively prevented with the use of antiscalants. However, according to literature, it is not clear if antiscalants can prevent calcium phosphate scaling in RO applications. A dominant question in the application of antiscalants is: “How to determine the optimum dose required for the prevention of scaling in RO systems”? In practice, the selection of antiscalant and the required dose of that antiscalant for a specific water composition is typically determined by the antiscalant manufacturers using one of their proprietary software programs. However, the method that is used by the manufacturers to calculate the antiscalant dose is unknown, and as a result, the end-users are unable to verify the doses that are recommended to them.

The main objectives of this study are: i) to develop an approach for determining the real-time optimal antiscalant dose required to achieve a target recovery in RO processes, and ii) to evaluate the performance of antiscalants in controlling calcium phosphate scaling in RO processes. This thesis is structured in six chapters, with chapter 1 providing a general introduction and chapter 6 summarizing the major conclusions of this study.

Chapters 2 and 3 deal with the optimization of antiscalant dose and reduction of antiscalant consumption in RO plants. In chapter 2, the potential of a dosing algorithm for optimizing antiscalant dose in RO processes was investigated. The algorithm defines a real-time optimal set-point of antiscalant dosing to the dosing pump by continuously and automatically adjusting the antiscalant dose based on observations of the net driving pressure (NDP) of the last stage of the RO system. During the process of finding the optimum antiscalant dose, the algorithm may temporarily underdose antiscalant, which

can result in scaling in the RO. For the application of the dosing algorithm in RO, it is crucial that scaling stops as the algorithm increases the antiscalant dose back to the optimum dose. The proof of principle of the algorithm was carried out for calcium carbonate scaling using induction time experiments (in glass batch-reactors) as well as lab-scale RO and pilot-scale RO measurements. It was demonstrated that in the case of scaling caused by the algorithm's underdose of antiscalant, further scaling can be stopped when the algorithm increases the antiscalant dose back to the optimum dose. This satisfied the basic criterion for the algorithm to be used in RO processes to determine the optimum antiscalant dose necessary to control scaling. It was shown that not only the underdose of antiscalant, but also the overdose of antiscalant could be detrimental to RO operation. For instance, in this study, an overdose of phosphonate antiscalant prevented calcium carbonate scaling, but resulted in permeability decline due to calcium phosphonate precipitation. The algorithm was applied to minimize antiscalant consumption in two pilot RO units; one treating anaerobic groundwater and located in the Netherlands, and the second one treating aerobic groundwater and located in Denmark. The algorithm was able to lower the antiscalant doses to 0.2 mg/L (for the pilot in the Netherlands) and 0.6 mg/L (for the pilot in Denmark), while the supplier's recommended antiscalant doses were 2.0 mg/L and 4.5 mg/L, respectively. As a result, the algorithm could reduce antiscalant consumption by up to 85–90% for the plants mentioned. This clearly showed that the suppliers' recommended doses were far greater than the optimum antiscalant dose and the dosing algorithm is a useful tool in minimizing antiscalant consumption in RO processes.

In Chapter 3, the effect of phosphate and humic substances, which are naturally present in the feedwater of the RO pilot unit in the Netherlands treating anaerobic groundwater, on calcium carbonate scaling and their impact on antiscalant dose were studied. Experiments were carried out with the RO unit (treating anaerobic groundwater), with a once-through lab-scale RO system (operating with artificially prepared groundwater), and with glass batch-reactors (measuring the induction times of the real anaerobic RO concentrate and the artificial RO concentrate). Despite operating the RO unit at 80% recovery (where calcium carbonate was highly supersaturated) without antiscalant for more than a month, calcium carbonate scaling was not observed and did not appear to result in any operational problems (e.g., NDP increase or permeability decrease) in the plant. On the other hand, the supplier's recommended dose (determined in chapter 2) to prevent calcium carbonate scaling at this recovery was 2.0 mg/L. The induction time of the real RO concentrate was greater than 168 h, while the artificial RO concentrate had an induction time of approximately 1 h. The artificial RO concentrate had the same supersaturation level as the real RO concentrate and contained only calcium, bicarbonate, sodium, and chloride ions. This suggested that the precipitation of calcium carbonate in the real anaerobic RO concentrate was suppressed by constituents present in the RO feedwater. Magnesium and sulphate ions had no influence on preventing calcium carbonate scaling as the induction time of the artificial RO concentrate did not increase in their presence. Phosphate ion and humic substances, on the other hand, had a

considerable role in hindering the precipitation of calcium carbonate. The induction time of the artificial RO concentrate increased to 168 h with the addition of 10 mg/L of phosphate, humic acid and fulvic acid. Furthermore, in lab-scale RO tests, the permeability of the membrane decreased when the artificial RO concentrate did not contain phosphate, while it remained constant when phosphate was present. These findings indicated that the presence of phosphate and humic substances in the RO feed may allow for a reduction in antiscalant dose required to control calcium carbonate scaling. It is important to note that the presence of phosphate and humic compounds in the feedwater should not be regarded as a means of preventing calcium carbonate scaling and lowering the dose of antiscalants, as these substances can also foul RO membranes. However, if they are present in the RO concentrate at concentrations that do not cause membrane fouling, their effect on antiscalant dosage reduction and determining the optimum antiscalant dose should not be neglected.

Chapters 4 and 5 deal with the effectiveness of antiscalants in controlling calcium phosphate scaling in RO processes. In Chapter 4, an investigation was conducted to determine whether the RO pilot unit in the Netherlands could be operated at 85% recovery without the use of antiscalants, and if not, what compounds would cause permeability decline and whether the precipitation of those compounds could be prevented with the use of antiscalants. As a Dutch water supply company will treat this anaerobic groundwater (via reverse osmosis) for drinking water production, it was crucial for them to understand if the RO could be operated at 85% recovery or higher. The projection programs of seven different antiscalant suppliers were used to identify the scalants and the maximum achievable recovery for the RO. The maximum achievable recovery for the RO unit according to the antiscalant suppliers varied in the range of 77–89 %. Three suppliers identified calcium phosphate, while other four indicated calcium carbonate as the scalant limiting RO recovery. During pilot testing, the permeability of the last stage of the RO unit decreased when the unit was operated at 85% recovery without antiscalant. Membrane autopsy was performed on the last element of the last stage. The scanning electron microscopy (SEM) analysis showed that the membrane surface was covered by a layer that appeared to be amorphous. Calcium carbonate (or any other crystalline compound) was not found on the fouled membrane surface using X-ray powder diffraction (XRD), which showed that calcium carbonate was not responsible for the permeability decline. The fluorescence excitation-emission matrix (FEEM) analysis suggested that humic substances were also not contributing to the permeability decline. The X-ray photoelectron spectroscopy (XPS) analysis indicated that calcium phosphate was the primary scalant causing permeability decline at 85% recovery. Five different commercially available (calcium phosphate) antiscalants were tested on the basis of their manufacturer recommended dose. The antiscalants were unable to prevent calcium phosphate scaling and increase RO recovery to 85% since the permeability of the last stage of the RO unit decreased with all tested antiscalants. This suggested that antiscalants may not be effective in preventing calcium phosphate scaling in RO processes. Nevertheless, some antiscalant suppliers claimed that the effectiveness of their

antiscalants was reduced because of the presence of iron (II) in the RO feed. Therefore, another study (Chapter 5) was carried out with artificial concentrate solutions in the absence of iron (II) to assess the performance of antiscalants in preventing calcium phosphate scaling in RO installations.

In chapter 5, the performance of antiscalants in preventing calcium phosphate scaling using synthetic concentrate solutions was evaluated. The synthetic concentrate solutions had the same calcium and orthophosphate concentrations that were present in the real RO concentrate of 85% recovery in the RO pilot unit treating anaerobic groundwater. The saturation level of calcium phosphate for the synthetic concentrate was determined using the projection programs of membrane suppliers and antiscalant suppliers. The projection programs of membrane suppliers indicated that calcium phosphate was supersaturated, while according to the projection programs of (some) antiscalant suppliers, calcium phosphate was undersaturated. These discrepancies make it difficult for RO operators to determine whether calcium phosphate is supersaturated and whether it will precipitate in RO systems. The effectiveness of eight calcium phosphate antiscalants from different suppliers in hindering the formation of calcium phosphate was assessed in batch (glass reactor) induction time experiments. None of the tested antiscalant could inhibit the formation of calcium phosphate in the synthetic concentrate. The formed calcium phosphate precipitates were identified as amorphous in the X-ray powder diffraction (XRD) analysis. Some antiscalants were able to suppress the agglomeration of formed calcium phosphate particles which are observed in particle size measurements. The antiscalants were tested in a once-through lab scale RO unit to see if the antiscalants, which could not prevent the formation of (amorphous) calcium phosphate particles, could prevent their deposition on the RO membrane surface. The flux of the RO element when fed with the synthetic concentrate with each antiscalant decreased which indicated that antiscalants were unable to prevent the deposition of amorphous calcium phosphate particles. This study revealed that the available antiscalants are ineffective in preventing calcium phosphate scaling in RO systems, as evidenced by pilot-scale RO measurements (Chapter 4) and lab-scale RO tests (Chapter 5).

Overall, this study showed that i) phosphate and humic substances naturally present in the RO feed can reduce the dose of commercial (synthetic) antiscalants in controlling calcium carbonate scaling, ii) the dosing algorithm is a useful tool that considers the variation in RO feedwater quality and identifies real-time optimum antiscalant doses necessary to prevent scaling for a given recovery in RO, and iii) the available calcium phosphate antiscalants, tested in this study, cannot provide acceptable inhibition of calcium phosphate scaling in RO applications.

Additional research, in collaboration with antiscalant suppliers, is recommended in order to further investigate and develop antiscalants that could prevent calcium phosphate scaling in RO systems. Furthermore, more research is needed to identify or develop a reliable method for determining the scaling potential of calcium phosphate in RO processes.

SAMENVATTING

In omgekeerde osmose (RO) processen is het essentieel dat de terugwinning (de verhouding van het permeaatwater tot het voedingswater) van het system zo hoog mogelijk is om de totale consumptie van elektriciteit per volume-eenheid van het permeaat te verlagen, de productie van water te verhogen, het volume van concentraat te verlagen en het gebruik van voorberhandelingschemicaliën en de daaraan gerelateerde kosten te verlagen. Bij het behandelen van zeewater wordt de terugwinning van het RO-systeem gelimiteerd door osmotische druk. Echter, bij omgekeerde osmose processen in brak water (BWRO), is aanslagvorming de belangrijkste barrière voor het opereren van RO-installaties bij hoge terugwinning. Aanslagvorming verwijst naar het neerslaan van slecht oplosbare stoffen (bijv. calciumcarbonaat, calciumsulfaat, bariumsulfaat, calciumfosfaat, enz.) die oververzadigd raken doordat de behouden zouten geconcentreerd worden in het RO-systeem. Aanslagvorming resulteert in verminderde prestatie van het systeem, verhoogde werkdruk, verhoogd energiegebruik, frequente chemische reiniging, verhoogde doorgang van zout, en ongewenste systeemuitval.

Om snelle terugwinning te bereiken, doseren veel RO-fabrieken antiscalanten in het voedingswater wat de neerslag van slecht oplosbare zouten op het membraanoppervlak voorkomt. Het is evident dat het aanslagvorming door calciumcarbonaat, calciumsulfaat en bariumsulfaat effectief voorkomen kan worden door het gebruik van antiscalanten. Echter, volgens de literatuur is het onduidelijk of antiscalanten het neerslaan van calciumfosfaat kan voorkomen in RO-applicaties. Een sterk aanwezige vraag in het toepassen van antiscalanten is: “Hoe is de optimale dosis vast te stellen die vereist om aanslagvorming in RO-systemen te voorkomen?” In de praktijk wordt de selectie van het antiscalant en de vereiste dosis daarvan voor een bepaalde watersamenstelling vastgesteld door de producenten van het antiscalant door middel van het gebruik van door henzelf ontwikkelde softwareprogramma’s. Echter, de methode die zij gebruiken voor het berekenen van de dosis antiscalant is onbekend, wat ertoe leidt dat de eindgebruikers niet in staat zijn om de doses die aan hen worden aanbevolen te verifiëren.

De hoofddoelen van deze studie zijn: i) het ontwikkelen van een aanpak voor het real-time vaststellen van de optimale dosis antiscalant die is vereist voor het bereiken van de gewenste terugwinning in RO-processen, en ii) het evalueren van de prestatie van antiscalanten in het controleren van aanslagvorming door calciumfosfaat in RO-processen. Deze scriptie is opgedeeld in zes hoofdstukken, waarvan hoofdstuk 1 een algemene introductie geeft en hoofdstuk 6 de belangrijkste conclusies van deze studie samenvat.

De hoofdstukken 2 en 3 behandelen de optimalisatie van de dosis antiscalant en de vermindering van antiscalant consumptie in RO fabrieken. In hoofdstuk 2 is het potentieel van een doseringsalgoritme voor het optimaliseren van de antiscalant dosis in RO-

processen onderzocht. Het algoritme definieert een real-time optimaal instelpunt van antiscalantdosering aan de doseerpomp door de dosis antiscalant continu en automatisch aan te passen op basis van waarnemingen van de netto aandrijfdruk (NDP) van de laatste fase van het RO-systeem. Tijdens het proces van het vinden van de optimale antiscalant dosis, kan het algoritme tijdelijk antiscalant onderdoseren wat kan resulteren in aanslagvorming in de RO. Voor het toepassen van het doseringsalgoritme in RO is het cruciaal dat aanslagvorming stopt op het moment dat het algoritme de dosis antiscalant weer verhoogt tot de optimale dosis. Het aantonen van de principiële bruikbaarheid van het algoritme was gedaan voor aanslagvorming door calciumcarbonaat door middel van zowel het gebruik van inductie-tijd experimenten (in glazen batch-reactoren) als laboratoriumschaal RO- en experimentschaal RO-metingen. Aangetoond werd dat in het geval van aanslagvorming veroorzaakt door het onderdoseren van antiscalant door het algoritme, verdere aanslagvorming tegen kan worden gegaan als het algoritme de antiscalant dosis verhoogd naar het optimum. Dit voldeed aan het basiscriterium voor het algoritme om gebruikt te kunnen worden in RO-processen om de optimale antiscalant dosis te bepalen die nodig is voor het controleren van aanslagvorming. Er is aangetoond dat niet alleen de onderdosering van antiscalant, maar ook de overdosering van antiscalant schadelijk kunnen zijn voor de RO-operatie. In deze studie verhinderde een overdosis fosfonaat-antiscalant bijvoorbeeld aanslagvorming door calciumcarbonaat, maar resulteerde in een afname van de permeabiliteit als gevolg van calciumfosfonaatprecipitatie. Het algoritme was toegepast om antiscalant consumptie te minimaliseren in twee RO test-eenheden: één die anaëroob grondwater behandelt en gevestigd is in Nederland, en de tweede die aëroob grondwater behandelt en gevestigd is in Denemarken. Het algoritme was in staat om de dosis antiscalant te verlagen naar 0.2mg/L voor de testeenheid in Nederland en 0.6 mg/L voor de testeenheid in Denemarken, terwijl de leveranciers antiscalant doses van respectievelijk 2.0 mg/L en 4.5mg/L adviseerden. Het resultaat was dat het algoritme de consumptie van antiscalant kon verlagen met 85-90% voor de genoemde fabrieken. Hieruit bleek duidelijk dat de aanbevolen doses van de leveranciers veel hoger waren dan de optimale dosis antiscalant en dat het doseringsalgoritme een nuttig hulpmiddel is om het gebruik van antiscalant in RO-processen te minimaliseren.

In Hoofdstuk 3 is het effect van fosfaat en humusstoffen, die van nature aanwezig zijn in het voedingswater van de RO-testeenheid in Nederland die anaëroob grondwater behandelt, op aanslagvorming door calciumcarbonaat en hun effect op de dosis antiscalant bestudeerd. Experimenten waren uitgevoerd met de RO-eenheid (behandeling van anaëroob grondwater), met een doorloop-RO-systeem op laboratoriumschaal (werkend met artificieel bereid grondwater) en met glazen batch-reactoren (meten van de inductietijden van het echte anaërobe RO-concentraat en het artificiële RO-concentraat). Ondanks dat de RO-eenheid gedurende meer dan een maand werd gebruikt met een terugwinning van 80% (waar calciumcarbonaat sterk oververzadigd was) zonder antiscalant, werd er geen aanslagvorming door calciumcarbonaat waargenomen en leek deze niet te leiden tot operationele problemen (bijv. NDP-toename of afname van de

permeabiliteit) in de fabriek. Aan de andere kant was de door de leverancier aanbevolen dosis (bepaald in hoofdstuk 2) om aanslagvorming door calciumcarbonaat te voorkomen bij dit herstel 2,0 mg/L. De inductietijd van het echte RO-concentraat was meer dan 168 uur, terwijl het artificiële RO-concentraat een inductietijd had van ongeveer 1 uur. Het artificiële RO-concentraat had hetzelfde oververzadigingsniveau als het echte RO-concentraat en bevatte alleen calcium-, bicarbonaat-, natrium- en chloride-ionen. Dit suggereerde dat de precipitatie van calciumcarbonaat in het echte anaërobe RO-concentraat werd onderdrukt door bestanddelen die aanwezig waren in het RO-voedingswater. Magnesium- en sulfaationen hadden geen invloed op het voorkomen van aanslagvorming door calciumcarbonaat, aangezien de inductietijd van het artificiële RO-concentraat niet toenam bij aanwezigheid van deze ionen. Fosfaationen en humusstoffen speelden daarentegen een aanzienlijke rol bij het belemmeren van de precipitatie van calciumcarbonaat. De inductietijd van het artificiële RO-concentraat nam toe tot 168 uur bij toevoeging van 10 mg/L fosfaat, humuszuur en fulvinezuur. Bovendien nam in RO-tests op laboratoriumschaal de permeabiliteit van het membraan af wanneer het kunstmatige RO-concentraat geen fosfaat bevatte, terwijl het constant bleef wanneer fosfaat aanwezig was. Deze bevindingen gaven aan dat de aanwezigheid van fosfaat en humusstoffen in de RO-aanvoer kan zorgen voor een verlaging van de dosis antiscalant die nodig is om aanslagvorming door calciumcarbonaat te beheersen. Noemenswaardig is dat de aanwezigheid van fosfaat en humusverbindingen in het voedingswater niet moet worden beschouwd als een middel waarmee aanslagvorming door calciumcarbonaat kan worden voorkomen en de dosis antiscalanten te verlagen, omdat deze stoffen ook RO-membranen kunnen vervuilen. Als ze echter in het RO-concentraat aanwezig zijn in concentraties die geen membraanvervuiling veroorzaken, moet hun effect op de verlaging van de dosis antiscalant en het bepalen van de optimale dosis antiscalant niet worden verwaarloosd.

Hoofdstukken 4 en 5 behandelen de effectiviteit van antiscalanten bij het beheersen van aanslagvorming door calciumfosfaat in RO-processen. In Hoofdstuk 4 is onderzocht of de RO-testeenheid in Nederland zonder gebruik van antiscalanten op 85% terugwinning zou kunnen draaien, en zo niet, welke verbindingen de permeabiliteit zouden verminderen en of de precipitatie van die verbindingen zou kunnen worden voorkomen door het gebruik van antiscalanten. Aangezien een Nederlands waterleidingbedrijf dit anaërobe grondwater (via omgekeerde osmose) gaat behandelen voor de productie van drinkwater, was het voor hen van cruciaal belang om te begrijpen of de RO kon worden gebruikt met een terugwinning van 85% of hoger. De projectieprogramma's van zeven verschillende leveranciers van antiscalant werden gebruikt om de aanslagvormende stoffen en het maximaal haalbare herstel voor de RO te identificeren. Het maximaal haalbare herstel voor de RO-eenheid volgens de leveranciers van antiscalant varieerde in het bereik van 77-89 %. Drie leveranciers identificeerden calciumfosfaat als beperking van de terugwinning in de RO, terwijl andere vier calciumcarbonaat aangaven als beperking. Tijdens de testen nam de permeabiliteit van de laatste fase van de RO-eenheid af wanneer de eenheid werd gebruikt met een terugwinning van 85% zonder antiscalant. Membraan

autopsie werd uitgevoerd op het laatste element van de laatste fase. De scanning elektronenmicroscopie (SEM) analyse toonde aan dat het membraanoppervlak bedekt was met een laag die amorf leek te zijn. Calciumcarbonaat (of welke andere kristallijne verbinding ook) werd niet gevonden op het vervuilde membraanoppervlak met behulp van röntgenpoederdiffractie (XRD), wat aantoonde dat calciumcarbonaat niet verantwoordelijk was voor de afname van de permeabiliteit. De fluorescentie-excitatie-emissiematrix (FEEM) analyse suggereerde dat humusstoffen ook niet bijdroegen aan de afname van de permeabiliteit. De röntgenfoto-elektronspectroscopie (XPS)-analyse gaf aan dat calciumfosfaat de primaire scalair was die de permeabiliteitsafname bij 85% terugwinning veroorzaakte. Vijf verschillende in de handel verkrijgbare (calciumfosfaat) antiscalanten werden getest op basis van de door de fabrikant aanbevolen dosis. De antiscalanten waren niet in staat calciumfosfaataanslag te voorkomen en de RO-terugwinning tot 85% te verhogen, aangezien de permeabiliteit van de laatste fase van de RO-eenheid afnam met alle geteste antiscalanten. Dit suggereerde dat antiscalanten mogelijk niet effectief zijn in het voorkomen van aanslagvorming door calciumfosfaat in RO-processen. Desalniettemin beweerden sommige leveranciers van antiscalant dat de effectiviteit van hun antiscalant was verminderd vanwege de aanwezigheid van ijzer (II) in de RO aanvoer. Daarom werd een andere studie (Hoofdstuk 5) uitgevoerd met artificiële concentraatoplossingen in afwezigheid van ijzer (II) om de prestatie van antiscalanten te beoordelen bij het voorkomen van aanslagvorming door calciumfosfaat in RO-installaties.

In hoofdstuk 5 werd de prestatie van antiscalanten in het voorkomen van calciumfosfaataanslag met behulp van synthetische concentraatoplossingen geëvalueerd. De synthetische concentraatoplossingen hadden dezelfde calcium- en orthofosfaatconcentraties die aanwezig waren in het echte RO-concentraat van 85% terugwinning in de RO-testeenheid die anaëroob grondwater behandelt. Het verzadigingsniveau van calciumfosfaat voor het synthetische concentraat is bepaald met behulp van de projectieprogramma's van membraanleveranciers en antiscalantleveranciers. De projectieprogramma's van membraanleveranciers gaven aan dat calciumfosfaat oververzadigd was, terwijl volgens de projectieprogramma's van (sommige) antiscalantleveranciers calciumfosfaat onderverzadigd was. Deze discrepanties maken het voor RO-operators moeilijk om te bepalen of calciumfosfaat oververzadigd is en of het zal neerslaan in RO-systemen. De effectiviteit van acht calciumfosfaat-antiscalanten van verschillende leveranciers bij het tegengaan van de vorming van calciumfosfaat werd beoordeeld in batch- (glazen reactor) inductietijd experimenten. Geen van de geteste antiscalanten kon de vorming van calciumfosfaat in het synthetische concentraat remmen. De gevormde calciumfosfaatprecipitaten werden geïdentificeerd als amorf in de röntgenpoederdiffractie (XRD) analyse. Sommige antiscalanten waren in staat om de agglomeratie van gevormde calciumfosfaatdeeltjes die worden waargenomen bij metingen van de deeltjesgrootte te onderdrukken. De antiscalanten werden getest in een RO-eenheid op laboratoriumschaal om te zien of de antiscalanten, die de vorming van calciumfosfaatdeeltjes niet konden voorkomen, hun

afzetting op het RO-membraanoppervlak wel konden voorkomen. De doorstroom van het RO-element wanneer gevoed met het synthetische concentraat met elk antiscalant nam af, wat aangaf dat antiscalanten de afzetting van amorfe calciumfosfaatdeeltjes niet konden voorkomen. Deze studie onthulde dat de beschikbare antiscalanten niet effectief zijn in het voorkomen van aanslagvorming door calciumfosfaat in RO-systemen, zoals blijkt uit RO-metingen op testeenheid schaal (Hoofdstuk 4) en RO-tests op laboratoriumschaal (Hoofdstuk 5).

Algeheel toonde deze studie aan dat i) fosfaat en humusstoffen die van nature in de RO-aanvoer zijn ingesteld, de dosis commerciële (synthetische) antiscalanten kunnen verminderen bij het beheersen van calciumcarbonaataanslag, ii) het doseringsalgoritme een bruikbaar hulpmiddel is dat rekening houdt met de variatie in RO-voedingswater kwaliteit en identificeert real-time optimale antiscalant-doses die nodig zijn om aanslagvorming te voorkomen voor een bepaalde terugwinning in RO, en iii) de beschikbare calciumfosfaat-antiscalant middelen, getest in deze studie, kunnen geen acceptabele remming van aanslagvorming door calciumfosfaat in RO-toepassingen bieden.

Aanvullend onderzoek, in samenwerking met leveranciers van antiscalant, wordt aanbevolen om antiscalanten die aanslagvorming door calciumfosfaat in RO-systemen kunnen voorkomen, verder te onderzoeken en te ontwikkelen. Daarnaast is er meer onderzoek nodig om een betrouwbare methode te identificeren of te ontwikkelen om het schaalpotentieel van calciumfosfaat in RO-processen te bepalen.

CONTENTS

1

INTRODUCTION AND THESIS OUTLINE

1.1 INTRODUCTION

One of the most significant advancements in water treatment over the past few decades has been the introduction of reverse osmosis (RO) technology. Because of the continuous development of RO, the decreasing prices of membrane technology, and its small footprint and excellent removal of contaminants (e.g., organic micropollutants (OMPs), viruses, etc.) (Beyer et al., 2014), RO is increasingly being used in the treatment of groundwater and surface water which are the primary sources for producing drinking water in many countries around the world. In the Netherlands, for instance, over 60% of the drinking water produced by water supply companies comes from the treatment of groundwater (Hiemstra et al., 2003, de Vet et al., 2009), and several of these Dutch water companies (Oasen, Vitens, PWN, etc.) have adopted (or are investigating) the use of RO technology to produce high-quality drinking water.

Although RO technology has gained acceptance and popularity in the water treatment industry, it still faces some challenges, such as membrane fouling, that need to be addressed. Membrane fouling has a negative impact on RO operation, including but not limited to membrane permeability loss, increased pressure requirements resulting in higher operating costs, an increase in salt passage of the RO permeate, and a shorter membrane lifetime as a result of frequent cleanings (Kucera, 2010, Peña et al., 2013, Ismail et al., 2019, Zaidi and Saleem, 2022). There are many different types of fouling that can occur in RO processes, including particulate fouling, organic fouling, biofouling, and scaling (Flemming, 1993, Tang et al., 2011, Fridjonsson et al., 2015, Okamoto and Lienhard, 2019). Particulate fouling is caused by the deposition of colloidal and suspended material (silt, clay, iron oxides, etc.) present in the RO feed onto the membrane surface (Potts et al., 1981, Salinas-Rodriguez, 2011, Pandey et al., 2012). Organic fouling is usually encountered when the RO feed contains high concentrations of natural organic matter (e.g., humic substances, etc.) that adsorb on the membrane surface (Xu et al., 2006, Martínez et al., 2014). Biofouling is the attachment and growth of microorganisms on the feed spacer and membrane surface in RO processes (Flemming, 1997, Vrouwenvelder et al., 1998, Vrouwenvelder et al., 2009). Lastly, scaling is the crystallization and precipitation of sparingly soluble salts on the membrane surface that can occur when the salts' concentration on the membrane surface exceeds their solubility limits (Lee and Lee, 2005, Kucera, 2010, Kostoglou and Karabelas, 2011, Fane, 2016).

Scaling is a major challenge in brackish water RO applications (BWRO) and is typically the key barrier in operating RO systems at high recovery rates. Maximizing recovery in BWRO is highly desirable to minimize the total electrical consumption per unit volume of permeate, maximize water production, decrease the amount of concentrate, and lower the use of pretreatment chemicals and their related costs. However, at high recoveries, the concentration of the dissolved inorganic compounds in the concentrate increases

considerably, as much as four to ten times for recoveries in the 75–90 % range, consequently, exceeding the solubility limits for several types of salts, which can lead to membrane scaling (Antony et al., 2011, Waly, 2011). Depending on the inorganic ion composition of the RO feed, various compounds such as calcium carbonate, calcium sulphate, calcium phosphate, silica, etc. can precipitate in RO installations. The focus of this study is primarily on calcium carbonate and calcium phosphate scaling.

Calcium carbonate is one of the most common scales found on RO membranes. The formation and degree of calcium carbonate scaling are affected by calcium and bicarbonate concentrations, as well as other factors including but not limited to the pH, temperature, and the presence of other inorganic/organic substances (Koutsoukos, 2010). The scaling potential of calcium carbonate in water increases with an increase in temperature and pH. On the other hand, its precipitation is hindered in the presence of magnesium, sulphate, phosphate, and natural organic matter. For instance, in applications other than RO, researchers have reported that the crystal growth rate of calcium carbonate is reduced when a water solution contains some common inorganic ions, such as magnesium ion (Berner, 1975, Bischoff, 1968, Chen et al., 2005), orthophosphate ion (Reddy, 1977, Giannimaras and Koutsoukos, 1987, Langerak et al., 1999), and sulphate ion (Nielsen et al., 2016) as well as when it contains dissolved organic substances such as humic substances (Hoch et al., 2000, Zuddas et al., 2003, Klepetsanis et al., 2002, Amjad et al., 1998, Inskeep and Bloom, 1986).

Calcium phosphate can be mainly encountered in water reuse applications as well as in RO treatment of groundwater when the RO feed contains a high concentration of calcium and orthophosphate ions (Chesters, 2009, Greenberg et al., 2005). Calcium phosphate can exist in various forms such as an amorphous phase, i.e., amorphous calcium phosphate (ACP) and in crystalline phases namely, monocalcium phosphate monohydrate ($Ca(H_2PO_4)_2{\cdot}H_2O$; MCPD) and its anhydrous form, dicalcium phosphate dihydrate ($CaHPO_4{\cdot}2H_2O$; DCPD) and its anhydrous form, β-tricalcium phosphate (β–$Ca_3(PO_4)_2$; β–TCP), hydroxyapatite ($Ca_5(PO_4)_3(OH)$) (Dorozhkin, 2016). In RO applications, not all of the mentioned phases could be encountered. For instance, the formation of MCPD, DCPD and their anhydrous forms occur at pH values below 6.5 (Dorozhkin, 2016), and therefore their precipitation in RO applications where pH is above 7 is less likely. Additionally, the formation of β-TCP occurs at temperatures above 700 °C (Bohner et al., 1997), thus it cannot be observed in RO systems. The formation of hydroxyapatite, which is the most thermodynamically stable and least soluble phase of calcium phosphate, could occur in the neutral to basic pH range (Eanes, 1998). However, its formation normally is preceded by ACP (Meyer and Weatherall, 1982, Brečević and Füredi-Milhofer, 1976, Eanes and Posner, 1965, Walton et al., 1967, Termine, 1972) which suggests that ACP, not hydroxyapatite, may be the primary species responsible for the flux decline in RO applications.

One of the most widely used strategies for preventing scaling and achieving high recoveries in RO applications is the addition of an antiscalant to the RO feed (Lee et al., 1999, Pervov, 1991, Greenlee et al., 2010). Antiscalants impede or delay the precipitation of sparingly soluble salts by interfering with one or more scale formation stages, such as nucleation, crystal growth, and/or agglomeration (Amjad, 1996, Antony et al., 2011, Koutsoukos, 2010, Fink, 2021). They function by one or more mechanisms to suppress scaling, including but not limited to threshold inhibition and dispersion (Darton, 2000). Threshold inhibition is one of the main mechanisms of antiscalants by which the process of crystallization, i.e., crystal formation and growth is hindered by the adsorption of antiscalants on the active sites of the first nucleating crystals (Koutsoukos, 2010, Cooper et al., 1979). Dispersion is the property of an antiscalant to adsorb on the crystals or colloidal particles and impart extra negative charge that then keeps the crystals or colloidal particles separated in the solution, limiting growth/agglomeration and deposition on the membrane surface (Amjad, 1996, Darton, 2000).

Antiscalants are blends of chemicals, the exact composition and amounts of which are known only to the antiscalant suppliers. There are a variety of commercial antiscalants available that are designed to combat specific types of scale. The most common antiscalants utilized in RO applications include, but are not limited to, phosphonates and polycarboxylates (Antony et al., 2011, van Engelen and Nolles, 2013). The selection of antiscalants in RO applications depends on the feed water composition. In practice, the selection of antiscalant and the dose of that antiscalant needed for a specific water composition is typically determined by the antiscalant manufacturers using one of their proprietary software programs. However, the method that is used by the manufacturers to calculate the antiscalant dose is not disclosed to the public, and as a result, the end-users are unable to verify the doses that are recommended to them.

1.2 PROBLEM STATEMENT

With the use of antiscalants, the main question which arises is: *How to determine the lowest (optimum) dose of antiscalants to prevent scaling in RO applications?* Operating the RO with the lowest antiscalant dose at which scaling does not occur is highly desirable, since high doses of antiscalant result in additional costs and pose environmental concerns (Boels and Witkamp, 2011). Some studies have reported that the presence of some inorganic ions (e.g., phosphate) and natural organic matter, i.e., humic substances have a noticeable inhibitory effect on the scaling species (Reddy, 1977, Giannimaras and Koutsoukos, 1987, Langerak et al., 1999, Zuddas et al., 2003, Klepetsanis et al., 2002, Inskeep and Bloom, 1986, Amjad et al., 1998). It is, therefore, likely that when these substances are present in the RO feed, a lower antiscalant dose may be applied. As the effect of these substances is not considered by suppliers in the dosing recommendation,

the actual required dose of antiscalant could be lower than the recommended dose. Furthermore, the required antiscalant dose may change in time, due to variations in the feedwater composition. Thus, dynamic adaptation is necessary to attain the lowest antiscalant dose. According to the author's current knowledge, no standard method exists for optimizing antiscalant dose in RO applications that considers the effect of inorganic and organic substances in the feedwater on the antiscalant dose and which could identify real-time optimum dose for any feedwater composition.

Furthermore, it is well established that the problem with the crystalline scales, i.e., $CaCO_3$, $BaSO_4$, $CaSO_4$, etc. can be alleviated with the addition of antiscalants to the RO feed (Greenlee et al., 2010, Rahman, 2013, Salman et al., 2015). However, it is not clear if antiscalants are effective in preventing calcium phosphate scaling in RO applications. For instance, antiscalant suppliers report that calcium phosphate scaling can be prevented by the addition of antiscalants (Chesters, 2009), where as some researchers reported that antiscalants were not effective in preventing calcium phosphate precipitation on the RO membrane (Greenberg et al., 2005). These researchers, however, tested the performance of antiscalants in recycled systems where permeate and concentrate were recirculated back to the feed tank. Antiscalant suppliers emphasize that antiscalants may not be as effective in recycled systems as they should be in once-through flow systems (like RO systems) and therefore the performance of antiscalants assessed in recycled systems may not be representative. From the available literature, one can realize that until now a study to investigate the performance of antiscalants in preventing calcium phosphate scaling in RO systems using once-through RO experiments with synthetic solutions (where calcium and phosphate are the only precipitating ions) is not available. Additionally, as new antiscalants have been introduced to the market over the years, there is a need for a study to assess the performance of commercially available antiscalants in preventing calcium phosphate scaling in RO systems.

1.3 RESEARCH OBJECTIVES

The main objectives of this study are:

- To develop an approach which can identify the real-time optimal antiscalant dose necessary to achieve a target recovery in RO processes
- To investigate the effectiveness of available calcium phosphate antiscalants in preventing calcium phosphate scaling in RO applications

1.4 THESIS OUTLINE

This thesis is organized into the following six chapters:

Chapter 1 provides a brief background on scaling and the use of antiscalants to control scaling in RO applications, as well as highlights the problem statement and main objectives of this research study.

Chapter 2 presents the proof of principle, the validity and the application of a control algorithm that defines a real-time optimal set-point of antiscalant dosing to minimize antiscalant consumption in RO processes. In addition, the effect of underdose and overdose of antiscalant, i.e., phosphonate antiscalant on membrane scaling and RO operation is demonstrated.

Chapter 3 demonstrates the effect of phosphate and humic substances (naturally present in RO feed) on calcium carbonate scaling prevention and their impact on antiscalant dose reduction for an anaerobic groundwater RO system.

Chapter 4 investigates the role of antiscalants in increasing the recovery of a future RO system of a Dutch water supply company, which will treat anaerobic groundwater in Kamerik (the Netherlands) for drinking water production, to at least 85 % and the scalants that could limit RO recovery.

Chapter 5 evaluates the performance of antiscalants in preventing calcium phosphate scaling using synthetic concentrate solutions.

Chapter 6 summarizes the main findings of this study and makes recommendations for future research.

2

APPLICATION OF A SMART DOSING PUMP ALGORITHM IN IDENTIFYING REAL-TIME OPTIMUM DOSE OF ANTISCALANT IN REVERSE OSMOSIS SYSTEMS

This chapter is based on the following publication:

M.N. Mangal, V.A. Yangali-Quintanilla, S.G. Salinas-Rodriguez, J. Dusseldorp, B. Blankert, A.J.B. Kemperman, J.C. Schippers, M.D. Kennedy, W.G.J. van der Meer, Application of a smart dosing pump algorithm in identifying real-time optimum dose of antiscalant in reverse osmosis systems, Journal of Membrane Science, 658 (2022) 120717. https://doi.org/10.1016/j.memsci.2022.120717

Abstract

The potential of membrane scaling control by a real-time optimization algorithm was investigated. The effect of antiscalant dosing was evaluated from the induction time measured in glass batch-reactors, and from the operational performance of a lab-scale reverse osmosis (RO) unit and two pilot-scale RO units. Step changes in the antiscalant dosing demonstrated that the accumulation of scaling is 'paused' during periods when the optimum dose is applied. This is paramount for the application of a dynamic dosing strategy that may briefly underdose, while searching for the optimum dose. It was found that antiscalant underdose and overdose were both detrimental to RO operation since underdose resulted in membrane scaling, while overdose led to membrane fouling due to calcium-antiscalant deposits. The dosing algorithm was used to minimize antiscalant consumption in two pilot RO units. The algorithm was able to lower the antiscalant doses to 0.2 mg/L and 0.6 mg/L, while the supplier's recommended antiscalant doses were 2.0 mg/L and 4.5 mg/L, respectively. As a result, the algorithm could reduce antiscalant consumption by up to 85–90% for the plants mentioned.

2.1 INTRODUCTION

In brackish water reverse osmosis (BWRO) processes, scaling is a major challenge and is typically the main barrier to operating RO installations at high recoveries. Scaling is caused by the precipitation (deposition) of sparingly soluble salts on the membrane surface when their saturation limits are exceeded. Scaling reduces permeate production (due to decreased membrane permeability), raises operational costs (due to higher operating pressure, cleaning costs, etc.), and degrades permeate water quality (due to increasing salt passage) (Kucera, 2010, Mangal et al., 2021c). A variety of inorganic compounds might cause scaling in BWRO, e.g., calcium carbonate, calcium sulphate, barium sulphate, calcium phosphate, silica, etc.

Antiscalant dosing in feedwater is one of the most extensively applied and effective scaling prevention strategies in RO applications (Antony et al., 2011, Kucera, 2010, Greenlee et al., 2010, van Engelen and Nolles, 2013, Yu et al., 2020). Antiscalants delay the precipitation process of the supersaturated sparingly soluble salts, allowing higher supersaturation without scale formation. There are several commercial antiscalants available, and the most commonly used ones in RO applications are phosphonates, polycarboxylates, and bio-based antiscalants (Antony et al., 2011, van Engelen and Nolles, 2013, Boels and Witkamp, 2011). The selection of antiscalants in RO applications depends on the feed water composition as well as other factors such as recovery and discharge regulations.

With the use of antiscalants, the main question which arises is: *How to determine the lowest (optimum) dose of antiscalants to prevent scaling in RO applications?* Operating the RO with the lowest antiscalant dose at which scaling does not occur is highly desirable, since high doses of antiscalant result in additional costs and pose environmental concerns (Boels and Witkamp, 2011). In practice, the antiscalant dose for a given water composition is generally determined using the antiscalant manufacturer's proprietary programs. However, the method used by the manufacturers to calculate the antiscalant dose is unknown and therefore the end-users cannot verify their recommended doses. In general, the suppliers' recommended antiscalant doses are in the range of 2–10 mg/L to prevent scaling in RO processes (Singh, 2005).

Some studies have reported that the presence of some inorganic ions (e.g., phosphate) and natural organic matter, i.e., humic substances have a noticeable inhibitory effect on the scaling species (Reddy, 1977, Giannimaras and Koutsoukos, 1987, Langerak et al., 1999, Zuddas et al., 2003, Mangal et al., 2021a, Klepetsanis et al., 2002, Inskeep and Bloom, 1986, Amjad et al., 1998). It is, therefore, likely that when these substances are present in the RO feed, a lower antiscalant dose may be applied. Mangal et al. (2021a) have demonstrated that both phosphate and humic substances present in an anaerobic groundwater in the Netherlands could prevent calcium carbonate scaling and thus were responsible for the reduction in the antiscalant dose. As the effect of these substances is not considered by suppliers in the dosing recommendation, the actual required dose of antiscalant could be lower than the recommended dose. It is therefore essential to consider the effect of the aforementioned substances (if present in RO feed) when determining the optimum dose in RO applications. According to the authors' current knowledge, no standard method exists for optimizing antiscalant dose in RO applications that considers the effect of inorganic and organic substances in the feedwater on the antiscalant dose and which could be applied for any feedwater composition.

The required antiscalant dose may change in time, due to variations in the feedwater composition. Thus, dynamic adaptation is necessary to attain the lowest antiscalant dose. A feedback algorithm continuously and automatically adapts the dose based on an observation of the performance of the membrane system. However, this implies that occasionally, brief periods with under- and over-dosing may occur. It is necessary that the adverse effect of the under- or over-dosing on the fouling rate is reversible (Blankert et al., 2007).

This study was performed in the context of the realization of a smart digital dosing pump (in cooperation with Grundfos A/S) with an integrated dosing control algorithm that is intended to identify the optimal antiscalant dose necessary to achieve a target recovery in RO processes and thus to minimize or prevent overdosing of antiscalant. The control module of the dosing pump is configured to vary the a of antiscalant in the RO feed based on the net driving pressure (NDP) or ($\Delta NDP/\Delta t$) of the last stage where scaling occurs.

The algorithm should preferably be applied to an external scale-guard unit to reduce the risk of scaling in full-scale RO installations while optimizing antiscalant dose. A scale-guard unit is an additional RO element that is fed with the concentrate of the last stage of a full-scale RO installation, and because the scale-guard provides additional recovery, scaling occurs in the scale-guard prior to the final stage of the full-scale RO installation (van de Lisdonk et al., 2000).

The working concept of the algorithm is described in more detail elsewhere (Yangali-quintanilla et al., 2019). The control algorithm, as illustrated in Figure 1, initially employs the supplier's recommended antiscalant dose and then reduces the dosage of antiscalant fed into the RO feed until an increase of the slope NDP (or $\Delta NDP/\Delta t$) is detected. Afterwards, the algorithm increases the dose to the lowest antiscalant dose at which the NDP remains constant. The dose at which an increase in NDP is observed is recognized as the underdose, and the lowest antiscalant dose at which no increase in NDP is observed is considered as the optimum antiscalant dose. The dosing pump algorithm is based on the hypothesis that when NDP increases (due to scaling) at a dose lower than the optimum dose, further scaling and thus increase in NDP will stop when the dose is raised back to the optimum dose. This hypothesis needs to be verified as it could be expected that once scaling occurs (during antiscalant underdose), further scaling could not be stopped when the dose is increased from the underdose to the optimum dose or even back to the supplier's recommended dose.

The objectives of this study are: *i*) to investigate whether once scaling occurs in an RO system due to antiscalant underdose, further scaling could be stopped with an optimum antiscalant dose, and *ii*) to evaluate the application of the dosing pump algorithm in minimizing antiscalant consumption and identifying optimum antiscalant doses in RO applications. This research work consists of two main parts. In the first part, step-changes are applied to the antiscalant dosing in controlled precipitation experiments (in glass reactors), once-through lab-scale RO tests, and pilot RO tests. In addition, the effect of underdose and overdose of antiscalant on calcium carbonate scaling and RO operation is demonstrated. In the second part, the antiscalant dosing algorithm is applied to determine the optimum antiscalant dose in two different RO plants; one treating anaerobic groundwater and located in Kamerik (the Netherlands), and the second one treating aerobic groundwater and located in Brabrand (Denmark).

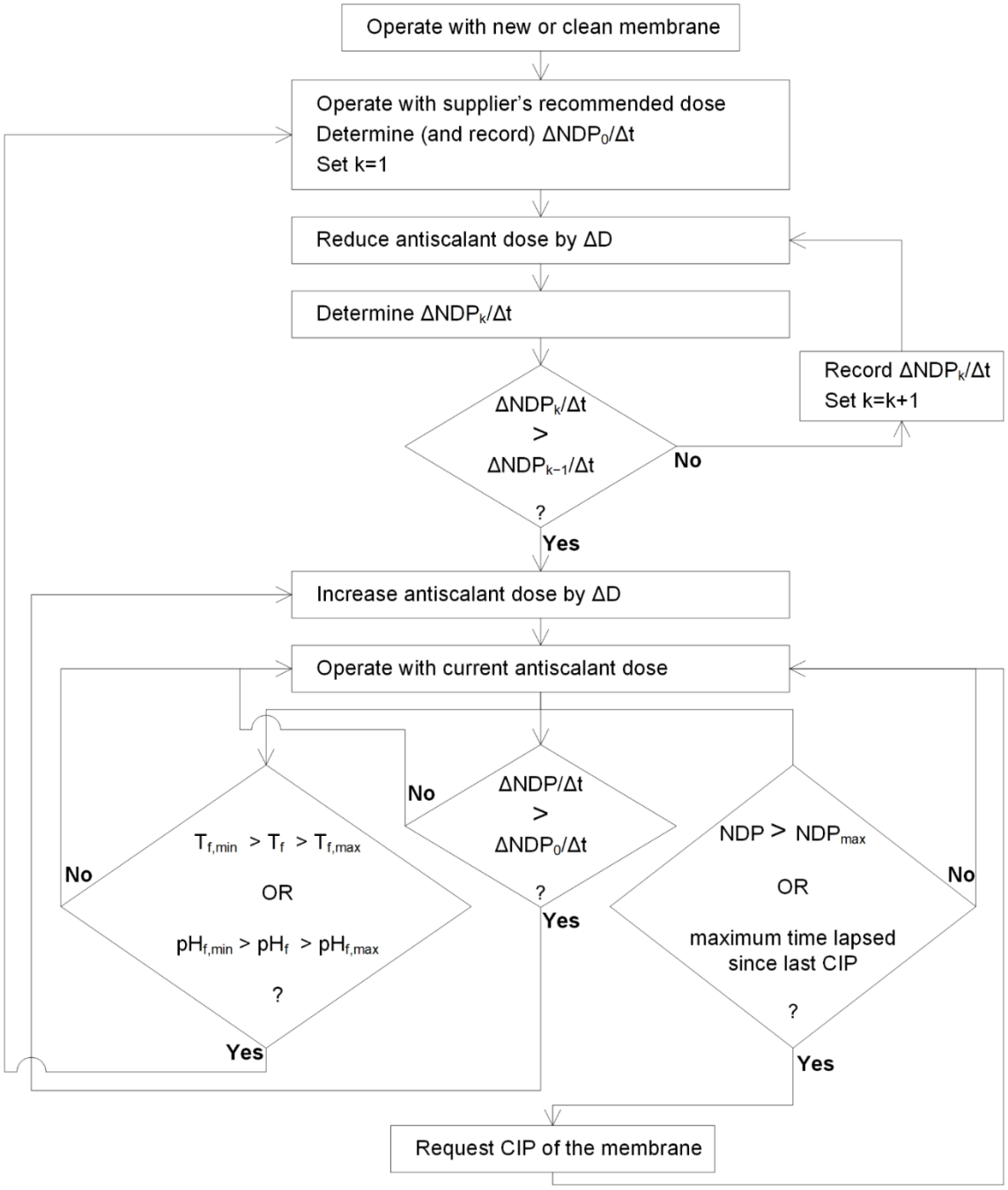

Figure 2.1 *Working principle of the dosing pump algorithm in identifying the optimum antiscalant doses in RO processes (Yangali-quintanilla et al., 2019)*

2.2 MATERIALS AND METHODS

2.2.1 Chemicals for preparing synthetic concentrate solutions

The controlled precipitation experiments in glass reactors, i.e., induction time measurements and the once-through lab-scale RO tests were executed with synthetic concentrate solutions where calcium carbonate was the only precipitating compound in the absence of antiscalant. The concentrations of Ca^{2+} and HCO_3^- in the synthetic concentrate solutions were equivalent to the concentrate concentration of the real anaerobic groundwater of Kamerik, the Netherlands (Table 2.1, section 2.2.5) treated at a certain recovery. For instance, a synthetic concentrate of 85% recovery comprised 765 mg/L of Ca^{2+}, 2670 mg/L of HCO_3^-, and had a pH 7.6, resulting in a Langelier Saturation Index (LSI) of 2.2. Performing experiments at such high supersaturation levels was done for two reasons: i) to have relatively short experiments with synthetic concentrates in the lab-scale RO tests that were performed in once-through mode, and ii) to carry out proof of principle tests at the most extreme conditions, so that if the algorithm can be successfully applied for the optimization of antiscalant dose at such high supersaturation levels, it can definitely be applied at low supersaturation levels as well.

Milli-Q water (Merck Millipore) was used to make synthetic concentrate solutions with $CaCl_2 \cdot 2H_2O$ and $NaHCO_3$ (Analytical Grade, Merck). The pH adjustments of the synthetic concentrate solutions were done using 0.2 M solutions of HCl (Analytical grade, ACROS Organics) or NaOH (Analytical Grade, J.T. Baker). All experiments in this study were performed with a commercial phosphonate antiscalant.

2.2.2 Induction time measurements

In this study, as in others (Söhnel and Mullin, 1988, Boerlage et al., 2000, Waly, 2011, Mangal et al., 2021a), induction time is defined as the time elapsed between the emergence of supersaturated conditions and the detection of crystallization. Figure 2.2 depicts a schematic diagram of the experimental setup which was used in this research to measure the induction time of calcium carbonate. The induction time tests were carried out in an airtight double-walled 3 L Applikon glass reactor with an Endress Hauser pH probe installed to continuously record the pH of the synthetic concentrate solution. Induction time was considered as the time it takes for the pH of the synthetic concentrate to drop by 0.03 units from its initial value as a result of the formation of calcium carbonate crystals (Waly et al., 2010).

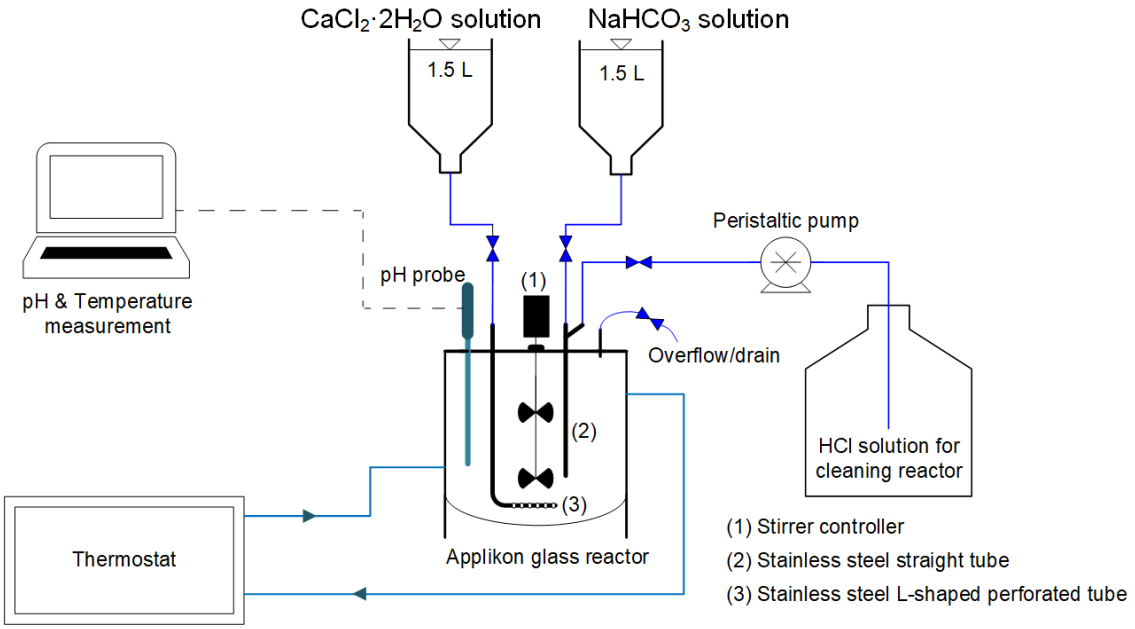

Figure 2.2 *Experimental setup for induction time tests*

To conduct an induction time test, the 3 L reactor was first half-filled with the $NaHCO_3$ solution and then the pH was adjusted to the desired value using a 0.2 M HCl solution. Following that, the other half of the reactor was filled with the $CaCl_2 \cdot 2H_2O$ solution while maintaining the stirring rate inside the reactor at 150 rpm to ensure uniform mixing of the solutions and to avoid the development of any local supersaturated zones (Waly et al., 2012). It is worth mentioning that all induction time tests were performed at 20 °C, which was controlled by a thermostat. After each induction time test, the reactor was cleaned with 0.2 M HCl to dissolve crystals that formed during the test, and then the reactor was rinsed twice with demineralized water (demi-water).

To investigate the effect of antiscalant underdose and overdose, induction time tests were performed with the synthetic concentrate of 85% recovery and antiscalant concentrations of 1.3 mg/L, 13.3 mg/L, and 33.3 mg/L which correspond to feedwater antiscalant doses of 0.2 mg/L, 2.0 mg/L, and 5.0 mg/L, respectively. According to antiscalant supplier, 5.0 mg/L was the upper limit of the antiscalant dose. For the algorithm's proof of principle, i.e., scaling reversibility with antiscalant, induction time measurements were carried out with synthetic concentrate solutions both with and without antiscalant, as well as in the absence and presence of calcium carbonate (seed) crystals. The calcium carbonate crystals employed were those that precipitated in the reactor during induction time tests with synthetic concentrate solutions without antiscalant. More precisely, to get freshly formed calcium carbonate crystals, an induction time test was performed with the synthetic concentrate solution having an initial pH of approximately 7.6. When the pH of the synthetic concentrate dropped to approximately 6.6 (nearly equilibrium pH) due to the precipitation of calcium carbonate in the reactor, the induction time test was stopped.

The synthetic concentrate was then filtered through a 0.1 µm filter to retain those crystals that were not settled in the reactor but were in suspension in the synthetic concentrate. The retained crystals were returned to the reactor. Following that, an induction time test with a new synthetic concentrate solution with antiscalant was performed in the reactor containing crystals to see if antiscalant could prevent the formation of calcium carbonate when the supersaturated synthetic concentrate was in contact with freshly produced seed crystals of calcium carbonate.

2.2.3 RO performance indicators

The performance of the RO is monitored by the permeability K_W (L/m^2/h/bar), defined as follows:

$$K_w = \frac{Q_P}{NDP \times A_M} \times \frac{1}{TCF_t} \quad \textit{(2.1)}$$

With permeate flow Q_p (L/h), net driving pressure NDP (bar), membrane area A_M (m^2), and temperature correction factor TCF_t. The temperature correction factor is calculated from the feedwater temperature T (°C) as follows:

$$TCF = e^{2700 \times \left(\frac{1}{298} - \frac{1}{273+T}\right)} \quad \textit{(2.2)}$$

and, the net driving pressure is given by:

$$NDP = P_f - \frac{\Delta P_{fc}}{2} - P_p - \pi_{fc} + \pi_p \quad \textit{(2.3)}$$

With feed pressure P_f (bar), feed-concentrate pressure drop ΔP_{fc} (bar), permeate pressure P_p (bar), feed-concentrate osmotic pressure π_{fc} (bar), and permeate osmotic pressure π_p (bar).

The control algorithm used the temperature corrected NDP as input, given by:

$$NDP_T = NDP \times TCF \quad \textit{(2.4)}$$

The equations 1–4 are obtained from the membrane manufacturer (Hydranautics) and the ASTM standard practice for standardizing RO performance data (Designation: D4516–00).

2.2.4 Lab-scale RO measurements

The once-through lab-scale RO tests were performed using the system depicted schematically in Figure 2.3, which included a SEPA cell (Sterlitech Corporation, USA) and an OSMO Titan unit (Convergence Industry B.V., the Netherlands). For each experiment, a new membrane sheet (effective area 140 cm^2) was harvested from a

brackish water RO element of Hydranautics (ESPA2-LD-4040) and placed in the SEPA cell. The lab-scale RO unit was operated at constant pressure and was equipped with a highly sensitive flow meter to measure the permeate flow produced from a small membrane sheet. Membrane permeability (Eq. 2.1) was used (instead of NDP) to monitor the occurrence of scaling.

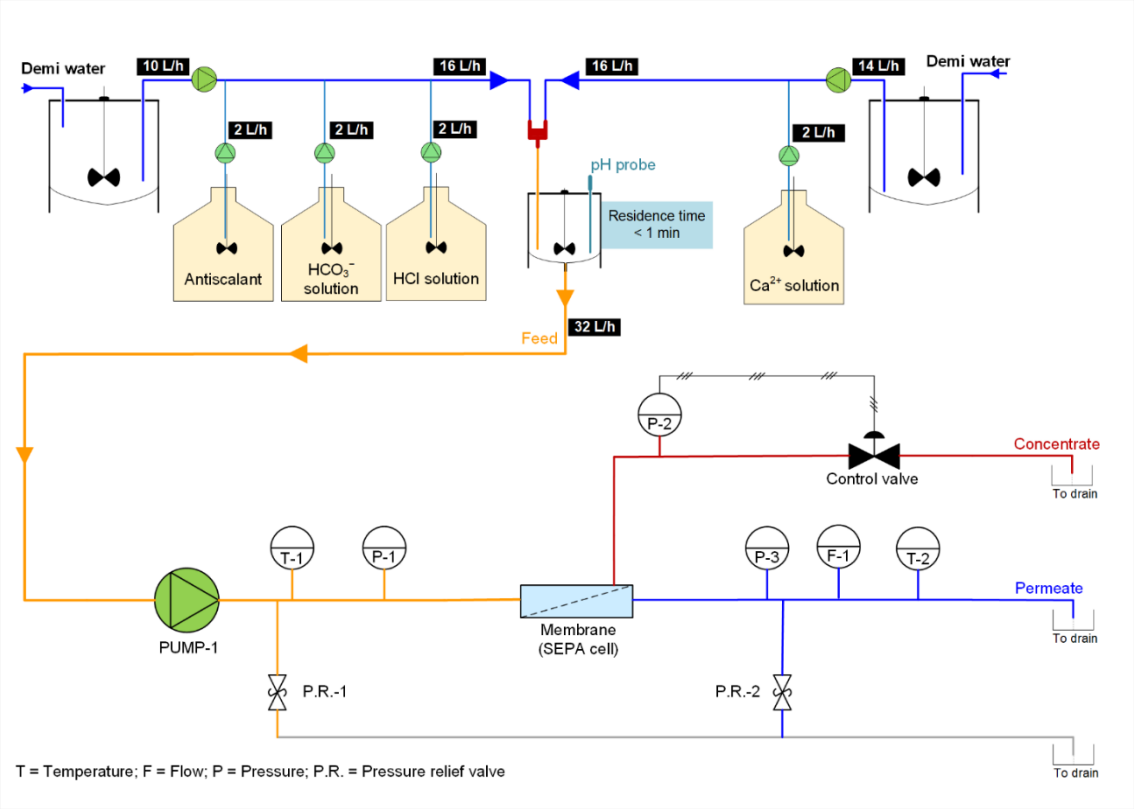

Figure 2.3 *Once-through lab-scale RO setup*

The lab-scale RO tests were executed with the synthetic concentrate solutions of 85% recovery with antiscalant concentrations of 1.3 mg/L, 13.3 mg/L, and 33.3 mg/L which correspond to feedwater antiscalant doses of 0.2 mg/L, 2.0 mg/L, and 5.0 mg/L, respectively. The synthetic concentrate solutions were prepared by continuously dosing salts (e.g., Ca^{2+}, HCO_3^-, etc.) into the demi-water feed stream at room temperature (20–23 °C). For tests that did not require the use of antiscalant, milli-Q water was dosed instead. The synthetic concentrate solution was first introduced to another reactor (before being fed to the SEPA cell), where it was stirred at 150 rpm for less than 1 minute. The residence time of less than 1 min was obtained by keeping the flow rates entering and leaving the reactor at 32 L/h and by maintaining the synthetic concentrate volume in the reactor to approximately 0.5 L. In all tests, the cross-flow velocity and recovery were approximately 0.10–0.12 m/s and 0.5–0.7%, respectively. After the experiment, the membrane sheets were examined using scanning electron microscopy (SEM) (JEOL, JSM-6010LA).

2.2.5 Pilot-scale RO measurements

In this study, two pilot-scale RO units (Figure 2.4) were used that were equipped with antiscalant dosing pumps fitted with the control algorithm, and could be operated with manual dosing or with automatically adapted dosing. An antiscalant manufacturer's projection program was used to understand the scaling potential of the RO concentrates for both RO pilot units and to obtain the recommended antiscalant type and doses to prevent scaling.

Figure 2.4a shows the schematic of the pilot RO located in Brabrand (Denmark) which treats aerobic groundwater (GW) with quality parameters given in Table 2.1. It is a single-stage RO unit with 3 pressure vessels in series where each pressure vessel is loaded with two FilmTec^{TM} brackish water RO elements (BW30-4040). The single-stage RO pilot unit was operated with constant permeate production in recirculation mode to achieve a recovery of 80%. During the tests, the RO feed flow (combined with the recirculated concentrated flow) was 2.0 m^3/h, and the permeate production was to 1.2 m^3/h. The concentrate discharge was 0.3 m^3/h, and 0.5 m^3/h concentrate was recirculated the feed. The used antiscalant was a phosphonate antiscalant. The RO unit was operated without and with a range of antiscalant doses.

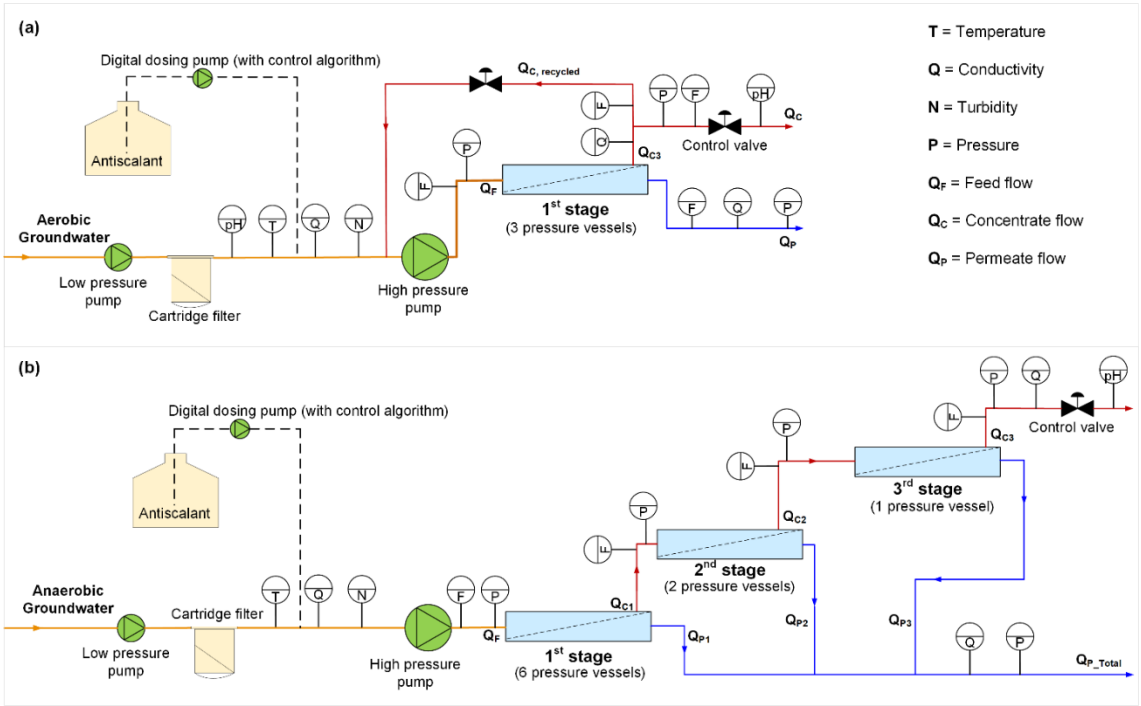

Figure 2.4 *Schematic diagram of the RO pilot unit (a) located in Brabrand, Denmark, and (b) located in Kamerik, the Netherlands*

Figure 2.4b shows a schematic representation of the pilot RO unit, located in Kamerik (the Netherlands), which treats anaerobic groundwater, with quality parameters shown in

Table 2.1. The RO unit comprised six pressure vessels in the first stage, two in the second stage and one in the third stage, with three Hydranautics ESPA2-LD-4040 membrane elements in each pressure vessel. The RO unit was operated at 80% recovery with various doses of a phosphonate antiscalant.

As both pilot units were operated at constant permeate production (flux) and the permeate flow of the entire stage was measured, the temperature corrected NDP (Eq. 2.4) of the last stage (rather than average permeability) was recorded to monitor the occurrence of scaling. In RO plants that are equipped with an external scale guard (monitoring) unit (van de Lisdonk et al., 2000) or could measure the permeate flow of the last element of the last stage, it is recommended to use permeability of that last element (or external scale guard unit) to monitor the occurrence of scaling and for the feedback control of the algorithm.

Table 2.1 *Feedwater compositions of the RO units in Brabrand (Denmark) and Kamerik (Netherlands)*

Cations	**Concentration (mg/L)**		**Anions**	**Concentration (mg/L)**	
	Aerobic GW (Denmark)	Anaerobic GW (Netherlands)		Aerobic GW (Denmark)	Anaerobic GW (Netherlands)
Calcium	155	115	Sulphate	80	43.4
Magnesium	9.5	17.4	Chloride	56	113.6
Sodium	50.6	55.2	Fluoride	< 0.1	0.1
Potassium	1.7	5.6	Bicarbonate	412	400
Barium	0.1	0.1	Carbonate	-	-
Strontium	0.4	0.5	Nitrate	7.6	0.2
Iron	0.2	8.5[△]	Silica	20	16.7
Ammonium	-	3.7	Orthophosphate	0	2.1
Other properties of the feed water:					
pH	7.2	7.1	TDS[*] (mg/L)	793	750–800
Temperature (°C)	12	12	DOC[*] (mg/L)	-	8.6
Turbidity (NTU)	< 0.1	< 0.1			

[*]TDS = Total dissolved solids; DOC = Dissolved organic carbon; [△]Iron in the anaerobic groundwater is in the ferrous state.

2.3 RESULTS AND DISCUSSION

2.3.1 Effect of an overdose of antiscalant on calcium carbonate scaling and RO operation

The objective of this section is to investigate the consequences of overdose as well as underdose of antiscalant on membrane scaling and RO operation and to illustrate why RO plants need to be operated with their optimum antiscalant dose.

Figure 2.5a presents the measured induction times of the synthetic RO concentrates (LSI 2.2) with the feedwater antiscalant doses of 0.2 mg/L, 2.0 mg/L and 5.0 mg/L. As can be seen, with both 2.0 mg/L and 5.0 mg/L antiscalant doses, the measured induction times were longer than 120 h, which suggested that the aforementioned doses of the antiscalants were able to delay the precipitation of calcium carbonate substantially. On the other hand, with 0.2 mg/L antiscalant dose, the measured induction time was shorter than 15 min and thus this dose was not sufficient to delay the precipitation of calcium carbonate and would most likely be unable to prevent the occurrence of calcium carbonate scaling in RO.

Figure 2.5b shows the permeability of the lab-scale RO unit when fed with the synthetic concentrate in the presence of feedwater antiscalant concentrations of 0.2 mg/L, 2.0 mg/L and 5.0 mg/L. As can be seen, the permeability decreased rapidly due to calcium carbonate scaling when the antiscalant dose was 0.2 mg/L. This result is in line with the one of Figure 2.5a where it was demonstrated that an antiscalant dose of 0.2 mg/L was not sufficient to hinder the formation of calcium carbonate substantially. On the other hand, the permeability of the membrane remained constant with an antiscalant dose of 2.0 mg/L which suggested that the mentioned antiscalant dose was able to prevent calcium carbonate scaling. This finding was expected when considering Figure 2.5a, where it was shown that the antiscalant dose of 2.0 mg/L was able to hinder the precipitation of calcium carbonate to a period longer than 120 h, thus minimizing the risk of scaling in RO. Unexpectedly, the permeability of the membrane decreased sharply with an antiscalant dose of 5.0 mg/L, and the drop was even greater than with a 0.2 mg/L antiscalant dose. As the induction time with the 5.0 mg/L antiscalant dose was greater than 120 h (similar to the dose of 2.0 mg/L), it was expected that the membrane permeability would remain constant. This suggested that calcium carbonate was not responsible for the permeability decline when the antiscalant dose was increased to 5.0 mg/L.

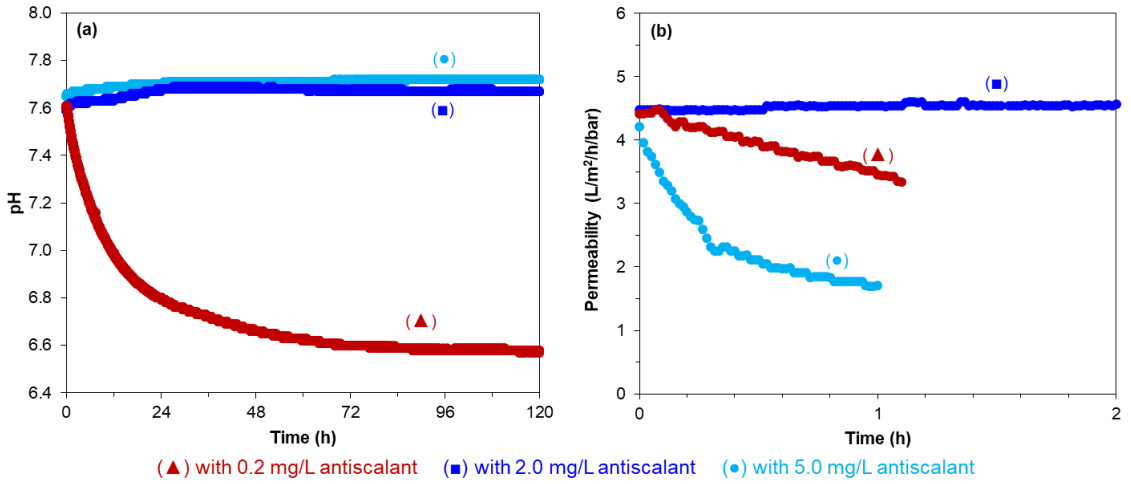

Figure 2.5 *(a) Induction time measurements (in glass reactor) with the synthetic RO concentrate with feedwater antiscalant doses of 0.2 mg/L, 2.0 mg/L, and 5.0 mg/L, and (b) Membrane permeability obtained from once-through lab-scale RO measurements with the synthetic RO concentrate with 0.2 mg/L, 2.0 mg/L, and 5.0 mg/L of antiscalant doses*

Figure 2.6 illustrates the SEM images of the fouled/scaled membranes with antiscalant doses of 0.2 mg/L and 5.0 mg/L, as well as the SEM image of a virgin (new) membrane. As can be seen in Figure 2.6a, the membrane surface was covered with cubical crystals when the antiscalant dose was 0.2 mg/L. The cubical crystals were identified as calcite, a form of calcium carbonate, in the X-ray powder diffraction (XRD) analysis. On the other hand, the membrane surface was covered by an amorphous compound when the antiscalant dose was 5.0 mg/L as shown in the SEM image in Figure 2.6b. This indicated that calcium carbonate was not responsible for the permeability decline at the high antiscalant dose of 5.0 mg/L. Figure 2.6c shows the SEM image of a new (clean) membrane to better visualize the presence of foulant in Figure 2.6b. The amorphous precipitates were sent to TZW DVGW-Technologiezentrum Wasser (Germany) for further examination with anion-exchange chromatography coupled to electrospray-ionization time-of-flight mass spectrometry (ESI-TOF) and inductively coupled plasma mass spectrometry (ICP-MS). The details on ESI-TOF and ICP-MS techniques have been published by other researchers elsewhere (Armbruster et al., 2019, Armbruster et al., 2020). The analysis revealed that the amorphous compound was calcium phosphonate. This showed that the high dose (5.0 mg/L) of phosphonate antiscalant in the presence of high concentration of calcium (765 mg/L) may lead to the formation of amorphous deposits of calcium-phosphonate. Therefore, the overdose of antiscalant may prevent calcium carbonate scaling in the RO process, but meanwhile may lead to the permeability decline due to the precipitation of a calcium-antiscalant compound.

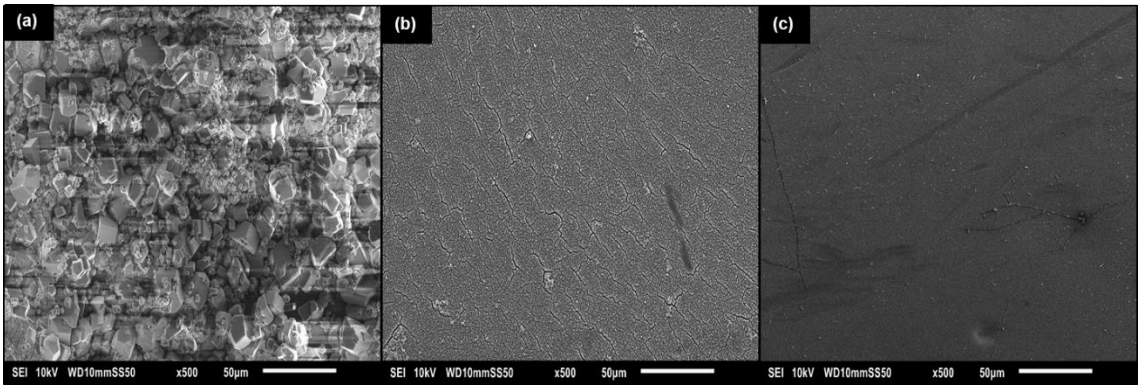

Figure 2.6 *SEM images of the (a) membrane with decreased permeability with 0.2 mg/L antiscalant dose, (b) membrane with decreased permeability with 5.0 mg/L antiscalant dose, and (c) new (virgin) membrane*

In RO processes, the adverse effect of a high dose of antiscalant is more pronounced at high recoveries (than at low recoveries) as the calcium concentration in the RO concentrate increases. Therefore, at high recoveries where the tendency of calcium carbonate scaling increases, the determination of the antiscalant dose as well as the selection of the type of antiscalant should be done carefully. This study briefly demonstrated the adverse effect of overdosing a commercial phosphonate antiscalant (which is one of the widely used antiscalants to control calcium carbonate scaling) in RO processes to show that optimizing antiscalant dose is not needed just because of environmental concerns and reducing additional costs, but also that higher doses may negatively affect the RO performance. It is essential to have information on the antiscalant concentrations at which the adverse effect of antiscalant is occurring. To answer when and under what conditions an antiscalant (e.g., phosphonate antiscalant) and calcium can precipitate on the membrane surface, both the solubility as well as the precipitation kinetics of the calcium antiscalant/phosphonate compound are required. It should be noted that the determination of the solubility of calcium and phosphonate antiscalant was not within the scope of this study, nor was an investigation of different types of antiscalants (e.g., polycarboxylates, etc.) to see if they showed a similar negative effect as was observed with the phosphonate antiscalant. However, it is recommended that this effect be further researched in a lab-scale/pilot installation to prevent precipitation of calcium–antiscalant amorphous deposits on RO membranes.

In brief, as both overdose and underdose of antiscalant are problematic, it is essential to operate RO plants as close as possible to their optimum antiscalant dose to minimize both the risk of scaling/fouling and the additional costs.

In this study, various terms for antiscalant doses are used, including overdose, optimum dose, underdose, and safe dose. Overdoes are defined as doses that prevent scaling but cause permeability decline due to the precipitation of a calcium-antiscalant compound.

The optimum dose is the lowest antiscalant dose that can prevent scaling. Underdose is defined as a dose that is less than the optimum dose and cannot prevent scaling. Safe antiscalant doses are those that fall between the overdose and the optimum dose, avoiding scaling without causing the calcium-antiscalant compound to develop.

2.3.2 Step changes in antiscalant dosing (Proof of principle of the dosing algorithm)

In this section, the effect of step-changes in antiscalant dosing is evaluated to investigate if once scaling occurs due to under-dosing, further accumulation of scaling can be stopped by increasing the antiscalant dose. This was evaluated with induction time measurements, lab-scale RO tests, and pilot-scale RO experiments.

2.3.2.1 Induction time measurements

Figures 7a and 7b show the induction times of synthetic RO concentrate solutions (LSI 2, Ca^{2+} = 675 mg/L, HCO_3^- = 2350 mg/L) in the absence of calcium carbonate crystals without and with 2.0 mg/L antiscalant, respectively. When antiscalant was not present, the pH of the synthetic RO concentrate started to decrease in approximately 15 min due to the formation of calcium carbonate crystals, while with 2.0 mg/L antiscalant dose, a decrease in pH was not observed within a 1-week period. This result showed that the feedwater dose of 2.0 mg/L of the phosphonate antiscalant could increase the induction time of the synthetic RO concentrate from 15 min to at least 1 week and thus could hinder the formation of calcium carbonate substantially when there were no seed crystals added to or in the reactor during the induction time test. Now the question was whether the antiscalant can hamper the formation/precipitation of calcium carbonate in the case when there are freshly formed seed crystals present in the synthetic concentrate solution (or in the glass reactor). To answer that, an induction time test was performed initially without antiscalant and when the pH started to decrease due to the formation of calcium carbonate crystals, antiscalant (with an equivalent feedwater dose of 2.0 mg/L) was added to the solution (Figure 2.7c).

As can be seen in Figure 2.7c, pH began to decline in the absence of antiscalant (similar to Figure 2.7a), but when 2.0 mg/L antiscalant was added after a 0.1 unit drop in pH, the subsequent decrease in pH stopped and thereafter, was constant for a duration longer than 1 week. This result showed that the antiscalant was able to prevent further formation and growth of calcium carbonate crystals in a highly supersaturated solution.

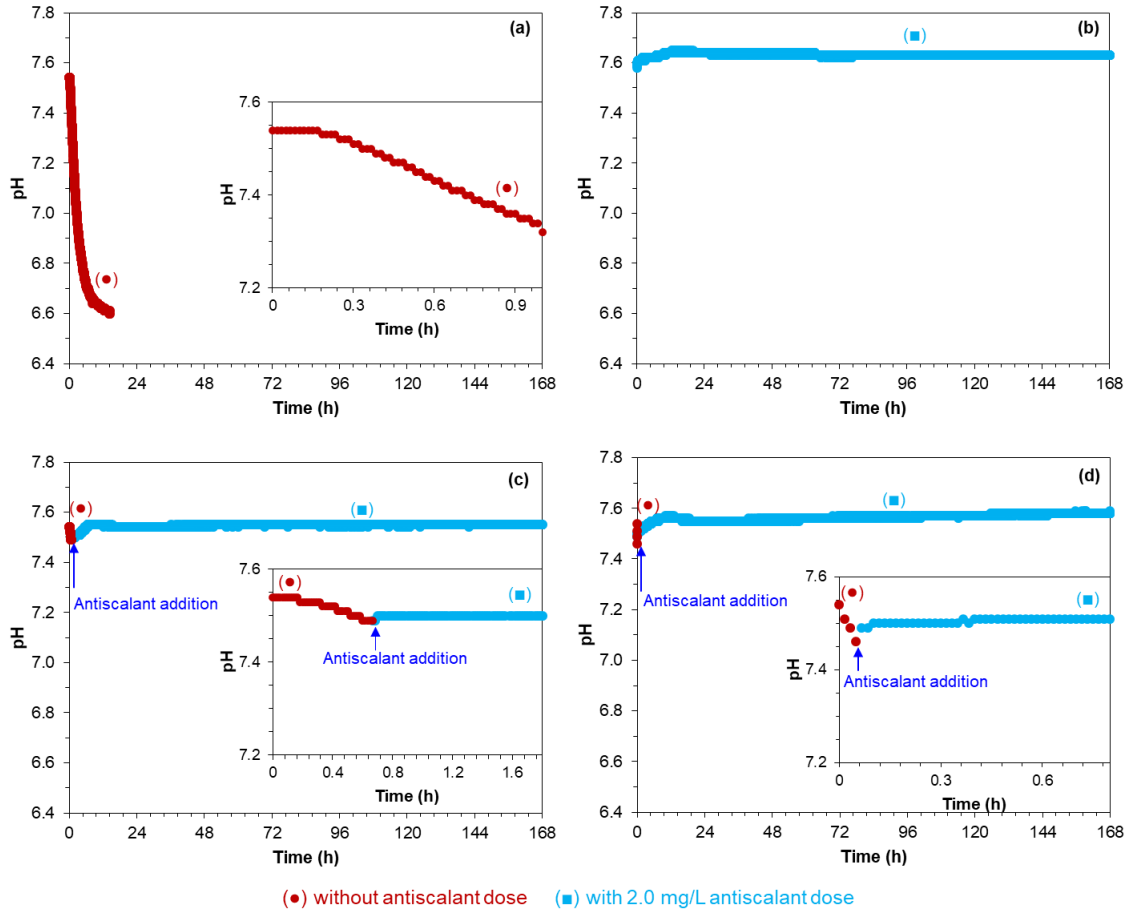

Figure 2.7 *Induction time measurements (in glass reactor) with the synthetic RO concentrate (a) without antiscalant and calcium carbonate crystals, (b) with 2.0 mg/L antiscalant dose in the absence of calcium carbonate crystals, (c) without and with 2.0 mg/L antiscalant dose in the absence of calcium carbonate crystals, and (d) without and with 2.0 mg/L antiscalant dose in the presence of calcium carbonate crystals*

Figure 2.7d presents the induction time of the synthetic RO concentrate (without and with 2.0 mg/L of antiscalant) where (fresh) calcium carbonate crystals were already present in the glass reactor prior to the addition of antiscalant. The freshly formed calcium carbonate crystals (in the glass reactor) were obtained from the induction time experiment with the synthetic RO concentrate in the absence of antiscalant shown in Figure 2.7a. In the presence of calcium carbonate crystals, pH decreased immediately as can be seen from Figure 2.7d which suggested that the induction time was very short and the growth phase started directly. With the addition of antiscalant after a 0.1 unit drop in pH, the further decrease in pH stopped, which indicated that the phosphonate antiscalant was able to prevent further crystallization of calcium carbonate in a supersaturated solution.

In brief, from Figures 2.7c and 2.7d, one can observe that in the case when scaling occurs in an RO system due to an underdose of antiscalant, further scaling can be stopped when a safe (or an optimum) dose of antiscalant is implemented.

2.3.2.2 Lab-scale RO measurements

Figure 2.8 shows the permeability of the RO membrane when fed with the synthetic RO concentrate (LSI 2.2) and with a feedwater antiscalant dose of 2.0 mg/L and 0.2 mg/L. As can be seen, the permeability remained constant with 2.0 mg/L dose, while it decreased when the dose was lowered to 0.2 mg/L. When the dose was increased back to 2.0 mg/L after a drop of approximately 27% in permeability, further decrease in the permeability stopped. This result clearly showed that a safe dose of phosphonate antiscalant can prevent further scaling in RO in the case when membrane elements are previously scaled due to an antiscalant underdose.

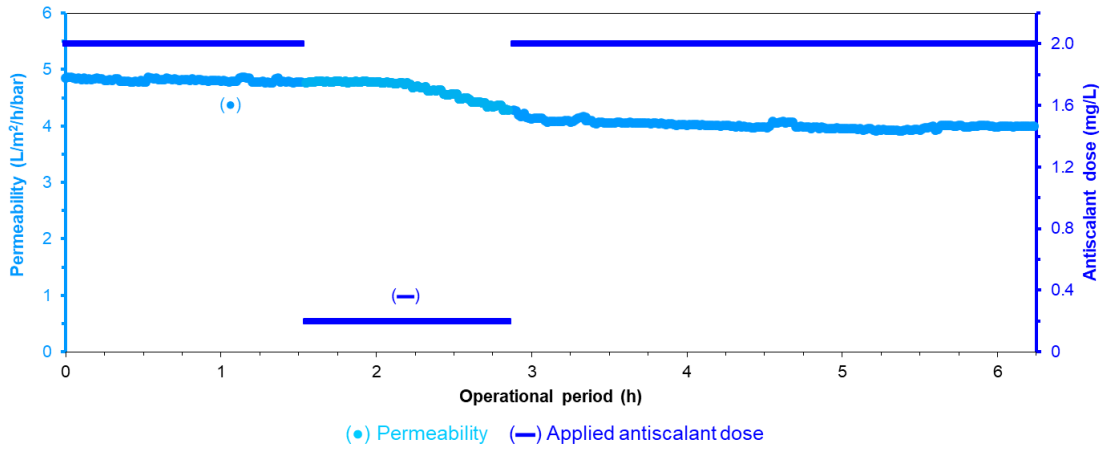

Figure 2.8 *Membrane permeability obtained from once-through lab-scale RO measurements with the synthetic RO concentrate (LSI 2.2) with feedwater antiscalant doses of 0.2 and 2.0 mg/L*

2.3.2.3 RO pilot measurements

Figure 2.9a illustrates the scaling potential of RO concentrate at 80% recovery which was determined with the projection program of an antiscalant supplier. According to the projection program, both calcium carbonate and barium sulphate had the tendency to scale the RO unit in the absence of antiscalant, while with the addition of antiscalant, precipitation of the abovementioned compounds was not expected. It is worth mentioning that the actual saturation level of the scaling compounds would remain the same in the presence and absence of antiscalants. In the presence of antiscalant, the crystallization of the scaling compounds is hampered, preventing them from precipitating in the RO unit.

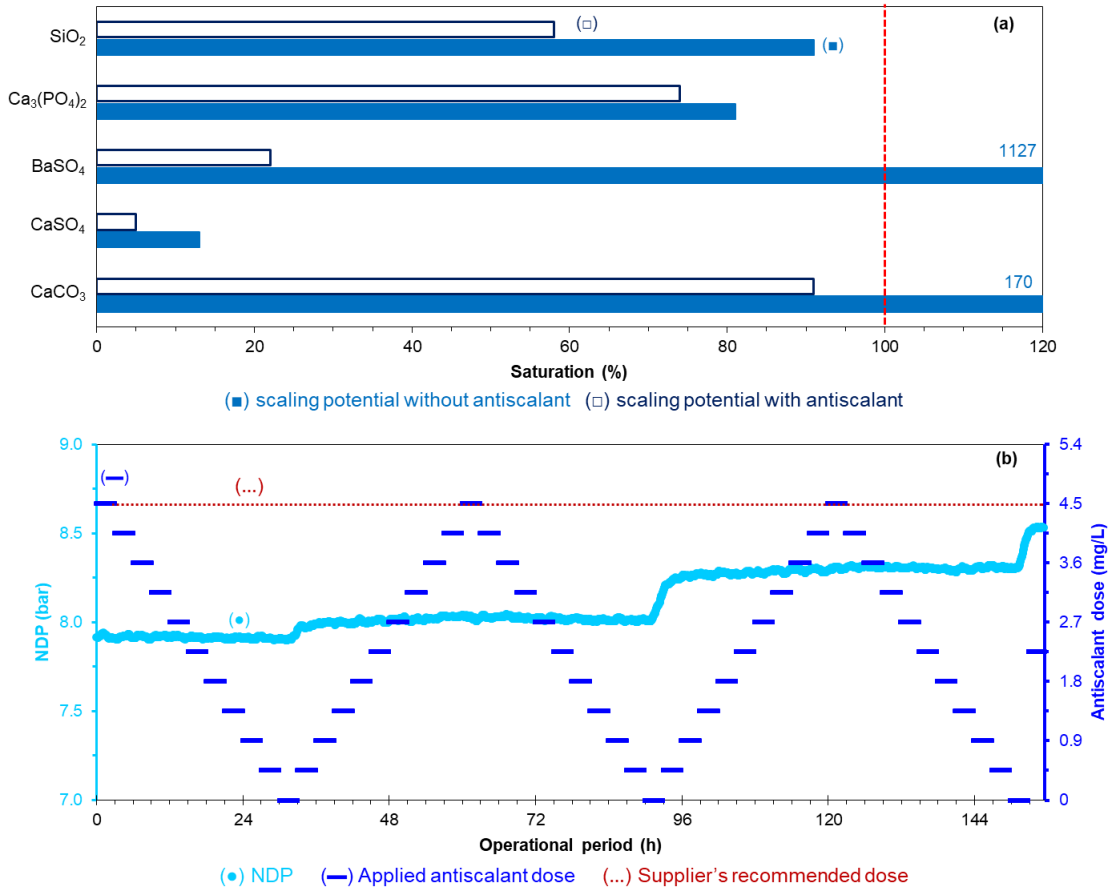

Figure 2.9 *(a) Scaling potential (according to the projection program of the antiscalant manufacturer) of the RO concentrate at 80% recovery in the absence and presence of antiscalant for the RO unit in Brabrand (Denmark), and (b) Operation of the RO pilot unit in Brabrand at 80% recovery with various doses of antiscalant*

This inhibitory effect of antiscalant is portrayed in the projection program as if antiscalant lowers the saturation level of the scaling compound (Figure 2.9a), which is not the case. The antiscalant projection programs provide a lower saturation level in the presence of antiscalant to qualitatively indicate that the given compound may not precipitate when antiscalant is added. As the barium concentration in the RO feed is very low (ca. 0.1 mg/L) and due to the very slow precipitation kinetics of barium sulphate reported by Boerlage et al. (2000), we consider that calcium carbonate is the main compound which will scale the RO unit in the absence of antiscalant. To prevent scaling in the RO unit in Brabrand, Denmark, the recommended dose given by the projection program was 4.5 mg/L.

Figure 2.9b presents the NDP when the RO pilot unit was operated at 80% recovery with various doses (including the supplier's recommended dose) of antiscalant and without the addition of antiscalant. As can be seen, no increase in NDP was observed when the antiscalant dose was lowered (in steps of 0.45 mg/L) from the supplier's dose of 4.5 mg/L

to 0.45 mg/L, which suggested that the supplier's recommended dose was far greater than the actual (optimum) dose required to control scaling.

When the dose was decreased to 0 mg/L, scaling started immediately which can be concluded from the NDP increase (during the operational periods 30–33h, 90–93 h, and 150–153 h) in Figure 2.9b. The sharp increase in NDP ceased each time when the antiscalant dose was increased from 0 mg/L to a higher dose. This result clearly demonstrated that when scaling occurs (due to under-dosing of antiscalant), further scaling can be prevented if the antiscalant dose is increased to the safe (or optimum) level.

2.3.3 Application of the dosing pump algorithm

In the previous section, it was demonstrated that the accumulation of scale due to under-dosing of antiscalant can be stopped by increasing the antiscalant dose to the optimum level. This satisfies the basic criterion for the dosing algorithm to be used in RO processes to determine the optimum antiscalant dose necessary to control scaling. The objective of this section is to evaluate the dosing algorithm in two different RO pilot plants in Kamerik (Netherlands) and in Brabrand (Denmark) to determine the optimum antiscalant dose at various recoveries.

2.3.3.1 Application of the algorithm to the RO plant in the Netherlands

Figure 2.10a depicts the scaling potential of the RO concentrate in the absence and presence of antiscalant for the Kamerik RO unit at 80% recovery. According to the projection program, calcium carbonate and barium sulphate were the compounds that could cause scaling in the RO unit in the absence of antiscalants, while in the presence of antiscalant, scaling was not expected. We consider calcium carbonate as the main compound causing scaling in the RO unit due to the slow precipitation kinetics of barium sulphate as described earlier (Boerlage et al., 2000). According to projection programs of the various suppliers, the proposed antiscalant was a phosphonate antiscalant, and the recommended dose was 2.0 mg/L.

In Figure 2.10b, the NDP of the last stage at 80% recovery with various doses of the phosphonate antiscalant is shown. The initial dose used in the algorithm was the supplier's recommended dose (2.0 mg/L). The algorithm was programmed to decrease the dose in 9 steps of 0.2 mg/L after each 12 h of operation. It was assumed that the optimal dose for the RO unit at 80% recovery was in the range of 0.2–2.0 mg/L. As can be seen, no increase in NDP was observed at all doses between 2.0 mg/L and 0.2 mg/L. It is possible that the optimal antiscalant dose for the RO unit at 80% recovery is between 0 and 0.2 mg/L. However, at this point, the algorithm was not programmed to implement doses below 0.2 mg/L. To summarize, Figure 2.10b showed that the supplier's recommended dose of 2.0 mg/L was considerably higher than the minimum dose required

to prevent scaling, and that by using the dosing algorithm, the antiscalant dose was reduced by approximately 90% for the RO pilot unit at 80% recovery.

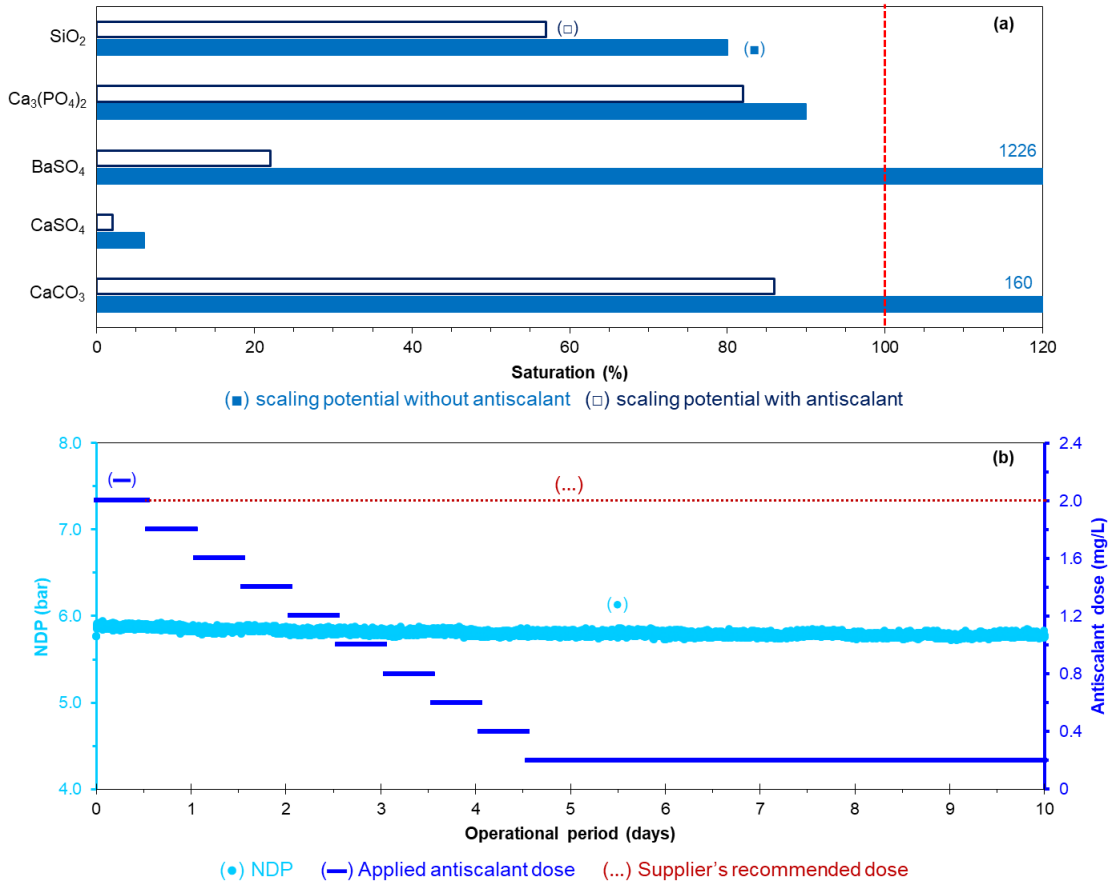

Figure 2.10 *(a) Scaling potential (according to the projection program of the antiscalant manufacturer) of the RO concentrate at 80% recovery in the absence and presence of antiscalant for the RO unit in Kamerik (Netherlands), and (b) Operation of the RO pilot unit in Kamerik at 80% recovery with the dosing algorithm to identify the optimal antiscalant dose*

It is worth mentioning that at recoveries above 80%, the determination of the optimal antiscalant dose with the algorithm was not possible, since (amorphous) calcium phosphate was the precipitating compound at those recoveries (Mangal et al., 2022). In our previous work Mangal et al. (2021b) have demonstrated that antiscalants are not effective in preventing amorphous calcium phosphate scaling.

2.3.3.2 Application of the algorithm to the RO plant in Denmark

In Figure 2.11a, the long-term operation of the RO unit (in Denmark) at 80% recovery with various doses of the antiscalant is illustrated. The algorithm was programmed to start

with an antiscalant dose of 6.0 mg/L and then reduce the dose by 0.5 mg/L every 24 h until it reached a minimum dose of 0.6 mg/L.

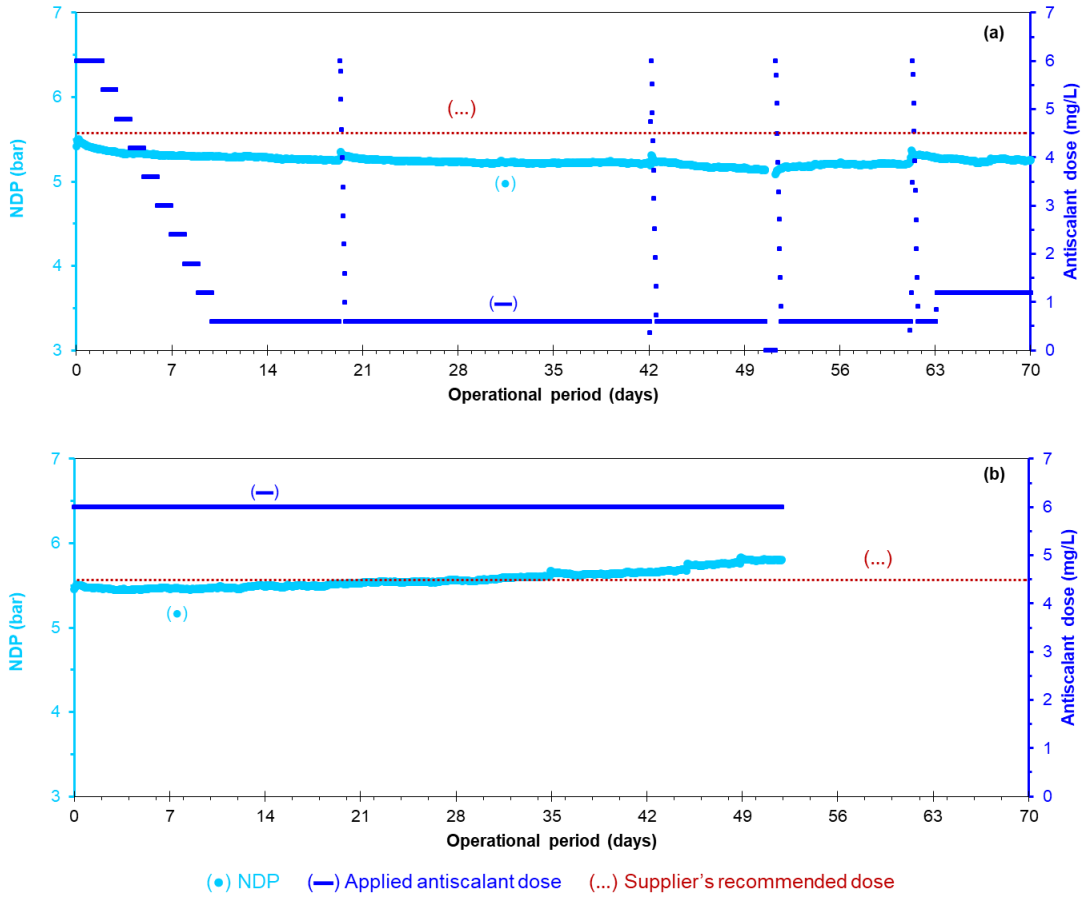

Figure 2.11 *(a) Long-term operation of the RO pilot unit in Brabrand at 80% recovery with the dosing algorithm to identify the optimal antiscalant dose, and (b) Long-term operation of the RO pilot unit in Brabrand at 80% recovery at constant antiscalant dose of 6.0 mg/L without the dosing algorithm*

As can be seen from Figure 2.11a, no increase in NDP was observed when the algorithm lowered the antiscalant dose from the initial dose of 6.0 mg/L to 0.6 mg/L. It should be noted that the algorithm was given a minimum (lower limit) dose of 0.6 mg/L, so the actual optimal dose could be even lower. The RO unit operated for 54 days with the 0.6 mg/L dose which was sufficient to prevent calcium carbonate scaling. In Figure 2.11a, one can see that at some points (e.g., between day 19 and 20, between day 42 and 43, and so on), the antiscalant dose jumped to 6.0 mg/L which was because of the disturbances in the RO operation. Nonetheless, the dose decreased back to 0.6 mg/L. The antiscalant dose was increased from 0.6 mg/L to 1.2 mg/L by the algorithm between days 63 and 70. This was again because of the disturbances in the RO operation which led to some short period

of NDP increase. As a result, the antiscalant dose was increased by the algorithm. The antiscalant dose will remain at 1.2 mg/L, according to the current algorithm's decision tree (Figure 2.1).

Figure 2.11a clearly shows that the NDP did not increase when the antiscalant dose was 1.2 mg/L, suggesting that the dose could be reduced to 0.6 mg/L. This means that operator intervention is needed when the algorithm increases the antiscalant dose. A warning message should appear on the human machine interface (HMI) indicating that the antiscalant dose has been increased. This prompts the operator to examine the RO performance (NDP) data and determine whether the algorithm's increase in antiscalant dose was caused by scaling or by disturbances in the RO operation. In the latter case, the operator has the option of adjusting the antiscalant dose and/or restarting the algorithm. Furthermore, if the NDP does not increase even with the lowest antiscalant dose given to the algorithm, an operator may restart the algorithm with smaller antiscalant reduction steps and a new minimum dose (lower limit) for the algorithm to determine the optimum antiscalant dose. For example, because no increase in NDP was observed at the lowest given dose of 0.6 mg/L in Figure 2.11a, the operator may re-run the algorithm with antiscalant reduction steps of 0.1 mg/L or 0.2 mg/L, with the starting dose (upper limit) set at 1.2 mg/L and the minimum dose (lower limit) fixed at 0.2 mg/L.

Nonetheless, Figure 2.11a clearly demonstrated that the supplier's recommended antiscalant dose (4.5 mg/L) was significantly higher than the actual optimum dose required for long-term calcium carbonate scaling control in the RO unit. Furthermore, the algorithm was capable of decreasing the antiscalant dose when the NDP remained constant at higher doses, as well as increasing the dose when an increase in NDP was detected. To summarize, the dosing algorithm has the potential to identify optimal doses and minimize antiscalant consumption in RO processes. In this study, the algorithm was applied where calcium carbonate was the precipitating compound. However, it is worth mentioning that the dosing algorithm should be able to identify the optimum dose of antiscalant for any scaling compound (e.g., calcium carbonate, calcium sulphate, silica, etc.) as long as the following two conditions are met: i) antiscalant is effective in preventing the precipitation of the scaling compound, and ii) the accumulation of scale due to under-dosing of antiscalant can be stopped by increasing the antiscalant dose to the optimum (safe) level.

Figure 2.11b illustrates the long-term operation of the RO unit with a constant antiscalant dose of 6.0 mg/L (1.5 mg/L higher than the supplier's recommended dose) in the absence of the dosing algorithm. As can be seen, the NDP increased at a constant antiscalant dose of 6.0 mg/L, which could not be due to calcium carbonate scaling because the NDP remained constant with the 0.6 mg/L antiscalant dose in Figure 2.11a. The calcium and antiscalant concentrations in the real RO concentrate of the RO unit in Denmark were 775 mg/L and 30 mg/L, respectively, which were comparable to the concentrations of calcium

(765 mg/L) and antiscalant (33 mg/L) present in the synthetic concentrate of the lab scale RO unit in Figure 2.5b (where permeability decreased sharply due to overdosing). This suggested that calcium-antiscalant compound, i.e., calcium phosphonate could be responsible for the increase in NDP in Figure 2.11b. However, the adverse effect of antiscalant overdosing in the RO pilot unit (Figure 2.11b) did not appear to be as severe as in the lab-scale RO unit (Figure 2.5b). This could be due to a number of factors, including: i) the lab-scale RO measurements were carried out at room temperature (22 °C), whereas the feedwater (groundwater) temperature in Figure 2.11b was 12 °C. As a result, the calcium-phosphonate compound in the lab-scale RO tests (Figure 2.5b) had a higher saturation level (and faster precipitation kinetics) than the RO pilot tests (Figure 2.11b), and ii) the increase in NDP of the lab-scale RO unit (if operated at constant permeate production (flux)) is more pronounced for a given decrease in membrane permeability than that of the pilot unit, because the lab-scale RO unit had only a single membrane sheet (total area = 0.014 m^2), whereas the pilot RO unit had 6 membrane elements in series (total area = 43.2 m^2). To summarize, the results of Figure 2.11b also indicated that an antiscalant overdose could be detrimental to RO operation, and establishing an optimum dose is important to prevent fouling due to overdosing of antiscalants in RO systems.

2.4 CONCLUSIONS

In this study, we investigated the proof of principle, the validity and the application of a control algorithm that defines a real-time optimal set-point of antiscalant dosing to minimize antiscalant consumption in RO processes. In addition, the effect of underdose and overdose of antiscalant, i.e., phosphonate antiscalant on membrane scaling and RO operation was demonstrated. We combined pilot-scale RO operation, lab-scale RO operation and controlled precipitation (induction time) experiments.

The major findings of this study can be summarized as follows:

- Underdose and overdose of phosphonate antiscalants can both be detrimental to the operation of RO systems, when trying to prevent calcium carbonate scaling.
    - Underdose of antiscalant results in RO flux decline due to the occurrence of (calcium carbonate) scaling on RO membranes
    - Overdose of antiscalant can lead to membrane fouling due to the precipitation of (amorphous) calcium-antiscalant deposits on RO membranes
- In the case of scaling caused by the control algorithm's underdose of antiscalant, further scaling can be stopped when the algorithm increases the antiscalant dose back to a safe (or the optimum) dose.

  - Using induction time measurements, it was demonstrated that the decrease in pH caused by the formation of calcium carbonate at underdose (or zero dose) ceased when a safe dose was implemented.
  - With lab-scale as well as pilot-scale RO measurements, it was shown that permeability decline (increasing NDP) caused by an underdose of antiscalant stopped when the dose was increased to a safe (or the optimum) dose.
- The dosing pump algorithm is a useful tool that considers the variation in RO feedwater quality and identifies real-time optimum antiscalant doses necessary to prevent scaling for a given recovery in RO.
  - For the RO pilot plant in the Netherlands, the supplier's recommended antiscalant dose at 80% recovery was 2.0 mg/L, while the dosing pump algorithm lowered the dose to 0.2 mg/L without any increase in NDP and thus resulted in a 90% reduction in antiscalant consumption.
  - For the RO pilot plant in Denmark, the supplier's recommended antiscalant dose was 4.5 mg/L, whereas the algorithm reduced the dose to 0.6 mg/L, which resulted in a stable NDP for over two months period and nearly 87% reduction in antiscalant consumption.

3

ROLE OF PHOSPHATE AND HUMIC SUBSTANCES IN CONTROLLING CALCIUM CARBONATE SCALING IN A GROUNDWATER REVERSE OSMOSIS SYSTEM

This chapter is based on the following publication:

M.N. Mangal, S.G. Salinas-Rodriguez, B. Blankert, V.A. Yangali-Quintanilla, J.C. Schippers, W.G.J. van der Meer, M.D. Kennedy, Role of phosphate and humic substances in controlling calcium carbonate scaling in a groundwater reverse osmosis system, Journal of Environmental Chemical Engineering, 9 (2021) 105651. https://doi.org/10.1016/j.jece.2021.105651

Abstract

The role of phosphate and humic substances (HS) in preventing calcium carbonate scaling and their impact on antiscalant dose was investigated for a reverse osmosis (RO) system treating anaerobic groundwater (GW) (containing 2.1 mg/L orthophosphate and 6–8 mg/L HS). Experiments were conducted with the RO unit (treating anaerobic GW), and with a once-through lab-scale RO system (operating with artificial feedwater). Additionally, (batch) induction time (IT) measurements were performed with, *i)* real RO concentrate, and *ii)* artificial RO concentrates in the presence and absence of phosphate and HS. It was found that at 80% recovery (Langelier saturation index (LSI) 1.7), calcium carbonate scaling did not occur in the RO unit when the antiscalant dose was lowered from 2.2 mg/L (supplier's recommended dose) to 0 mg/L. The IT of the real RO concentrate, without antiscalant, was longer than 168 h, while, at the same supersaturation level, the IT of the artificial concentrate was approximately 1 h. The IT of the artificial concentrate increased to 168 h with the addition of 10 mg/L of phosphate, humic acid (HA), and fulvic acid (FA). Furthermore, in the lab-scale RO tests, the normalized permeability (K_w) of the membrane decreased by 20% in 2-h period when fed with artificial concentrate of 80% recovery containing no phosphate, whereas, with phosphate, no decrease in K_w was observed in 10-h period. These results indicate that phosphate and HS present in the GW prevented calcium carbonate scaling in the RO unit and reduced the use of commercial (synthetic) antiscalants.

3.1 INTRODUCTION

In the Netherlands, over 60 % of the produced drinking water by Dutch water supply companies is obtained from the treatment of GW (Hiemstra et al., 2003, de Vet et al., 2009). Although, in general, the quality of GW is already very good, it is often desirable to remove a wide range of components, such as salinity, specific ions, organic micropollutants (OMPs), colour, all of which can be obtained by RO. For this reason, several of the Dutch water supply companies have embraced (or are exploring) the use of RO technology for producing drinking water of impeccable quality.

In RO applications, the recovery (ratio of the permeate water to the feed water) strongly affects the economic and operational performance due to the total energy consumption per unit volume of product water, concentrate volume, and the scale of the pretreatment. When treating seawater, the osmotic pressure limits the recovery of the system. Conversely, in brackish water RO (BWRO), it is usually economically favourable to increase the recovery. However, membrane scaling is the main obstacle in operating BWRO systems at high recovery rates. The consequences of scaling are increase in feed channel pressure drop, increase salt passage, higher feed pressure requirement resulting

in higher operational costs and shorter lifetime of membranes caused due to frequent cleanings (Kucera, 2010).

Scaling is the precipitation of poorly soluble species (e.g., calcium carbonate, calcium sulphate, barium sulphate, calcium phosphate, etc.), which become oversaturated as the retained salts are concentrated in the RO system. Thus, scaling in RO systems is related to the composition of feed water (e.g., concentration of inorganic compounds, pH, temperature etc.), as well as to the recovery of the RO (Antony et al., 2011).

In this study, we focus on calcium carbonate scaling, which is one of the most common type of scale encountered in RO systems (Antony et al., 2011). The formation of calcium carbonate in RO concentrate is directly related to the concentration of calcium and bicarbonate/carbonate and various other factors including but not limited to temperature and pH. The solubility of calcium carbonate in water decreases with an increase in temperature and pH. The scaling potential of calcium carbonate for a given water composition can be expressed by various indicators, such as the saturation ratio (S_r), the saturation index (SI), and the LSI. These indices only provide information about the saturation level. Whether calcium carbonate may or may not precipitate on the surface of the membrane depends not only on supersaturation, but also depends on the precipitation kinetics such as nucleation and growth rates. The mentioned indices do not provide information about the precipitation kinetics or the time required for precipitation to occur. To obtain information about reaction kinetics, growth tests and/or IT measurements are generally performed. In this study, we focused on IT measurements where IT is considered as the elapsed time between the development of the supersaturated conditions and the detection of crystallization (Söhnel and Mullin, 1988, Boerlage et al., 2000, Waly, 2011).

At supersaturated conditions, the precipitation of calcium carbonate in RO applications is controlled by the addition of antiscalants. Antiscalants allow much higher supersaturation without scale formation. The crystallization process of calcium carbonate and other scaling species (e.g. calcium sulphate, barium sulphate, etc.) is hindered in the presence of antiscalants, resulting in prolonged IT (Prisciandaro et al., 2006, El-Shall et al., 2002, Ahmed et al., 2008). Various types of antiscalants are available such as polyphosphates, phosphonates/organophosphates, polyacrylates and biobased, and their effectiveness is reported to depend on the functional groups of the molecules, their molecular weight, and charge density (Antony et al., 2011, Yu et al., 2020). Threshold inhibition is one of the main mechanisms of antiscalants by which the process of crystallization is hindered by the adsorption of antiscalants on the active sites of the first nucleating crystals. (Koutsoukos, 2010, Cooper et al., 1979). More specifically, when the crystal formation starts to occur at submicroscopic level, the negative groups of the antiscalant attach to the cationic sites of the scale nuclei which then disrupts the electronic balance that is required to encourage the growth of the crystals (Antony et al., 2011,

Darton, 2000, Koutsoukos, 2010). As a result, antiscalants not only delay the formation of calcium carbonate, i.e., prolonging the IT, but also decreases the crystal growth rate of calcium carbonate (Koutsoukos, 2010).

In applications other than RO, researchers have reported that the crystal growth rate of calcium carbonate is also reduced when a water solution contains some common inorganic ions, including but not limited to the magnesium ion (Berner, 1975, Bischoff, 1968, Chen et al., 2005), orthophosphate ion (Reddy, 1977, Giannimaras and Koutsoukos, 1987, Langerak et al., 1999), and sulphate ion (Nielsen et al., 2016) as well as when it contains dissolved organic substances such as HS (Hoch et al., 2000, Zuddas et al., 2003, Klepetsanis et al., 2002, Amjad et al., 1998, Inskeep and Bloom, 1986). It is, therefore, likely that when these substances are present in RO feed, they may have an inhibitory effect on calcium carbonate scaling and could result in the reduction of antiscalant dose. Operating the RO with the lowest antiscalant dose at which scaling does not occur is necessary, since high doses of antiscalant not only result in additional costs, but may pose environmental concerns. To the authors' knowledge, no study to date has examined the effects of aforementioned ions and HS on reducing the antiscalant dose to tackle calcium carbonate scaling in RO applications.

The objective of this study is to investigate the effect of inorganic ions, particularly phosphate, and HS on calcium carbonate scaling for an RO system treating anaerobic GW in the Netherlands. The results from an RO pilot, operating with anaerobic GW, a lab-scale RO system, operating with artificial feedwater, and controlled precipitation experiments are combined. By systematically varying the composition of the artificial feedwaters, different aspects of the complex anaerobic GW are isolated and investigated separately.

3.2 MATERIALS AND METHODS

3.2.1 Chemicals

In this study, to investigate the effects of inorganic ions (e.g., phosphate, magnesium and sulphate) and HS on the inhibition of calcium carbonate scaling in RO processes, experiments (e.g., IT measurements) were performed with both real RO concentrates and artificial RO concentrates. To identify the effect of the mentioned ions and HS individually on the precipitation of calcium carbonate, it was necessary to carry out experiments with the artificial RO concentrates, which was not possible with the real RO concentrate. The artificial solutions were prepared using Milli-Q water (Merck Millipore, conductivity < 10 µS/cm and TOC < 30 µg/L). The chemicals used include Na_2SO_4, $CaCl_2 \cdot 2H_2O$, KH_2PO4, and $MgCl_2 \cdot 6H_2O$ (Analytical Grade, Merck), $NaHCO_3$, NaOH, and $NaHSO_3$ (Analytical Grade, J.T. Baker), HA and FA (International Humic

Substances Society, (IHSS)). For pH adjustments, 0.2 M solutions of HCl (Analytical grade, ACROS Organics) or NaOH were employed. The artificial concentrate solutions are prepared such that the Ca^{2+} and HCO_3^- concentrations were equivalent to the concentrate concentration of real ground water (Table 3.1) treated at a certain recovery value. The antiscalant used in this study was OSM92 (Aquacare Europe) which is a phosphonate antiscalant.

3.2.2 GW composition

The anaerobic GW was abstracted from several wells of a drinking water production plant in Kamerik, Netherlands. Table 3.1 shows the composition of the anaerobic GW (RO feed) as determined by a commercial lab (Vitens Laboratorium, Netherlands). For the identification and quantification of HS, the dissolved organic carbon (DOC) was characterized with liquid chromatography–organic carbon detection (LC–OCD) (DOC-Labor, Germany).

Table 3.1 *Anaerobic GW composition (RO feed)*

Cations	**Concentration (mg/L)**	**Anions**	**Concentration (mg/L)**
Calcium	115.2 [100–120]◊	Sulphate	38.2 [20–44]
Magnesium	17.4 [16–18]	Chloride	79.4 [70–95]
Sodium	49.2 [40–60]	Fluoride	0.1 [0.1–0.14]
Potassium	5.6 [5–7]	Bicarbonate	391.8 [380–410]
Barium	0.1 [0.09–0.15]	Carbonate	-
Strontium	0.5 [0.5–0.6]	Nitrate	< 0.2
Iron (II)	8.5 [7.4–8.6]	Silica	16.7 [14.4–16.7]
Ammonium	3.7 [3.6–4.4]	Orthophosphate	2.1 [1.8–2.5]
Other properties of the feed water:			
pH	7.0–7.1	TDS* (mg/L)	750-800
Temperature (°C)	12	DOC (mg/L)	8.6 [8–8.8]
Turbidity (NTU)	< 0.1		

◊ Values in brackets [ ] represents the range of concentrations that could be present in the RO feed due to the various combination of wells, *TDS = Total dissolved solids

The assessment of the scaling potential of the RO concentrates at various recoveries was performed using the projection programs of antiscalant manufacturers. For the scaling tendency of calcium carbonate, the programs calculated LSI, where a positive LSI value for a solution implies that the solution is supersaturated in calcium carbonate and precipitation might occur, while a negative LSI value denotes that the solution is undersaturated and calcium carbonate will not precipitate. In addition, the projection programs also suggested a required antiscalant dose to prevent scaling. To determine the speciation of calcium and phosphate ions, Visual MINTEQ program (version 3.1) was

employed. Furthermore, the Visual MINTEQ program was also used to identify the complexation of calcium ions with HS.

3.2.3 Induction time measurements

A schematic diagram of the IT setup is illustrated in Figure 3.1. This setup was also used by Waly et al. (2012). An air-tight double wall 3 L Applikon glass reactor was used for the IT experiments. The Applikon reactor had an internal diameter of 12 cm and a height of 24 cm. The reactor included a mixing controller with mixing shaft that was used to adjust the stirring rate of the solution. The stirring rate could vary between 0 and 1250 rpm. A stirring rate of 150 rpm was used for the IT measurements (Waly et al., 2012, Waly, 2011). The top of the reactor was closed using a stainless-steel lid equipped with a thin rubber gasket to avoid the escape of CO_2 from the solution into the air and vice versa. In this study, IT experiments were performed by measuring the pH of the solution using a pH probe (Endress + Hauser) with an accuracy of ± 0.01 pH units. The probe was inserted in the reactor and the pH values were continuously recorded during the entire experiment. The interval for pH measurements was set to 1 min. IT was defined as the time when the solution pH decreased by 0.03 units from the initial value, due to calcium carbonate precipitation (Waly et al., 2010). It is worth mentioning that a part of the measured IT may also include (part of) the growth phase of calcium carbonate.

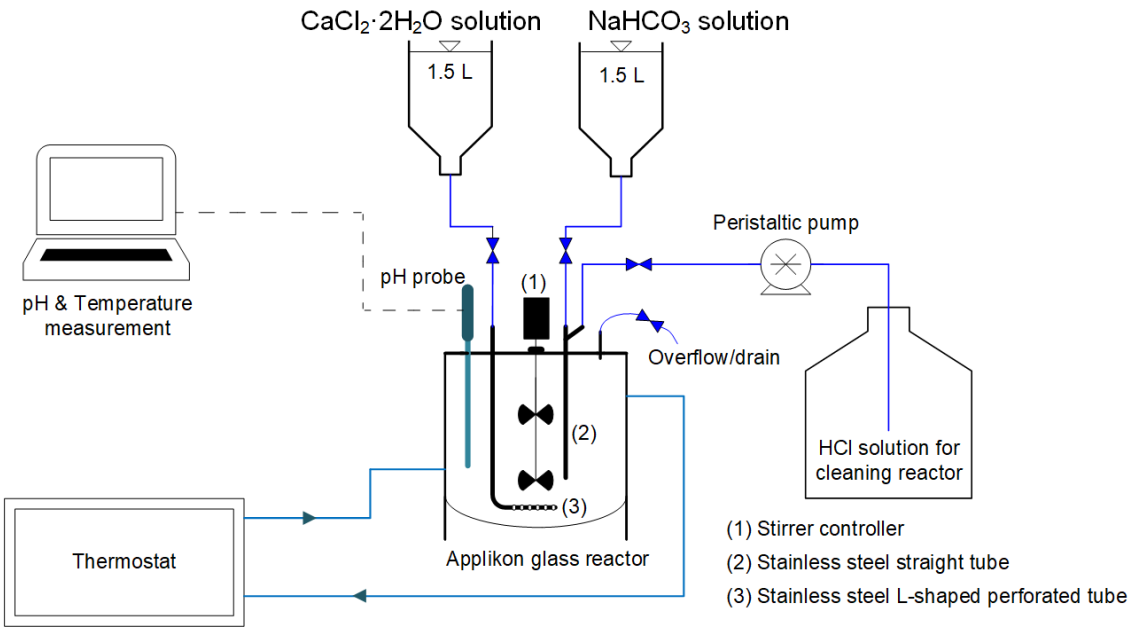

Figure 3.1 *Experimental setup for IT measurement*

At the end of each experiment, the reactor was filled with 0.1 M HCl to dissolve any crystals formed during the experiment. Acid cleaning was performed for 30 min and the stirring rate was set to 1250 rpm. After acid cleaning, the reactor was flushed twice with

demineralized water (demi-water) for 10 min. A thermostat was used to maintain a constant temperature of 20 °C during the experiments.

IT measurements were performed using both anaerobic real RO concentrates (Table 3.2) and artificial concentrate solutions (Table 3.3). It should be noted that the real RO concentrates (Table 3.2) include all the ions (substances) present in the anaerobic GW, but only the relevant ions to this study are listed in Table 3.2.

Table 3.2 *IT measurement with the anaerobic real RO concentrate of various recoveries without antiscalant*

Exp.	**Recovery** (%)	**pH**	**Ca^{2+}** (mg/L)	**HCO_3^-** (mg/L)	**DOC** (mg/L)	**PO_4^{3-}** (mg/L)	**Mg^{2+}** (mg/L)	**SO_4^{2-}** (mg/L)
A	70	7.2	384	1306	29	7.0	58	145
B	80	7.4	576	1959	42	10	87	217

Table 3.3 *IT measurement with the artificial concentrate solutions of various recoveries without antiscalant*

Exp.	**Recovery** (%)	**pH**	**Ca^{2+}** (mg/L)	**HCO_3^-** (mg/L)	**HA** (mg/L)	**FA** (mg/L)	**PO_4^{3-}** (mg/L)	**Mg^{2+}** (mg/L)	**SO_4^{2-}** (mg/L)
A	70	7.2	384	1306	-	-	-	-	-
B	80	7.4	576	1959	-	-	-	-	-
C	80	7.4	576	1959	-	-	-	87	-
D					-	-	-	-	217
E					-	-	10	-	-
F					-	-	5	-	-
G					-	-	2.5	-	-
H					-	10	-	-	-
I					-	5	-	-	-
J					10	-	-	-	-
K					5	-	-	-	-

It was crucial to keep the anaerobic RO concentrate anaerobic and eliminate the oxidation of Fe^{2+} while filling the reactor. For this, the 3 L reactor was filled (at approximately 10 L/min flow rate) with the anaerobic RO concentrate, in a bottom to top manner, from a tube equipped with fine nozzles located 3 cm from the bottom of the reactor. At the same time, the concentrate was drained from the overflow tube (Figure 3.1) located on the top of the reactor. After 30 min, the concentrate flow was stopped and the overflow tube of the reactor was closed. Thus, the reactor was completely filled with the anaerobic RO concentrate. In the case of the presence of some (trace) amount of dissolved oxygen that might have intruded during filling, $NaHSO_3$ (< 10 mg/L) was used to prevent Fe^{2+} oxidation, and then NaOH was used to correct the pH.

To run an IT experiment with the artificial concentrate, the 3 L reactor was initially half-filled with the $NaHCO_3$ solution and the pH was set at the desired value. Afterwards, the remaining half of the reactor was filled with the $CaCl_2 \cdot 2H_2O$ solution through the fine nozzles located 3 cm from the bottom of the reactor to maintain the uniform distribution of the solution. While adding the $CaCl_2 \cdot 2H_2O$ solution, the stirring rate inside the reactor was set to 150 rpm to allow uniform mixing of the solutions and avoid the formation of any local supersaturated zones.

3.2.4 RO pilot

The RO pilot plant is schematically represented in Figure 3.2. The RO consisted of three stages, with a variable number of parallel pressure vessels containing three 4 inch membrane elements (Hydranautics ESPA2-LD-4040) each. The anaerobic GW, after passing through a cartridge filter (10 µm), was directly fed to the RO unit and the unit was operated at constant permeate production. The normalized K_w (Eq. 3.1) and the normalized pressure drop (ΔP, Eq. 3.7) for the last element of the third stage (internal scale guard) were recorded separately. The equations used to normalize the RO operational data were obtained from the membrane manufacturer (Hydranautics). The purpose of including an internal scale guard in the last pressure vessel is to monitor the occurrence of scaling. The internal scale guard is the last element in the last stage of RO for which the permeate flow (thus K_w) and the ΔP across the element are measured. The permeate of the internal scale guard is collected separately from the permeate outlet (located on the concentrate side of the pressure vessel) and the permeate of the other membrane elements in the pressure vessel is collected from the permeate outlet which is located on the feed side as illustrated in Figure 3.2.

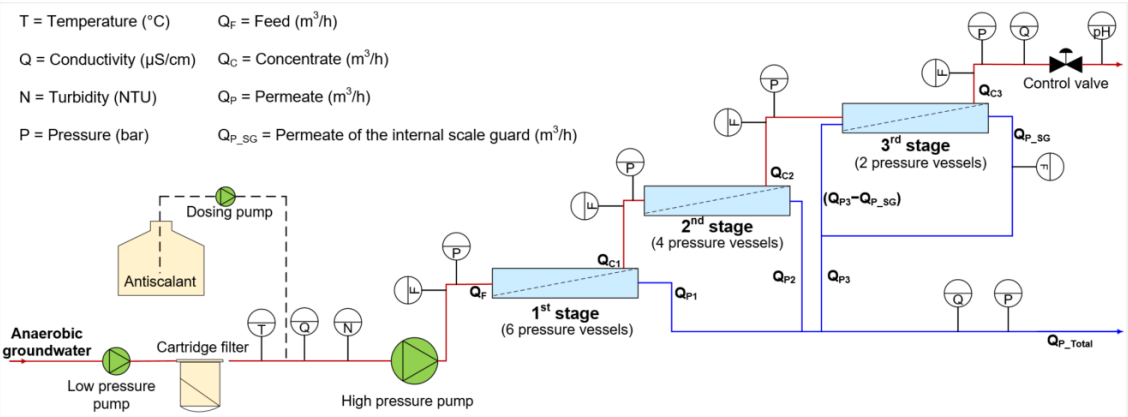

Figure 3.2 *Schematic diagram of the RO pilot*

$$K_w = \frac{Q_P}{NDP \times A_M} \times \frac{TCF_r}{TCF_t} \qquad \textit{(3.1)}$$

Where: Q_p = permeate flow (L/h); NDP = net driving pressure (bar); A_M = membrane area (m^2); TCF_r = temperature correction factor at reference conditions (25 °C) which is equal to 1; TCF_t = temperature correction factor at time t.

$$NDP = P_f - \frac{\Delta P_{fc}}{2} - P_p - \pi_{fc} + \pi_p \quad \textbf{(3.2)}$$

Where: P_f = feed pressure (bar); ΔP_{fc} = pressure drop (bar); P_p = permeate pressure (bar); π_{fc} = feed-concentrate osmotic pressure (bar); π_p = permeate osmotic pressure (bar).

$$\pi_{fc} = 0.002654 \times C_{fc} \times \frac{(T + 273)}{(1000 - \frac{C_{fc}}{1000})} \quad \textbf{(3.3)}$$

$$\pi_p = 0.002654 \times C_p \times \frac{(T + 273)}{(1000 - \frac{C_p}{1000})} \quad \textbf{(3.4)}$$

$$C_{fc} = \frac{C_f + C_c}{2} \quad \textbf{(3.5)}$$

Where: C_f = TDS of the feed (mg/L); C_c = TDS of the concentrate (mg/L); C_p = TDS of the permeate (mg/L); T = Temperature (°C)

$$TCF = e^{2700 \times \left(\frac{1}{298} - \frac{1}{273 + T}\right)} \quad \textbf{(3.6)}$$

In RO processes, it is essential to normalize the operational data (e.g., K_w, etc.) to account for the changes occurring in the RO feed. It can be misleading if the data is not normalized. For instance, if the temperature of the RO feed drops, the K_w will decrease suggesting that fouling/scaling is occurring which in reality may not be the case. To account for the temperature changes in the RO feed, temperature correction factor (Eq. 3.6) is given by the membrane manufactures. It is assumed that by normalizing the data (e.g., K_w) with the temperature correction factor, the effect of temperature change on the K_w is omitted completely. It is worth mentioning that the RO feed in this study is anaerobic GW which has more or less constant temperature, and therefore the effect of temperature change on the K_w is negligible.

$$\Delta P = \Delta P_t \times \left(\frac{Q_{fc,ref}}{Q_{fc,t}}\right)^m \times \left(\frac{\eta_{T,ref}}{\eta_{T,t}}\right)^n \quad \textbf{(3.7)}$$

Where: $Q_{fc,ref}$ = average reference feed/concentrate flow; $Q_{fc,act}$ = average feed/concentrate flow at time t; $\eta_{T,ref}$ = viscosity at reference temperature; $\eta_{T,act}$ = viscosity at actual temperature; m = 1.4; n = 0.34.

Table 3.4 *Operation of the RO pilot with various antiscalant doses and without antiscalant at 70 and 80 % recoveries*

Run	Recovery (%)	Recommended dose* (mg/L)	Initial dose (mg/L)	Final dose (mg/L)	Pressure vessel configuration△	Run period (days)
A	70	2.8	3.0	0.2	6-2-1	10
	80	2.2	2.2	0.2	6-2-1	16
B	80	2.2	0	0	3-2-1	32

*Recommended dose was the antiscalant dose determined by the projection program of the antiscalant manufacturer. △Pressure vessels with a 6-2-1 configuration had three membrane elements, whereas pressure vessels with a 3-2-1 configuration had six membrane elements.

The RO pilot was operated with various antiscalant doses and without dosing antiscalant as described in Table 3.4. In the first set of experiments, the RO unit was operated at 70 and 80 % recoveries initially with the antiscalant dose recommended by the projection programs of the antiscalant suppliers, and then the dose was lowered by 0.5 mg/L and/or 0.2 mg/L after each 12 h of RO operation to a final dose of 0.2 mg/L. In the second set of experiments, the RO unit was operated without antiscalant addition. The average operating flux of the last stage was in the 10–20 L/h/m^2/bar range for all experiments.

3.2.5 Lab-scale RO measurements

Lab-scale RO measurements were done with a system schematically represented in Figure 3.3. The setup comprised of a SEPA CF cell (140cm^2, Sterlitech Corporation, USA) and the OMSO Inspector unit (Convergence Industry B.V., Netherlands). Membrane sheets harvested from a Hydranautics ESPA2-LD-4040 element were used. A new membrane sheet was used for each experiment. In all experiments, the recovery was in the range of 0.5–0.7 % and the cross-flow velocity was approximately 0.12 m/s. Both permeate and concentrate were directed to the drainage. All experiments were carried out at room temperature (20–23 °C). When a drop in K_w was observed, scanning electron microscopy (SEM) (JEOL, JSM-6010LA) was used to examine the membrane sheets.

Several artificial feed solutions (Table 3.5) were used, that were realised by continuous dosing of additives (e.g., Ca^{2+}, HCO_3^-, PO_4^{3-}, etc.) to the feed stream of demi-water as illustrated in Figure 3.3a. If no chemical dosing was applied, Milli-Q water was dosed instead. The final solution (artificial concentrate solution) was introduced to a 5 L reactor in which the artificial concentrate solution was stirred at a rate of 150 rpm with a residence time shorter than 1 min. The residence time of less than 1 min was achieved by maintaining equal flow rates (32 L/h) of the artificial concentrate solution entering and leaving the 5 L reactor and by keeping the volume of the artificial concentrate solution in the reactor to approximately 0.5 L.

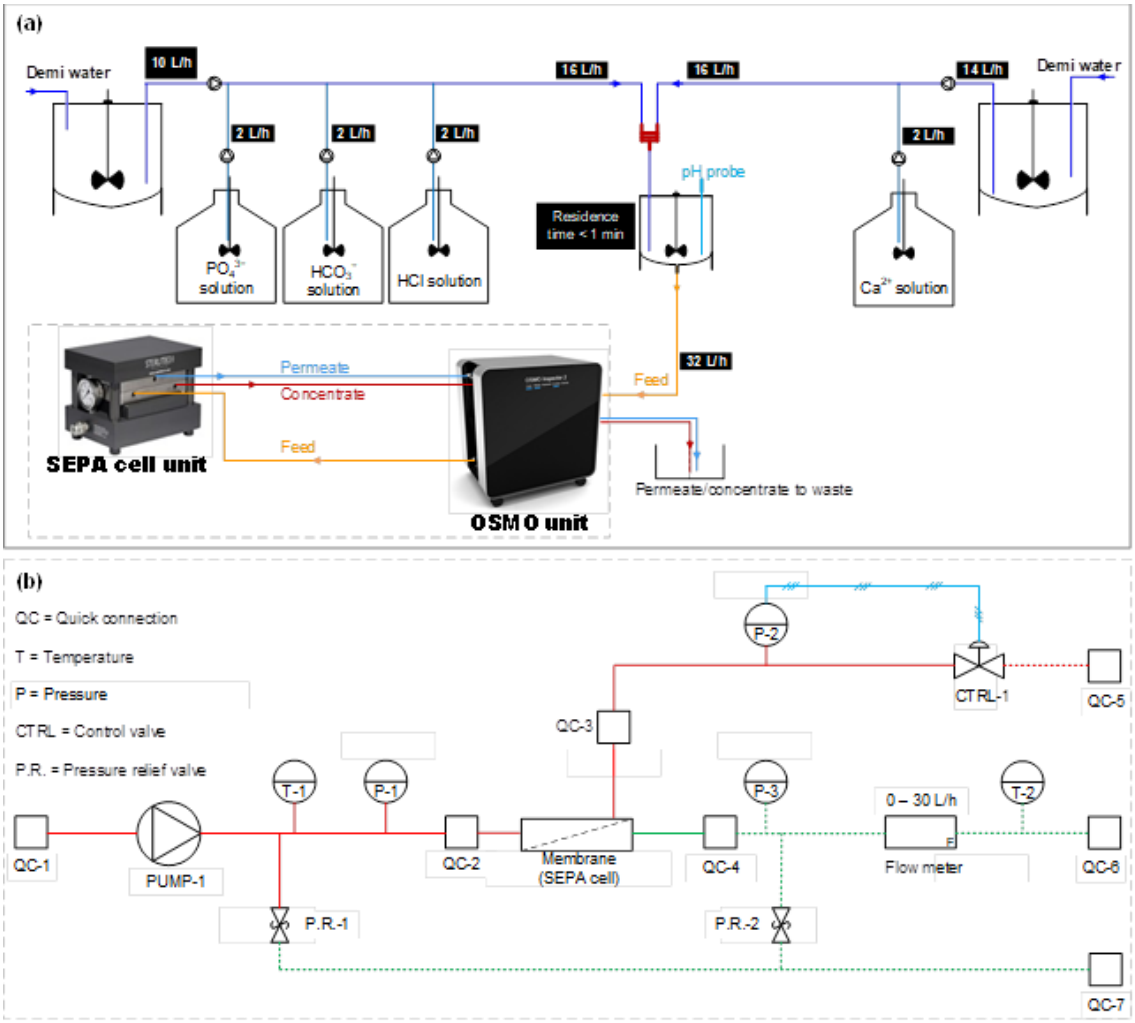

Figure 3.3 *(a) Once-through lab-scale RO setup, and (b) Piping and instrumentation diagram (P&ID) of the OSMO unit with SEPA cell*

In this study, the once-through lab-scale RO measurements with the HA and FA (IHSS) were not performed as those experiments were cost-wise not feasible.

Table 3.5 *Lab-scale RO measurements with the artificial concentrate of 80 % recovery without and with PO_4^{3-} ions*

Exp. #	Feed solution*	Equivalent recovery	Flow rate (L/h)	pH	Ca^{2+} (mg/L)	HCO_3^- (mg/L)	PO_4^{3-} (mg/L)
1	Artificial concentrate	80%	32	7.4	576	1959	0
2	Artificial concentrate	80%	32	7.4	576	1959	10

*Feed solution to the SEPA CF cell

3.3 RESULTS AND DISCUSSION

3.3.1 Scaling potential and the recommended antiscalant doses at 70 and 80 % recoveries

The scaling tendency, for several commonly encountered scaling compounds, of the anaerobic RO concentrate at recovery values of 70 % and 80 % with and without antiscalant addition is presented in Figure 3.4. The figure shows that both calcium carbonate and barium sulphate are supersaturated and may be expected to cause scaling in the absence of antiscalant. The LSI values were 1.2 and 1.7 for the real RO concentrates at 70 % and 80 % recovery, respectively. We expect that calcium carbonate will precipitate prior to barium sulphate. Boerlage et al. (2000) demonstrated that barium sulphate has very slow precipitation kinetics even at saturation levels as high as 4.5.

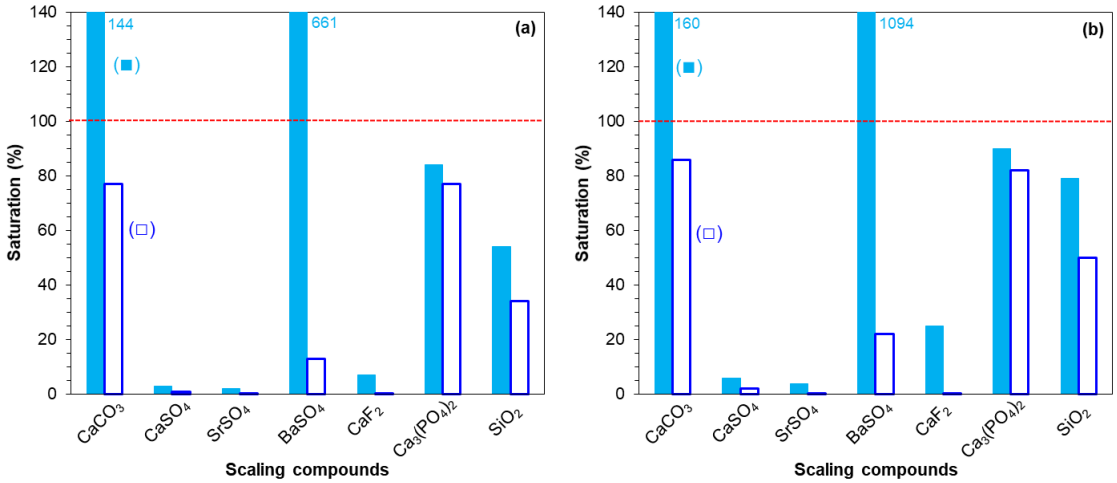

Figure 3.4 *Scaling potential of various scaling species with the projection program of an antiscalant manufacturer at (a) 70 % recovery (■) without antiscalant and (□) with antiscalant addition, and (b) 80 % recovery (■) without antiscalant and (□) with antiscalant addition*

Furthermore, Figure 3.4 shows that calcium carbonate and barium sulphate scaling may not occur in the presence of antiscalant. The projection software recommended a phosphonate antiscalant for controlling scaling at 70 and 80 % recoveries. It is worth mentioning that we have some concerns with the results from the projection software. Firstly, according to the projection program, the recommended antiscalant dose in the feed water was approximately 2.8 mg/L for the RO operation at 70 % recovery and a lower dose of about 2.2 mg/L for operation at a higher recovery of 80 %. We consider that the required dose must increase with the recovery, because the system operating at 80% contains, at some location, concentrate that is equivalent with 70% recovery and therefore requires at least a dose that is required for 70%. Secondly, by varying the feedwater composition, we noticed that the recommended dose (given by the projection programs) does not depend on phosphate, magnesium, sulphate or DOC concentration.

For instance, at 80 % recovery, the recommended dose by the projection program was 2.2 mg/L when the feed water contained 2.1 mg/L of phosphate and when phosphate was eliminated from the feedwater input of the projection program. However, precipitation studies suggest that these factors affect the precipitation of calcium carbonate (Reddy, 1977, Dove and Hochella, 1993, Giannimaras and Koutsoukos, 1987, Nielsen et al., 2016, Hoch et al., 2000, Zuddas et al., 2003, Klepetsanis et al., 2002, Amjad et al., 1998, Inskeep and Bloom, 1986).

3.3.2 Effect of antiscalant dose on RO pilot performance

The appropriate antiscalant dose was determined experimentally by operating the RO pilot with 70% and 80% recovery and varying antiscalant dose. The results are illustrated in Figure 3.5.

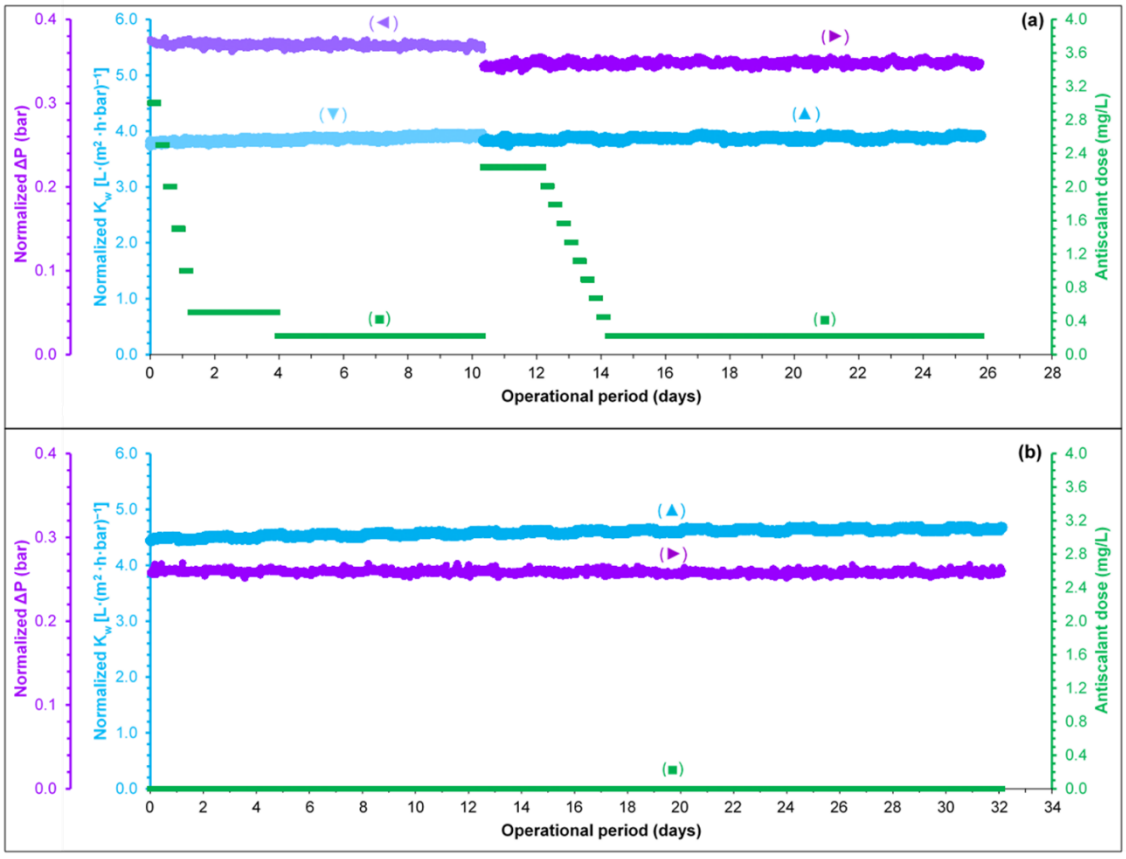

Figure 3.5 *(a) RO operation with a phosphonate antiscalant: (◄) Normalized ΔP at 70 % recovery, (►) Normalized ΔP at 80 %, (▼) Normalized K_w of the last element of the RO unit at 70 % recovery, (▲) Normalized K_w of the last element of the RO unit at 80 % recovery, (■) antiscalant dose, (b) RO operation at 80 % recovery without antiscalant addition: (►) Normalized ΔP, (▲) Normalized K_w of the last element of the RO unit, (■) antiscalant dose*

In Figure 3.5a, the normalized K_w and the normalized ΔP of the last element (the internal scale guard) are shown when the RO unit was operated at 70 and 80 % recoveries with various doses of a phosphonate antiscalant. As shown, the RO unit was operated for 10 days at 70 % recovery (LSI 1.2) with an initial dose of 3 mg/L (0.2 mg/L higher than the recommended dose) which was then lowered every 12 h to a final dose of 0.2 mg/L. During this period, the normalized ΔP remained constant and also no decrease in the normalized K_w was observed even when the antiscalant dose was as low as 0.2 mg/L. It could be that the antiscalant dose of 0.2 mg/L was sufficient to target calcium carbonate scaling or perhaps calcium carbonate scaling might not occur in 6–10 days of RO operation at 70 % recovery.

After 10 days of RO operation at 70 % recovery, the RO recovery was increased to 80 % (Figure 3.5a) where calcium carbonate was highly supersaturated (LSI 1.7). The starting antiscalant dose was 2.2 mg/L (equivalent to the supplier's recommended antiscalant dose) for the first day of the RO operation at 80 % recovery which was afterwards lowered by 0.2 mg/L after every 12 h of operation to a final dose of 0.2 mg/L. As can be seen, the normalized K_w remained constant and also no increase in the normalized ΔP was observed when the RO unit was operated for 12 days with an antiscalant dose as low as 0.2 mg/L.

The RO unit was operated at 80 % recovery without antiscalant addition (Figure 3.5b). As can be seen, both the normalized K_w and the normalized ΔP remained constant for an experimental period of 32 days at 80 % recovery which indicated that there was no need to add antiscalant even when the LSI of the RO concentrate was as high as 1.7. This suggested that calcium carbonate scaling might have been inhibited by some constituents (possibly phosphate and HS) present in the feedwater (anaerobic GW) that might have functioned as natural antiscalant.

3.3.2.1 Comparing anaerobic real RO concentrate and artificial concentrate

To understand why the RO pilot did not scale at high supersaturation levels, IT measurements were performed with the anaerobic real RO concentrate at 70 and 80 % recoveries in the absence of antiscalant (Exp. A and B, Table 3.2). In parallel, IT measurements were also executed using artificial concentrate solutions (Exp. A and B, Table 3.3).

In Figure 3.6, we show that the measured ITs of the real RO concentrate at 70 and 80 % recoveries were both longer than 168 h (7 days), while for the artificial concentrates corresponding to 70 and 80 % recoveries, the measured ITs were approximately 6 h and 1 h, respectively. Thus, at the same supersaturation level, the IT of the real RO concentrate at 80 % recovery was at least 168 times longer than that of the artificial concentrate. This result clearly shows that the formation of calcium carbonate was suppressed in the anaerobic real RO concentrate by some constituents present in the RO feedwater (anaerobic GW).

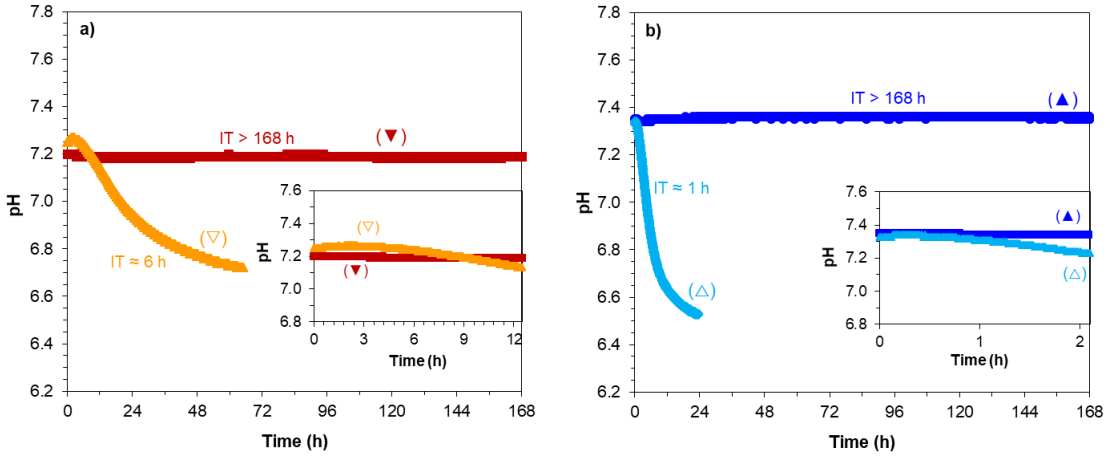

Figure 3.6 *(a) IT of the (▼) real RO concentrate at 70 % recovery without antiscalant, (▽) artificial concentrate at 70 % recovery without antiscalant, (b) IT of the (▲) real RO concentrate at 80 % recovery without antiscalant, (△) artificial concentrate at 80 % recovery without antiscalant*

3.3.3 Effects of phosphate and HS on the precipitation of calcium carbonate

In Table 3.6, the DOC characterization of the anaerobic GW with LC-OCD analysis is presented. The analysis revealed that from 8.62 mg/L of DOC in the GW, 5.26 mg/L (61.1 %) was represented by HS of FA type.

Table 3.6 *LC-OCD analysis of the anaerobic GW from Kamerik (Netherlands)*

DOC			Approximate molecular weight (g/mol)						
	HOC[1]	CDOC[2]	>> 20000	~ 1000			300-500	< *350*	< 350
			Biopolymers	HS			Building blocks	LMW[3] neutrals	LMW acids
					Aromaticity (SUVA-HS)	Molecular weight			
ppb-C[4]	**ppb-C**	**ppb-C**	**ppb-C**	**ppb-C**	**L/(mg·m)**	**(g/mol)**	**ppb-C**	**ppb-C**	**ppb-C**
% DOC	*% DOC*	*% DOC*	*% DOC*	*% DOC*	-	-	*% DOC*	*% DOC*	*% DOC*
8620	**1023**	**7597**	**46**	**5263**	**3.93**	**679**	**989**	**1252**	**48**
100 %	*11.9 %*	*88.1 %*	*0.5 %*	*61.1 %*	-	-	*11.5 %*	*14.5 %*	*0.6 %*

[1] HOC: hydrophobic organic carbon, [2] CDOC: chromatographic dissolved organic carbon

[3] LMW: low molecular weight, [4] ppb-C: parts per billion carbon

We consider that the difference between the ITs of the anaerobic RO concentrate and the artificial concentrate, demonstrated in the previous section, is caused by phosphate and/or HS present in the GW (Table 3.1, Table 3.6). We investigated this hypothesis by varying the composition of the artificial concentrate (Table 3.3), evaluating the effect of magnesium and sulphate (Figure 3.7a), phosphate (Figure 3.7b), FA (Figure 3.7c) and HA (Figure 3.7d) which is presented in the next section.

3.3.3.1 Induction time measurements

In this section, the effects of phosphate and HS on hindering calcium carbonate precipitation is presented with the IT measurements. Additionally, IT tests with some other ions such as Mg^{2+} and SO_4^{2-}, which are reported in literature to have a positive effect on the suppression of calcium carbonate, are also presented here to identify if those ions have played a role in the long IT of the real RO concentrate.

Fig. 7a compares the ITs of the artificial concentrate of 80% without the addition of Mg^{2+} and SO_4^{2-}, with the addition of Mg^{2+}, and with the addition of SO_4^{2-} (Exp. B, C, and D in Table 3.3). As can be seen, in the absence of mentioned ions, IT was approximately 1 h, whereas with 87 mg/L of Mg^{2+} and with 217 mg/L of SO_4^{2-}, IT increased to approximately 2 h and 1.2 h, respectively. This result is in agreement with the findings of Waly et al. (2012), where they reported that Mg^{2+} ions offer stronger inhibition for calcium carbonate than SO_4^{2-} ions. In addition, the results of Figure 3.7a are also in line with the observations of other researchers, such as Berner (1975), Bischoff (1968) and Chen et al. [16], that the formation of calcium carbonate is hindered in the presence of Mg^{2+} ions. However, it is clear from Figure 3.7a that neither Mg^{2+} nor SO_4^{2-} was accountable for the long IT (>168 h) of the real RO concentrate at 80 % recovery.

In Figure 3.7b, the measured ITs of the artificial concentrate of 80 % recovery in the presence of various concentrations of phosphate (Exp. E, F, and G in Table 3.3) are illustrated. We show that phosphate has a considerable effect on delaying calcium carbonate precipitation. In the presence of 10 mg/L of phosphate (which is equal to the concentration of phosphate in the real RO concentrate of 80 % recovery), IT of the artificial concentrate increased from 1 h to a period longer than 168 h which indicated that phosphate was one of the constituents of the feedwater which was responsible for the long IT (>168 h) of the real RO concentrate. When 5 mg/L of phosphate was added to the artificial concentrate solution, the measured IT was also longer than 168 h, which suggested that if the GW contained 1 mg/L of phosphate, it would still reduce the need of antiscalants to control calcium carbonate scaling at 80 % recovery. However, in the presence of 2.5 mg/L phosphate, the formation of calcium carbonate was not hindered substantially, as IT with the mentioned phosphate concentration increased to 4 h.

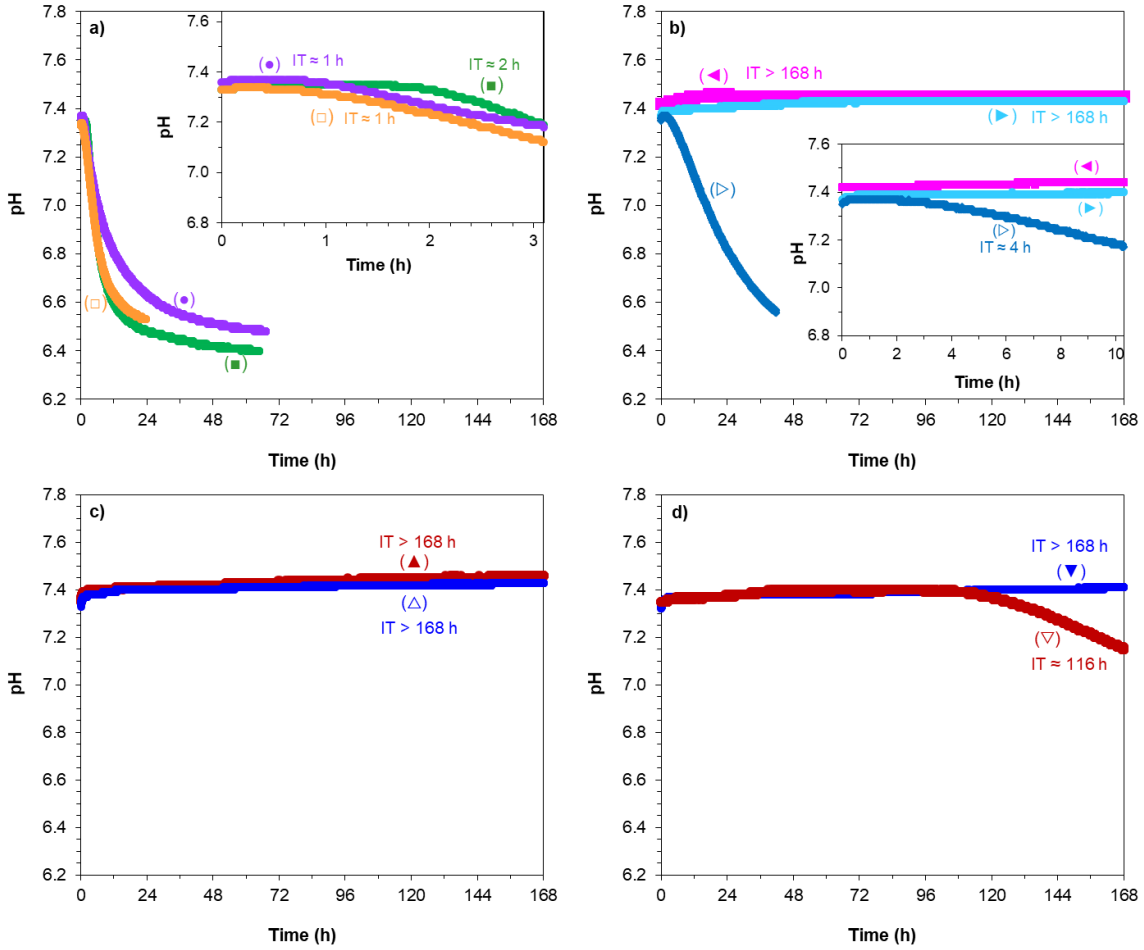

Figure 3.7 *(a) IT of artificial concentrate of 80 % recovery (□) in the absence of foreign substances, (●) with 217 mg/L sulphate, and (■) with 87 mg/L magnesium, (b) IT of the artificial concentrate of 80 % recovery (◄) with 10 mg/L phosphate, (►) with 5 mg/L phosphate, and (▷) with 2.5 mg/L phosphate, (c) IT of the artificial concentrate of 80 % recovery (▲) with 10 mg/L of IHSS FA, and (△) with 5 mg/L of IHSS FA, and (d) IT of the artificial concentrate of 80 % (▼) with 10 mg/L of IHSS HA and (▽) with 5 mg/L of IHSS HA*

It should be noted that the aforementioned phosphate concentrations are referred to the total dissolved phosphate which includes various species of phosphate such as HPO_4^{2-}, $H_2PO_4^-$, PO_4^{3-}, etc. In other words, when 10 mg/L of phosphate was added to the artificial concentrate solution of 80 % recovery, not all the mentioned concentration existed in the form of PO_4^{3-} ion. Actually, based on the speciation of phosphate which was carried out with the Visual MINTEQ, the PO_4^{3-} form was negligible in the artificial concentrate and the dominant specie was HPO_4^{2-}. Simkiss (1964), Griffin and Jurinak (1973), Reddy (1977), and Pytkowicz (1973) have demonstrated that phosphate adsorbs onto the calcium carbonate crystals and hinder their growth. Among the various forms of phosphate, PO_4^{3-} and HPO_4^{2-} are the adsorbing species that hinder the crystal growth of calcium carbonate

(Burton and Walter, 1990). This suggests that the long IT of the artificial concentrate in Figure 3.7b could be due to the adsorption of phosphate, i.e., HPO_4^{2-} on the newly formed calcium carbonate nuclei in the nucleation phase, consequently preventing the nuclei from growing further and initiating crystallisation.

In summary, the results of Figure 3.7b indicate that when phosphate is present in the feedwater in concentrations that can hinder calcium carbonate precipitation, the antiscalant dose to target calcium carbonate scaling can be reduced significantly, as demonstrated in Figure 3.5, where the antiscalant dose at 80 % recovery of the RO pilot (Kamerik, Netherlands) was lowered from the recommended dose of 2.2 mg/L to 0.2 mg/L and then to zero dose. It is worth mentioning that the presence of high concentrations of phosphate in the feed water should not be considered as a way to prevent calcium carbonate scaling and to reduce the dose of antiscalants, since they may lead to calcium phosphate scaling at high recovery rates when the solubility limits of calcium phosphate is exceeded. If, however, they are present in the RO concentrate at concentrations where they do not lead to calcium phosphate scaling, then their effect on the reduction of antiscalant dose and in determining the optimum dose of antiscalants should not be neglected.

The effect of HS was investigated by comparing the IT of the artificial concentrate of 80% with and without HA and FA (Exp. B, H, I, J and K in Table 3.3). Figure 3.7(c) presents the ITs of the artificial concentrate of 80 % recovery in the presence of FA. As shown, the effect of FA on prolonging the IT of calcium carbonate is also noticeable. In the presence of 5 mg/L and 10 mg/L FA, IT of the artificial concentrate of 80 % recovery increased from 1 h to a period longer than 168 h. Figure 3.7(d) illustrates the ITs of the artificial concentrate solution of 80 % recovery when HA was used. The IT values, when 5 and 10 mg/L HA were used, were approximately 116 h and longer than 168 h, respectively. These results suggested that the formation of calcium carbonate was also considerably hindered by HA. The results of Figure 3.7c–d are in agreement to the findings of Klepetsanis et al. (2002). In their study, they investigated the effects of HA and FA at concentrations in the 0.1–0.5 mg/L range on the IT of calcium carbonate. They reported that both HA and FA prolonged the IT of calcium carbonate. In their study, however, IT tests were performed for a maximum duration of approximately 3 h.

It is well established that Ca^{2+} ions interact with HS leading to the formation of calcium complexes with HS (Choppin and Shanbhag, 1981, Paxéus and Wedborg, 1991). Based on this, one may suggest that upon the formation of complexes, the concentration of free calcium in the artificial concentrate solution of 80 % recovery (in Figure 3.7c and Figure 3.7d) might have reduced, and as a consequence, the supersaturation was lowered, thus resulting in longer ITs. However, this mechanism seemed less likely to predominate, as the concentration of calcium was much higher than those of FA and HA. For instance, in Figure 3.7c and 7d, the concentration of calcium in the artificial concentrate of 80 %

recovery was approximately 576 mg/L, while the concentrations of FA and HA were each approximately 10 mg/L and that might have not substantially lowered the supersaturation levels. Various models exist that theoretically determine the binding of metal ions with HS. One of the models that is used by researchers is the NICA-Donnan model which is incorporated in the Visual MINTEQ program. With the NICA-Donnan model, it was found that 10 mg/L of each FA and HA would bind approximately 1.8 and 1.2 mg/L of Ca^{2+}, respectively. Therefore, the reduction in the concentrations of free Ca^{2+} ions due to HS was negligible. This indicated that the complexation of calcium with HS was not the main mechanism for delaying the precipitation of calcium carbonate. It should be noted that the concentrations of Ca^{2+} ions that might have been complexed with FA (Figure 3.7c) and HA (Figure 3.7d) could be different from those calculated by the NICA-Donnan model as the structure and chemistry of the HS may differ. The use of the NICA-Donnan model was to illustrate that 10 mg/L of each FA and HA would not complex a high concentration of Ca^{2+} ions.

Various researchers, such as Hoch et al. (2000), Klepetsanis et al. (2002), and Amjad et al. (1998) have studied the effect of HS on the crystal growth rate of calcium carbonate in seeded growth tests. They all reported that the adsorption of humic molecules on the active growth sites of calcium carbonate crystals (which, as a result, hamper further growth) is the dominant mechanism in retarding the crystal growth of calcium carbonate. This suggest that the long ITs in Figure 3.7c and Figure 3.7d were due to the adsorption of humic molecules on the newly formed nuclei in the nucleation phase which, as a result, did not allow the nuclei to further grow and to initiate crystallisation.

To summarize the effect of HS on calcium carbonate, one can propose that HS, particularly FA, present in the anaerobic GW in Kamerik (Netherlands) could also be one of the reasons for the long IT of the real RO concentrate at 70 and 80 % recoveries (Figure 3.6) and for preventing calcium carbonate scaling in the RO unit at 80 % recovery when no antiscalant was used (Figure 3.5b). The results indicated that when HS, which have the same inhibitory effect on calcium carbonate as the HA and FA of IHSS, are present in the RO feed, the required dose of antiscalants can be lowered substantially.

It should be taken into account that although the natural presence of HS in the RO feed may prevent calcium carbonate scaling at high recovery rates, it may foul the RO membranes since some researchers (Tanaka et al., 2016, Tang et al., 2007a, Tang et al., 2007b, Zhao et al., 2019) have reported that HS lead to the fouling of RO membranes. Therefore, the presence of HS in the RO feed should not be favoured as a way to control calcium carbonate scaling. It is, however, not known that if HS from every location can lead to the fouling of the RO membranes as their structure and chemistry may differ from one location to another. For instance, in Figure 3.5b, the normalized K_w of the last element of the RO unit did not decrease in 1-month period when the unit was operated at 80 % recovery (DOC concentration in the concentrate was approximately 42 mg/L) which

suggested that HS present in the GW was not causing fouling. Membrane fouling due to HS is a different topic and requires further research to answer if all HS can cause fouling of RO membranes, which fractions of HS lead to the fouling, at what concentrations and operational conditions and in the presence of what ions do they lead to the fouling of RO membranes, etc. Characterization of HS and to investigate their fouling propensity was not in the scope of this study.

To sum up, the IT measurements for the various artificial concentrate compositions of 80 % recovery are summarized in Figure 3.8. The figure clearly shows that both phosphate and HS, i.e., HA and FA can substantially hinder the precipitation of calcium carbonate in RO applications.

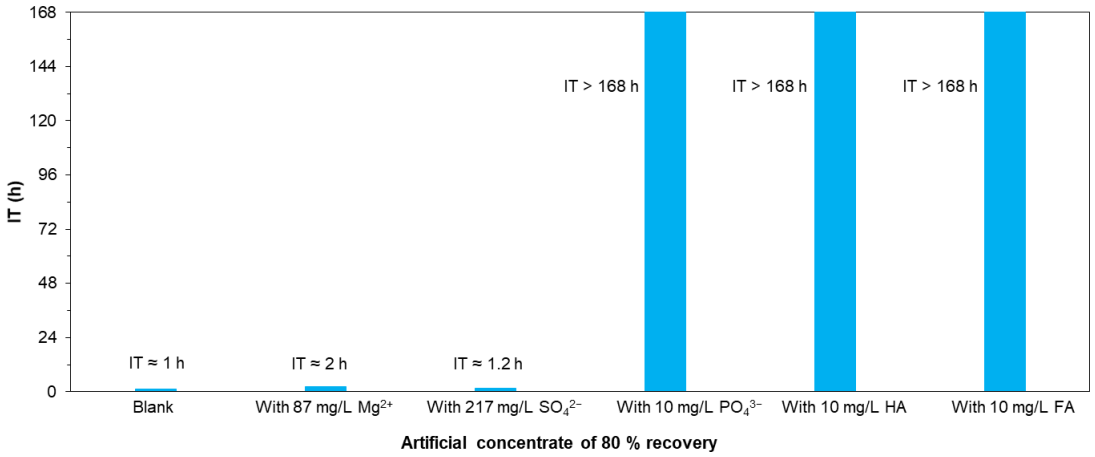

Figure 3.8 *IT of the artificial concentrate of 80 % recovery with various compositions*

3.3.3.2 Lab-scale RO measurements

In the previous section, the effect of phosphate and HS on delaying the formation of calcium carbonate in glass reactors was investigated. However, the condition in such a reactor differs from an RO system, in terms of residence time, geometry, material and hydro-dynamics. In this section, the effect of phosphate on calcium carbonate scaling in RO systems is investigated using the once-through lab-scale RO setup.

Figure 3.9a presents the normalized K_w of the Hydranautics ESPA2-LD-4040 membrane when fed with the artificial concentrate of 80 % recovery, *i*) in the absence of phosphate and *ii)* in the presence of 10 mg/L of phosphate (Table 3.5). The feedwater composition was equivalent with the artificial concentrate used in the IT measurements. In both experiments, the filtration flux was in the 30–35 L/m^2/h range which was higher than the average flux of the last stage of the RO pilot unit.

As can be seen, when phosphate was absent, the normalized K_w of the membrane decreased by approximately 20 % in less than 2 h due to calcium carbonate scaling. In Figure 3.9b, the SEM image of the membrane scaled with calcium carbonate is illustrated.

On the other hand, when approximately 10 mg/L of phosphate was added to the artificial concentrate, the normalized K_w of the membrane remained constant for a 10–hour experimental period which is consistent with the IT results shown in Figure 3.7b. As presented earlier in Figure 3.7b, IT of the artificial concentrate in the presence of 10 mg/L of phosphate was longer than 1 week, which suggested that if the lab-scale RO test was continued for a 1-week period or even longer, calcium carbonate scaling would have not occurred. It was cost-wise not feasible to run the lab-scale RO test for a 1-week duration due to the consumption of large amount of chemicals in once-through experiment. The result of Figure 3.9 clearly showed that the presence of phosphate can prevent calcium carbonate scaling in RO systems and therefore can reduce the need for the addition of commercial antiscalants. Furthermore, this result verified that phosphate was one of the reasons for the constant normalized K_w of the last element of the RO pilot unit (Kamerik, Netherlands) when no antiscalant was used (Figure 3.5b).

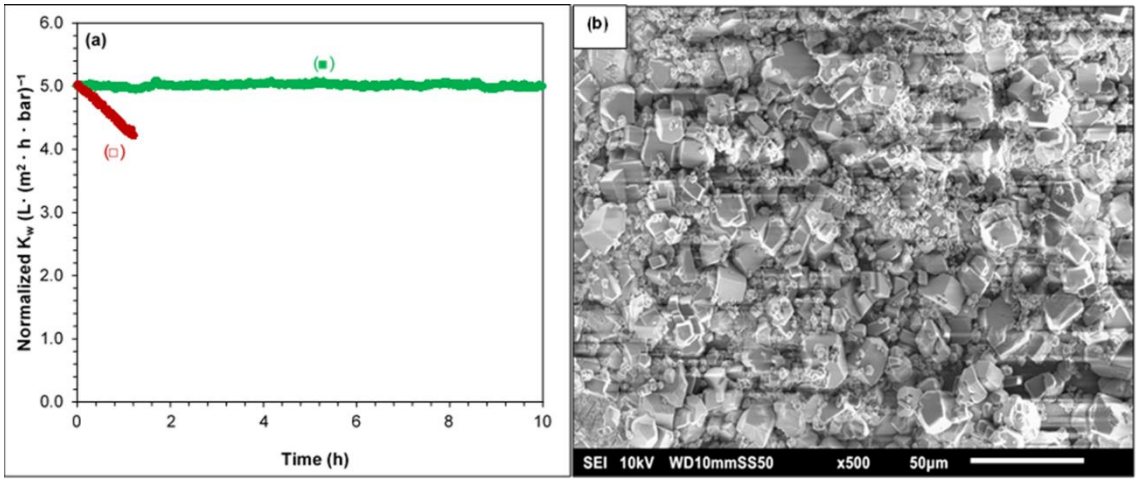

Figure 3.9 *(a) Normalized K_w of the ESPA2-LD-4040 membrane in the lab-scale RO test when fed with the artificial concentrate of 80 % recovery (□) in the absence of phosphate and (■) in the presence of 10 mg/L of phosphate, and (b) SEM image of the ESPA2-LD-4040 membrane after being fed with the artificial concentrate of 80 % recovery in the absence of phosphate*

Furthermore, one can perceive from Figure 3.9 that the addition of antiscalant was a must to prevent calcium carbonate scaling when the membrane (in the lab-scale RO test) was fed with the artificial concentrate of 80 % recovery in the absence of phosphate. This result also suggested that, in case, when phosphate (and also HS) were not present in the GW, the dosage of antiscalant to the RO feed would have been crucial to prevent calcium carbonate scaling in the RO unit of Kamerik when the unit was operated at 80 % recovery.

We emphasize that it is important to conduct these experiments in a flow through mode, rather than in a circulation mode, due to the difference in residence time and the possibility of recirculating seed crystals. Due to the required feedwater volume, it was not possible to perform these experiments with HS.

From the results in this study, it became obvious that the required antiscalant dose is significantly impacted by the feedwater composition (e.g., the presence of phosphate and HS) and that those factors are insufficiently considered when antiscalant dosing is recommended. It is therefore beneficial to experimentally determine optimal dosing or to use feedback control.

3.4 CONCLUSIONS

In this study, we investigated the effect of phosphate and HS on membrane scaling. We combined pilot scale RO operation, lab-scale RO operation and controlled precipitation experiments.

The major findings of this study can be summarized as follows:

- We demonstrated that both phosphate and HS considerably hinder the formation of calcium carbonate and therefore can prevent calcium carbonate scaling in RO applications.
    - At 80 % recovery of the RO pilot unit without antiscalant, the IT of the anaerobic real RO concentrate (containing phosphate and HS) was longer than 168 h, whereas, at the same supersaturation level, the IT of the artificial RO concentrate (without phosphate and HS) was approximately 1 h.
    - With the addition of 10 mg/L phosphate to the artificial RO concentrate of 80 % recovery, the IT of the concentrate increased from 1 h to at least 168 h. Likewise, the IT of the artificial RO concentrate of 80 % recovery was longer than 168 h when 10 mg/L of HA and FA was added to the artificial concentrate.
    - In the absence of phosphate, the normalized K_w of the ESPA2-LD-4040 membrane decreased by approximately 20 % in 2-h period when the membrane was fed with the artificial concentrate of 80 % recovery containing no phosphate, while the normalized K_w remained constant for a 10-h experimental period when the membrane was fed with the same artificial concentrate in the presence of 10 mg/L of phosphate.
- It was found that the presence of phosphate and HS in the RO feed has a noticeable effect on the reduction of antiscalant dose required to control calcium carbonate scaling.
    - The supplier's recommended antiscalant dose to prevent calcium carbonate scaling in the RO unit at 80 % recovery was 2.2 mg/L. Due to the presence of phosphate and HS in the RO feed, the RO unit could be operated with an antiscalant dose as low as 0.2 mg/L and even without antiscalant.

4

FOULANT IDENTIFICATION AND PERFORMANCE EVALUATION OF ANTISCALANTS IN INCREASING THE RECOVERY OF A REVERSE OSMOSIS SYSTEM TREATING ANAEROBIC GROUNDWATER

This chapter is based on the following publication:

M.N. Mangal, S.G. Salinas-Rodriguez, J. Dusseldorp, B. Blankert, V.A. Yangali-Quintanilla, A.J.B. Kemperman, J.C. Schippers, W.G.J. van der Meer, M.D. Kennedy, Foulant identification and performance evaluation of antiscalants in increasing the recovery of a reverse osmosis system treating anaerobic groundwater, Membranes, 12 (2022) 290. https://doi.org/10.3390/membranes12030290

Abstract

The objectives of this study are to assess the performance of antiscalants in increasing the recovery (≥ 85%) of a reverse osmosis (RO) plant treating anaerobic groundwater (GW) in Kamerik (the Netherlands), and to identify scalants/foulant that may limit RO recovery. Five different commercially available antiscalants were compared on the basis of their manufacturer recommended dose. Their ability to increase the recovery from 80% to a target of 85% was evaluated in pilot-scale measurements with anaerobic GW. Membrane autopsy was performed on the tail element(s) with decreased permeability. X-ray photoelectron spectroscopy (XPS) analysis indicated that calcium phosphate was the primary scalant causing permeability decline at 85% recovery and limiting RO recovery. Calcium carbonate scaling did not occur in the RO unit. The addition of antiscalant had no positive effect on RO operation and scaling prevention, since at 85% recovery, permeability of the last stage decreased with all five antiscalants, while no decrease in permeability was observed without the addition of antiscalant at 80% recovery. In brief, calcium phosphate appeared to be the main scalant limiting RO recovery, and antiscalants were unable to prevent calcium phosphate scaling and to achieve a recovery of 85% or higher.

4.1 INTRODUCTION

One of the main developments in water treatment over the last few decades has been the advent of RO technology. Due to continuous development of RO, decreasing prices of membrane technology, and due to its small footprint and excellent removal of contaminants (e.g., organic micropollutants (OMPs), viruses, etc.) (Beyer et al., 2014), the use of RO is increasingly applied in the treatment of GW and surface water which are the main sources for producing drinking water in many countries worldwide. For instance, in the Netherlands, over 60 % of the produced drinking water by Dutch water supply companies is obtained from the treatment of GW (Hiemstra et al., 2003, de Vet et al., 2009) and several of these companies have adopted (or are investigating) the use of RO technology to produce high-quality drinking water.

Though RO technology has gained popularity in the water treatment sector and is widely accepted, it still faces some challenges such as membrane fouling that need to be addressed. Membrane fouling has adverse effect on the operation of RO, including but not limited to the permeability loss of the membranes, increased pressure needs leading to higher operating expenses, an increase in salt passage of the RO permeate, and a shorter membrane lifetime as a result of frequent cleanings (Kucera, 2010). In RO processes, various types of fouling can be encountered such as particulate fouling, organic fouling, biofouling, and scaling (Tang et al., 2011, Fridjonsson et al., 2015, Okamoto and Lienhard, 2019, Flemming, 1993). Particulate fouling is caused by the deposition of colloidal and

suspended material (silt, clay, iron oxides, etc.) present in the RO feed onto the membrane surface (Potts et al., 1981, Pandey et al., 2012, Salinas-Rodriguez, 2011). Organic fouling is usually encountered when the RO feed contains high concentrations of natural organic matter (e.g., humic substances (HS)) (Martínez et al., 2014, Xu et al., 2006). Biofouling is the attachment and growth of microorganisms on the feed spacer and membrane surface in RO processes (Vrouwenvelder et al., 2009, Vrouwenvelder et al., 1998, Flemming, 1997). In GW applications, especially RO treatment of anaerobic GW, biofouling is not encountered (Hiemstra et al., 1999, Beyer et al., 2014). Lastly, scaling refers to the crystallization and precipitation of sparingly soluble salts on the membrane surface that can occur when the concentration of the salts on the membrane surface exceeds their solubility limits (Kucera, 2010).

Scaling is a major challenge in brackish water RO applications (BWRO) and is typically the key barrier in operating RO systems at high recovery rates. Maximizing recovery in BWRO is highly desirable to minimize the total electrical consumption per unit volume of permeate, maximize water production, decrease the amount of concentrate, and lower the use of pretreatment chemicals and their related costs. At high recoveries, the concentration of the dissolved inorganic compounds in the concentrate can increase considerably, as much as four to ten times for recoveries in the 75–90 % range, consequently, exceeding the solubility limits for several types of salts, which can lead to membrane scaling.

Depending on the inorganic ion composition of the RO feed, various compounds such as calcium carbonate, calcium phosphate, silica, etc. can precipitate in RO installations. Calcium carbonate is one of the most commonly encountered scales on RO membranes. The formation and degree of calcium carbonate scaling depend on the calcium and bicarbonate concentrations (Antony et al., 2011, Tzotzi et al., 2007) as well as on pH and temperature (Koutsoukos, 2010). When the RO feed contains a high concentration of calcium and orthophosphate ions, calcium phosphate scale can form on the membrane surface (Chesters, 2009, Greenberg et al., 2005). Calcium phosphate can be mainly encountered in water reuse applications as well as in RO treatment of GW. Calcium phosphate can exist in amorphous form and various crystalline forms (Dorozhkin, 2016). In RO applications, the amorphous phase of calcium phosphate is reported to be responsible for flux decline (Chesters, 2009, Mangal et al., 2021b). Silica degrades membrane performance by precipitating as colloidal silica or as metal silicates with ions such as calcium, magnesium, aluminium, etc. (Neofotistou and Demadis, 2004, Luo and Wang, 2001, Antony et al., 2011). In GWRO applications, aluminium silicates (e.g., clay in colloidal form) are one of the most commonly encountered compounds which could be present in the RO feedwater and can cause permeability decline in the first stage as well (Gallego et al., 2008).

Antiscalant addition to the RO feed is one of the most effective and widely used methods for preventing scaling and achieving high recoveries in RO applications. (Lee et al., 1999, Pervov, 1991, Greenlee et al., 2010). One factor that makes antiscalant addition appealing is the low dose required to overcome scaling (Antony et al., 2011). Antiscalants disrupt the crystallization process; more specifically, hinder the nucleation phase and/or retard the growth phase of crystallization (Amjad, 1996, Antony et al., 2011, Koutsoukos, 2010), allowing for higher recovery in RO applications (Drak et al., 2000). There are a variety of commercial antiscalants available that are designed to combat specific types of scale, and the most common ones used in RO applications are phosphonates, polycarboxylates and biobased antiscalants (Antony et al., 2011, van Engelen and Nolles, 2013). The selection of antiscalants in RO applications depends on the feed water composition. The antiscalant dose is generally recommended by the antiscalant suppliers which they calculate using their projection programs. The projection programs of the antiscalant suppliers also predict the maximum achievable recovery and identify the scalants that may limit RO recovery.

This study was performed in the context of the realization of a future RO plant by a Dutch water supply company (Oasen Drinkwater) in treating anaerobic groundwater for drinking water production. Due to the anticipated increase in salinity and higher standards in the removal of OMPs, the water company aims to replace the existing conventional plant (spray aeration on the surface of rapid sand filters, tower aeration, pellet softening, rapid sand filtration, and granular activated carbon filtration) with RO. The abstraction of anaerobic groundwater and the discharge of concentrate are limited by strict regulations. It is therefore desirable, in this situation, to operate the RO plant at 85% recovery or higher.

The objectives of this work are:

- To identify the foulant/scalants that would precipitate in the RO unit at 85 % recovery
- To examine the role of antiscalants in increasing the RO recovery to at least 85 %

In this study, an RO pilot unit was operated with and without antiscalant at 80–85 % recoveries. Membrane autopsy was carried out to identify the scalants/foulant.

4.2 MATERIALS AND METHODS

4.2.1 Feedwater (anaerobic GW) composition

The RO feed was anaerobic GW which was obtained from several wells of a (conventional) water treatment plant in Kamerik, the Netherlands. Table 4.1 shows the composition of the feedwater. The water analysis was carried out by a commercial lab (Vitens Laboratorium, the Netherlands). The major fraction (approximately 62%) of the dissolved organic carbon (DOC) in the GW was humic substances (HS) of the fulvic acid (FA) type, which was identified with liquid chromatography–organic carbon detection (LC–OCD) (DOC-Labor, Germany).

Table 4.1 *Feedwater (anaerobic GW) composition*

Cations	**Concentration (mg/L)**	**Anions**	**Concentration (mg/L)**
Calcium	115.2	Sulphate	43.4
Magnesium	17.4	Chloride	113.6
Sodium	55.2	Fluoride	0.1
Potassium	5.6	Bicarbonate	391.8
Barium	0.1	Carbonate	-
Strontium	0.5	Nitrate	0.2
Iron (II)	8.5	Silica	16.7
Ammonium	3.7	Orthophosphate	2.1
Other properties of the RO feed:			
pH	7.0	TDS (mg/L)	750-800
Temperature (°C)	12	DOC [HS] (mg/L)	8.6 [5.3]
Turbidity (NTU)	< 0.1		

The RO feedwater data (Table 4.1) was entered into the projection programs of seven different antiscalant manufacturers (names are not included in this study) to identify the suppliers' recommended maximum achievable recovery and the scaling compound(s) which may limit RO recovery. The projection programs were also used to assess the scaling potential of the RO concentrates at various recoveries (with and without antiscalant addition).

4.2.1.1 Tested antiscalants to increase RO recovery to at least 85%

Based on the RO feed analysis (Table 4.1), various antiscalants were recommended by the antiscalant manufacturers with which the RO recovery could be increased to 85%. Table 4.2 lists the arbitrary names of the tested antiscalants, along with some basic information provided by the antiscalant suppliers.

Table 4.2 *Tested antiscalants as recommended by suppliers for increasing RO recovery to at least 85%*

Antiscalants▲	**Chemical nature**	**Target scalants**	
		Primary scalants targeted	Additional scalants targeted
AS–1	Blend of phosphonates and carboxylic acids	Calcium phosphate/carbonate	Silica, iron/clay fouling, etc.
AS–2	Proprietary acrylic polymer with chelate agent	Silica, calcium phosphate	calcium carbonate, etc.
AS–3	Information not available	Calcium phosphate/carbonate	Silica, clay, metal oxides, etc.
AS–4	A modified polycarboxylate	Calcium phosphate/carbonate	Silica, etc.
AS–5	Sulfonated Polycarboxylate	Calcium phosphate	Silica, calcium carbonate, etc.

▲ The antiscalants' real names are replaced with arbitrary names.

4.2.2 RO pilot

Figure 4.1 depicts a schematic representation of the RO pilot plant. The RO installation had three stages where the pressure vessel configuration for each stage could be varied. Each pressure vessel contained three Hydranautics membrane elements (ESPA2-LD-4040). The anaerobic GW (feedwater) was passed through a cartridge filter (10 µm) and then fed to the RO unit. The RO installation was operated at constant permeate water production. To assess the occurrence of scaling, the average normalized (temperature corrected) permeability (K_w) of the last stage was monitored.

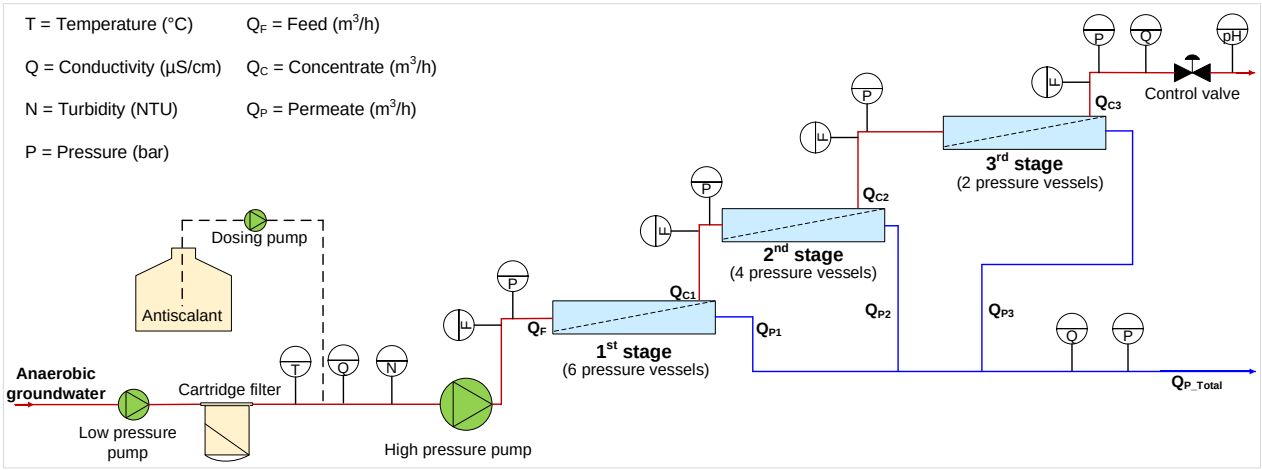

Figure 4.1 *Schematic representation of the RO pilot installation in Kamerik*

Table 4.3 *RO operation without antiscalant (to identify scalants that cause permeability decline), and with antiscalants (to increase RO recovery to 85 %)*

Run	Pressure vessel configuration	Recovery (%)	Antiscalant	Antiscalant dose• (mg/L)	Run period (days)
A	3-2-1 (6 elements)	80	-	0	10
		85	-	0	32
B	6-2-1 (3 elements)	85	-	0	5
			AS–1	2.5	3
			AS–2	2.5	5
			AS–3	2.5	4
			AS–4	5.0	5
			AS–5	5.0	4

•Tested antiscalant doses were the suppliers' recommended doses.

In the first set of experiments, the RO pilot was operated without antiscalant as described in Table 4.3 to realize which compounds will precipitate in the RO unit in the absence of antiscalant. After observing a permeability drop (> 20%) in the last stage, the tail membrane element was taken for autopsy. In the second set of experiments (as shown in Table 4.3), the RO unit was operated at 85% recovery with various antiscalants. These experiments were conducted to recognize if a recovery of 85% (or higher) could be achieved with the use of antiscalants for the RO unit in Kamerik, since according to some antiscalant suppliers, 85% recovery was an achievable recovery with their antiscalants. The average flux of the last stage in all experiments was in the 10–20 L/h/m^2/bar range.

4.2.3 Foulant characterization

After operating the RO unit without antiscalant, all three stages were flushed with RO permeate. As the membranes were in contact with anaerobic concentrate containing high concentrations of ferrous, flushing with RO permeate was necessary to avoid iron oxidation (and precipitation) while taking out the membranes for autopsy. Membrane autopsy was performed on the tail element of the 3rd stage and 1st stage. It is worth mentioning that the membrane elements in the 3rd stage were brand new, whereas the membrane elements in the 1st stage had been in use for over 5 years.

To identify the foulant/scalant which was responsible for the permeability decline of the RO, various techniques were employed such as scanning electron microscopy with energy dispersive X-ray (SEM-EDX) spectroscopy (JEOL, JSM-6010LA), X-ray powder diffraction (XRD) (Bruker D8 Advance), fluorescence excitation–emission matrix (FEEM) spectrophotometry (FluoroMax-3), and X-Ray photoelectron spectroscopy (XPS) (Quantera SXM-Scanning XPS microprobe).

SEM-EDX was used to visualize the foulant and to identify the mass percentages of the elements present in the foulant. To investigate whether the foulant disappears in acidic or basic solutions (or both), membrane coupons of the fouled RO with a total area of approximately 1000 cm^2 were stirred for about 24 h at 35 °C in beakers containing either 0.05 M HCl or 0.05 M NaOH. Afterwards, the membrane coupons were flushed with demineralized water, dried and then analyzed with SEM-EDX. In the case where foulant was not observed on the membrane coupons (after cleaning) in SEM-EDX analysis, the cleaning solutions then were filtered through 0.45 µm (cellulose acetate) filters. Afterwards, the 0.45 µm filters were flushed with demineralized water, dried, and analyzed with SEM-EDX to find out if the foulant dissolved in the cleaning solutions or was just physically detached from the membrane.

XRD analysis was performed on the fouled RO membrane to examine if the foulant was crystalline and if so, which scales were present on the fouled membrane. FEEM analysis was used to examine the cleaning solutions (0.05 M HCl and 0.05 M NaOH) to identify the presence of HS on the fouled RO membrane. XPS was used to obtain the binding energies of the foulant present on the membrane surface and to identify the foulant.

4.3 RESULTS AND DISCUSSION

4.3.1 Maximum achievable recovery based on antiscalant suppliers' projection programs

In this section, the maximum achievable recovery and the scalants that limit RO recovery according to projection programs of the antiscalant suppliers are discussed. In addition, the scaling potential (of some commonly encountered scalants) at 80 % and 85 % recovery with and without antiscalant (according to the projection software) is presented.

Figure 4.2a shows the maximum achievable recoveries in the presence of antiscalants for the RO unit which were determined by the projection programs of seven different antiscalant suppliers. As can be seen, the recommended maximum achievable RO recovery was different for all projection programs of the antiscalant suppliers. In addition, the scalant compound which may limit RO recovery was also not the same according to the projection programs of different suppliers. For instance, according to the projection programs of suppliers A, E, C and G, recovery of the RO unit was limited due to calcium carbonate scaling, while calcium phosphate scaling was limiting RO recovery according to suppliers B, D, and F. The maximum achievable RO recovery (limited due to calcium carbonate) was 89% according to suppliers E and G, and 83% and 87% according to suppliers A and C, respectively. The maximum achievable RO recovery (limited due to calcium phosphate) was 77%, 80% and 85% according to suppliers B, D and F,

respectively. From Figure 4.2a, one can clearly recognise that the projection programs of the antiscalant suppliers are not consistent in identifying the maximum RO recovery.

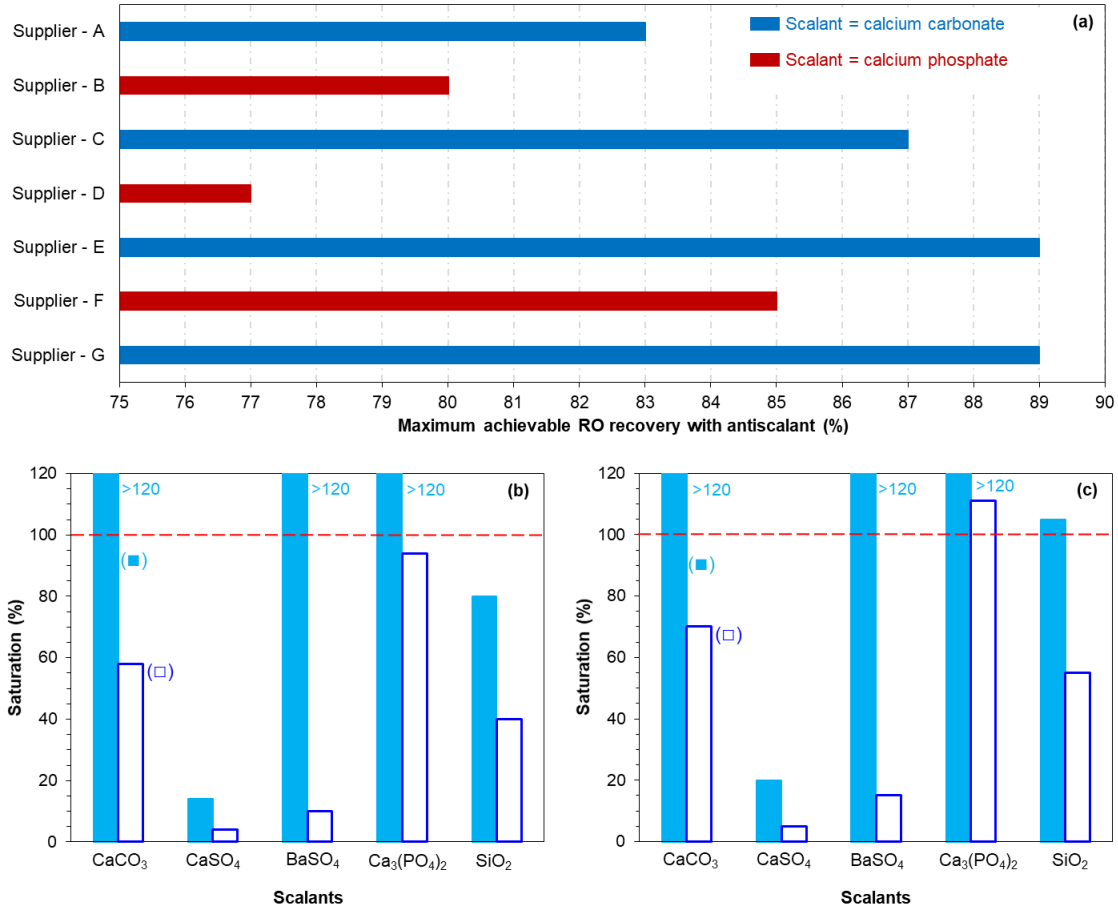

Figure 4.2 *(a) Maximum achievable recovery of the RO unit in the presence of antiscalants determined with the projection programs of various antiscalant suppliers, (b) scaling potential of commonly encountered scalants at 80% recovery of the RO unit (■) in the absence of antiscalant, and (□) in the presence of antiscalant, and (c) scaling potential of commonly encountered scalants at 85% recovery of the RO unit (■) in the absence of antiscalant, and (□) in the presence of antiscalant. (b) and (c) are determined with the projection program of Supplier-B*

Figure 4.2b and Figure 4.2c present the scaling tendency (performed with the projection program of Supplier-B) of some commonly encountered scalants in the RO concentrate at 80% and 85% recovery, respectively. The scaling tendency of the RO concentrates at 80 and 85% recoveries is presented because the RO pilot, in this study, was operated initially at 80% recovery and then at 85% recovery. The scaling tendency is shown both with and without the addition of antiscalant to the RO feed.

The projection program of supplier-B advised that at 80% recovery without antiscalant, the RO unit may experience calcium carbonate, barium sulphate and calcium phosphate scaling, while with the addition of antiscalant to the RO feed, none of the mentioned scalants will precipitate in the RO unit. Furthermore, at 85% recovery with no antiscalant, the program indicated that silica may also precipitate together with calcium carbonate, barium sulphate and calcium phosphate. The program suggested that, with the addition of antiscalant, calcium carbonate, barium sulphate and silica may not precipitate in the RO unit at 85% recovery, while calcium phosphate may precipitate even with the addition of antiscalant.

In short, with the use of projection programs, it is not clear if the RO unit in Kamerik can be operated at 85% recovery (or higher) as the highest achievable recovery according to antiscalant suppliers varied from 77 to 89%.

4.3.2 Foulant (scalant) characterization

In this section, the aim was to understand which compounds may limit RO recovery. For this, the RO unit was initially operated at various recoveries without antiscalant, and in the case of a decrease in permeability, the membranes were taken out for autopsy to identify the scalants responsible for the observed permeability decline in the absence of antiscalants. After identifying the scalant(s), the RO was operated with various antiscalants of different suppliers in an attempt to inhibit the precipitation of those scalants and to maximize RO recovery.

4.3.2.1 RO operation at 80–85% recoveries in the absence of antiscalants

Figure 4.3 presents the average normalized permeability of the 1st, 2nd and 3rd stages of the RO unit at 80–85% recoveries when no antiscalant was added to the RO feed.

At 80% recovery without antiscalant, the normalized permeability remained constant where calcium carbonate, barium sulphate and calcium phosphate had the tendency to scale the RO unit according to the projection program of supplier-B. On the other hand, at 85% recovery, the normalized permeability of the last stage decreased in the absence of antiscalants. At 85% recovery, the normalized permeability of the 2nd stage remained constant where the total recovery of the 1st and 2nd stages was approximately 77%. As no decrease in membrane permeability of the last stage at 80% recovery without antiscalant was observed, it was expected that permeability would remain constant at 77% recovery. Surprisingly, the average normalized permeability of the 1st stage with a recovery of 52% had a slight decreasing trend (with a −0.005 slope). The slight decrease in the 1st stage may not be due to the deposition/precipitation of newly formed particles/crystals. It could be that the RO feed contained particles that deposited in the 1st stage and caused permeability decline. To understand what compounds caused permeability decline in the

3rd stage and in the 1st stage, the tail elements of the mentioned stages were taken out for autopsy.

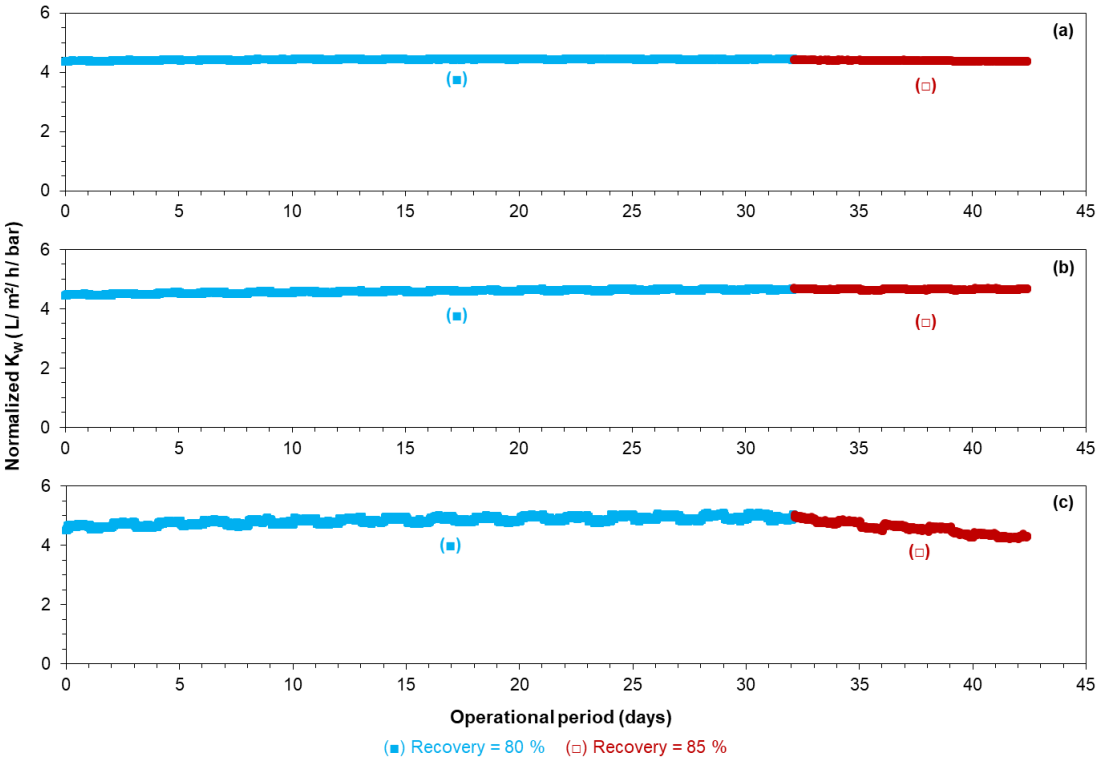

Figure 4.3 *Average normalized permeability of the (a) 1st stage, (b) 2nd stage, and (c) 3rd stage of the RO unit at 80 and 85% recoveries without antiscalant addition*

4.3.2.2 SEM-EDX of the tail element of the 1st stage

The SEM and EDX analyses of the tail element of the 1st stage (with decreased permeability) are presented in Figure 4.4a and Figure 4.4b, respectively. The SEM picture showed that the membrane surface was covered by deposits. The EDX results in Figure 4.4b indicated that the deposited material on the membrane surface consisted of aluminium, silicon and iron. In the EDX analysis (Figure 4.4b), only those elements that are not part of the membrane material are presented. The presence of aluminium and silicon on the membrane surface could be attributed to clay particles that might be present in the RO feedwater and were not retained by the 10 µm cartridge filter. The presence of iron may be related to the deposited clay particles as iron may be present in the composition of the clay particles, and/or to the iron oxide particles that may be present in very low concentrations in the RO feed.

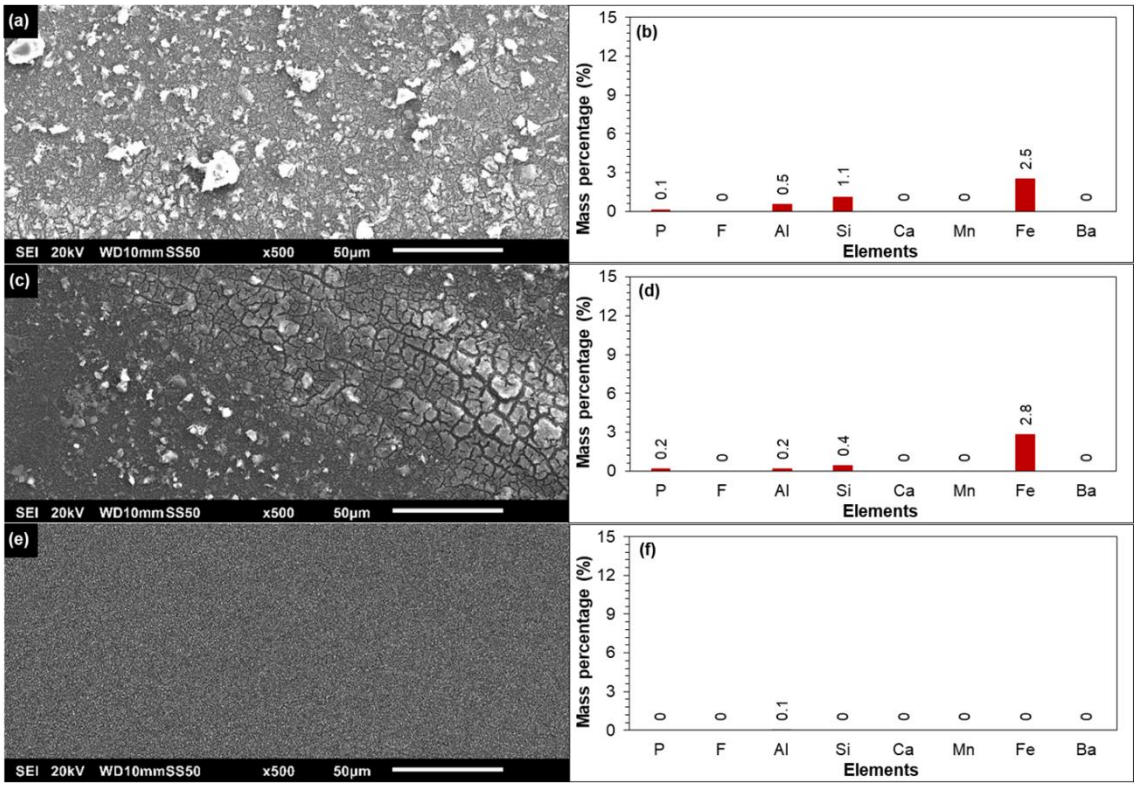

Figure 4.4 *(a) SEM, (b) EDX analyses of the tail element of the 1st stage with decreased permeability, (c) SEM, (d) EDX analyses of the tail element of the 1st stage cleaned with a 0.05 M NaOH solution, and (e) SEM, (f) EDX analyses of the tail element of the 1st stage cleaned with a 0.05 M HCl solution*

Figure 4.4c and Figure 4.4d present the SEM image and the EDX of the membrane cleaned with 0.05 M NaOH solution, respectively. It was observed that the NaOH solution was unable to remove the deposited particles from the membrane surface, and the layer (after cleaning) still consisted of aluminium, silicon and iron. On the other hand, the deposited particles disappeared when the membrane was stirred in 0.05 M HCl solution (Figure 4.4e). In the EDX analysis (Figure 4.4f), no aluminium, silicon and iron were detected. This showed that the deposited layer was removed with HCl solution. At this point, it was not clear if the deposited particles were dissolved in the HCl solution and/or were detached from the membrane surface due to mechanical forces.

In Figure 4.5, the SEM-EDX analysis of the retained deposits on the 0.45 µm filter (after filtering the 0.05 M HCl cleaning solution) is shown. As can be seen, the retained deposits consisted of aluminium, silicon and iron suggesting that clay particles from the membrane surface were not dissolved in the HCl solution, but actually were detached from the membrane surface. Figure 4.5b also indicated that a part of iron on the membrane surface of the tail element of the 1st stage (Figure 4.4a and Figure 4.4b) could be linked to clay

particles since if all iron was present as iron oxides, then it should have been dissolved in 0.05 M HCl solution. In Figure 4.5b, the mass percentage of iron (on the filter surface) was approximately half the mass percentage of silicon. However, in Figure 4.4b, the mass percentage of iron on the membrane surface of the tail element of the 1st stage was higher than silicon. This may indicate that the additional mass percentage of iron in Figure 4.4b could be due to the iron oxide particles.

In brief, based on the SEM-EDX results of Figure 4.4 and Figure 4.5, it may be concluded that the deposition of clay and iron oxide particles (present in the RO feed) were contributing to the slight permeability decline of the 1st stage.

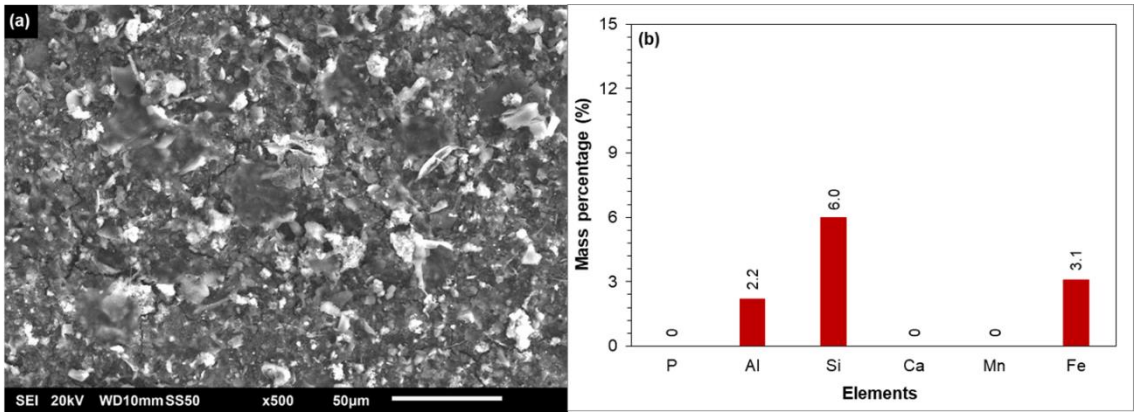

Figure 4.5 *(a) SEM image and (b) EDX analysis of the 0.45 µm filter after filtration of the 0.05 M HCl solution (of the tail element of the 1st stage)*

4.3.2.3 SEM-EDX of the tail element of the 3rd stage

In Figure 4.6a and Figure 4.6b, SEM-EDX analysis of the fouled/scaled RO membrane of the tail element of the 3rd stage is shown. As can be seen, the membrane surface apparently was covered with an amorphous layer. According to the EDX analysis, the foulant was composed of calcium, phosphorous, and iron. A small mass percentage of manganese could also be observed. In the EDX analysis, aluminium and silicon were not observed on the membrane surface which suggested that clay particles did not contribute to the permeability decline of the 3rd stage at 85% recovery. According to the antiscalant projection program of Supplier-B (Figure 4.2c), calcium carbonate, barium sulphate, calcium phosphate and silica have the potential to scale the RO at 85% recovery in the absence of antiscalant. As silica was not observed on the membrane surface in the EDX analysis (Figure 4.6b), it can be concluded that silica scaling did not occur in the RO unit at 85% recovery without antiscalant.

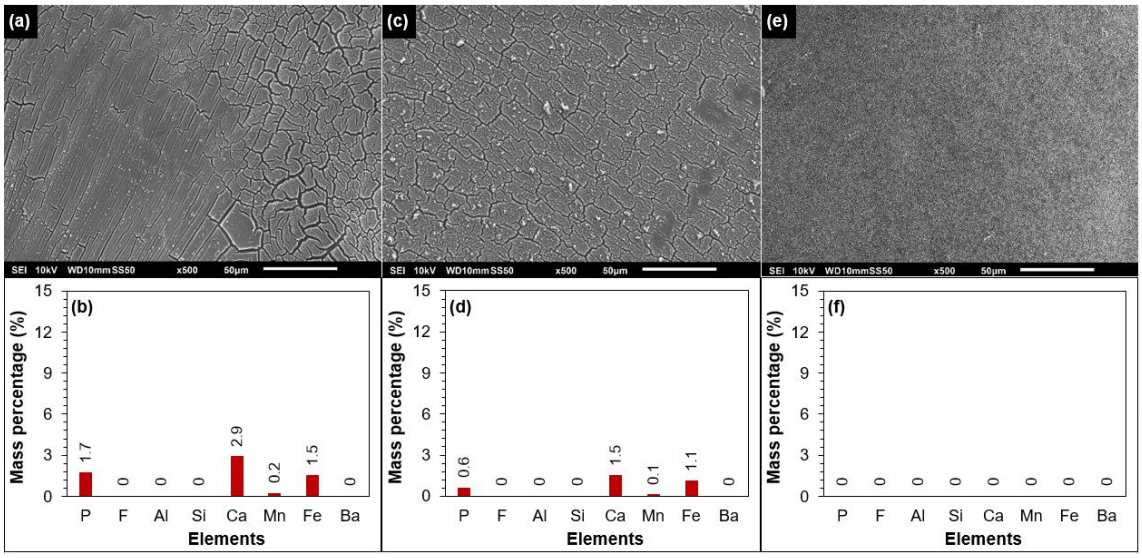

Figure 4.6 *(a) SEM, (b) EDX analyses of the fouled tail element of the 3rd stage, (c) SEM, (d) EDX analyses of the tail element of the 3rd stage cleaned with 0.05 M NaOH solution, and (e) SEM, (f) EDX analyses of the tail element of the 3rd stage cleaned with 0.05 M HCl solution*

Furthermore, barium sulphate scaling did not occur at 85% recovery as barium was not present on the fouled membrane surface (Figure 4.6b). Based on a study by Boerlage et al. (2000), where they reported that barium sulphate has very slow precipitation kinetics and its precipitation is hindered by humic substances (HS), it was expected that the barium sulphate scale would not occur in the RO unit in Kamerik. In the anaerobic groundwater of Kamerik (RO feed), the concentration of HS was approximately 5.3 mg/L (Table 4.1) which might inhibit barium sulphate scaling in the RO unit. Several researchers (Hoch et al., 2000, Zuddas et al., 2003, Klepetsanis et al., 2002, Amjad et al., 1998, Inskeep and Bloom, 1986) have reported that HS significantly hinder the formation of calcium carbonate. Also, in a study by the current authors (Mangal et al., 2021a), it was demonstrated that HS as well as phosphate present in the GW were able to inhibit calcium carbonate scaling in the RO unit in Kamerik. We showed that due to the presence of HS and phosphate, the induction time of the real RO concentrate at 80% recovery was longer than 7 days, whereas at the same supersaturation level in the absence of phosphate and HS, the induction time of the synthetic RO concentrate of 80% recovery was around 1 h. Due to the long induction time (> 168 h) of the RO concentrate of 85% recovery in the absence of antiscalants (Figure S4.1), it is also expected that calcium carbonate scaling would not occur at 85% recovery when antiscalants are not added to the RO feed. In the XRD analysis (Figure S4.2), calcium carbonate crystals were not detected which also indicates that calcium carbonate scaling was not the reason for the permeability decline in the last stage in Figure 4.3c.

In Figure 4.6b, the mass percentage of calcium and phosphorous on the membrane surface could be attributed to (amorphous) calcium phosphate scaling which was also predicted by the projection programs of suppliers B, D, and F (Figure 4.2a). However, the presence of iron on the fouled membrane is not clear. As aluminium and silicon were not observed on the fouled membrane of the 3rd stage (Figure 4.6a), the presence of iron could not be due to clay particles. One may suggest that the presence of iron on the membrane could be due to the presence of iron oxide particles in the RO feed. The presence of iron (and also of calcium and phosphorous) on the fouled membrane is elucidated via XPS analysis (discussed later in this chapter).

Figure 4.6c and Figure 4.6d present the SEM-EDX analysis of the fouled membrane which was cleaned with 0.05 M NaOH solution. As can be seen, the alkaline solution (0.05 M NaOH) was unable to remove the foulant from the membrane surface. After cleaning at high pH, calcium, phosphorous and iron were still present on the membrane surface. On the other hand, the acidic solution (0.05 M HCl) was able to remove the foulant from the membrane surface as can be seen from the SEM image (Figure 4.6e) and the EDX analysis (Figure 4.6f). As calcium, phosphorous and iron were not detected on the membrane surface (Figure 4.6e), the acidic solution was filtered through a 0.45 µm filter and then the filter was examined by SEM-EDX. It was found that the foulant (composed of calcium, phosphorous and iron) on the tail element of the 3rd stage was dissolved in the acidic solution (Figure S4.3).

In brief, from Figure 4.6 one can conclude that the foulant (on the membrane surface of the tail element of the 3rd stage) was mainly inorganic which could be dissolved in an acidic solution (0.05 M HCl) but not in an alkaline solution (0.05 M NaOH).

4.3.2.4 XPS analysis of the tail element of the 3rd stage

The fouled membrane (tail element of the 3rd stage) was analysed with XPS analysis in an attempt to identify the scalant(s) to which calcium, phosphorous and iron could be attributed. The survey spectrum of the analysis is shown in Figure S4.4. Calcium, phosphorous, iron, manganese, oxygen, nitrogen, sulphur and carbon were all detected. In Table 4.4, the average atomic concentrations (obtained with the XPS analysis) from four different spots of the fouled membranes are shown. As the foulant layer was thin, nitrogen, sulphur, carbon and partly oxygen could be attributed to the polyamide membrane. In the survey spectrum, aluminium and silicon were not observed which further verified the results of SEM-EDX of Figure 4.6a and Figure 4.6b showing that clay particles were not (mainly) present on the membrane surface.

Table 4.4 *Atomic concentrations of various elements (obtained via XPS analysis) of the fouled membrane*

Elements	**C**	**N**	**O**	**P**	**S**	**Ca**	**Mn**	**Fe**
Average atomic concentration (%)	46.35	1.9	38.47	3.45	1.18	6.19	0.47	1.98
Standard deviations	0.9	0.29	0.48	0.42	0.06	0.32	0.17	0.26

In Table 4.5, the binding energies of calcium, phosphorous, iron and manganese (present on the fouled membrane surface) are given. In addition, for the determined binding energies, the identified compounds based on the XPS database of the National Institute of Standards and Technology (NIST) (NIST) are included in Table 4.5. The binding energies of calcium and phosphorous were 347.2 eV and 132.9 eV, respectively, which corresponded to calcium phosphate compounds in the NIST database. This suggested that the presence of calcium and phosphorous on the fouled membrane surface (tail element of the 3rd stage) can be attributed to calcium phosphate scaling as predicted by the projection programs of suppliers B, D, and F (Figure 4.2a).

Table 4.5 *Binding energies of various elements on the fouled membrane (determined via XPS analysis)*

Element	**Binding energy (eV)**	**Identified compound(s) according to the NIST database**
Carbon [C1s]	284.8	Reference value
Calcium [$Ca2p_{3/2}$]	347.2	$Ca_3(PO_4)_2$, $Ca_8H_2(PO_4)_6.5H_2O$, $Ca_{10}(PO_4)_6(OH)_2$
Phosphorous [$P2p_{3/2}$]	132.9	$Ca_3(PO_4)_2$
Iron [$Fe2p_{3/2}$]	711.1	Fe_2O_3
Manganese [$Mn2p_{3/2}$]	642.4	MnO_2

In the XPS analysis, the binding energies of iron and manganese were found to be 711.1 eV and 624.4 eV, respectively. According to the NIST database, the presence of iron and manganese on the fouled membrane of the tail element of the 3rd stage could be due to the precipitation of oxidized iron and manganese. This may suggest that iron oxide particles have been present in the raw water (RO feed) before entering the plant. It may also be that iron oxide particles were formed (and precipitated on the membrane surface) when the anaerobic RO concentrate (containing a ferrous concentration of approximately 57 mg/L) come in contact with the aerobic RO permeate during flushing of the last stage which was needed for membrane autopsy. If iron oxide particles were formed during flushing, then they were not responsible for the observed permeability decline of the last stage in Figure 4.3c.

Nevertheless, from the SEM-EDX analysis (Figure 4.6a and Figure 4.6b) and XPS analysis (Table 4.4 and Table 4.5), it can be concluded that calcium phosphate scaling

was one of the reasons for the permeability decline of the 3rd stage at 85% recovery (Figure 4.3c) when no antiscalant was added to the RO feed.

4.3.2.5 FEEM analysis of the 0.05 M HCl and 0.05 M NaOH cleaning solutions

As discussed earlier in section 4.2.1 (Table 4.1), the dissolved organic carbon (DOC) concentration in the RO feed was approximately 8.6 mg/L of which 5.3 mg/L were HS. This means that the concentration of HS in the RO concentrate at 85% recovery could increase to approximately 35 mg/L. In RO processes, HS are recognized by various researchers (Tanaka et al., 2016, Tang et al., 2007a, Tang et al., 2007b, Zhao et al., 2019) to cause membrane fouling. Therefore, it was essential to investigate if HS also contributed to the permeability decline of the 3rd stage (Figure 4.3c).

In Figure 4.7, fluorescence excitation-emission matrix (FEEM) analysis of the RO concentrate (at 85% recovery) and the HCl and NaOH cleaning solutions of the tail elements of the 3rd stage is shown. In this study, the locations of the EEM peaks of humic acid (HA) and fulvic acid (FA) were based on the EEM regions reported by Chen et al. (2003). The HA peaks were observed in the 380–500 and 250–400 nm emission and excitation wavelength ranges, respectively, while the 380–400 and 200–250 nm emission and excitation wavelength ranges, respectively, were attributed to FA (Chen et al., 2003).

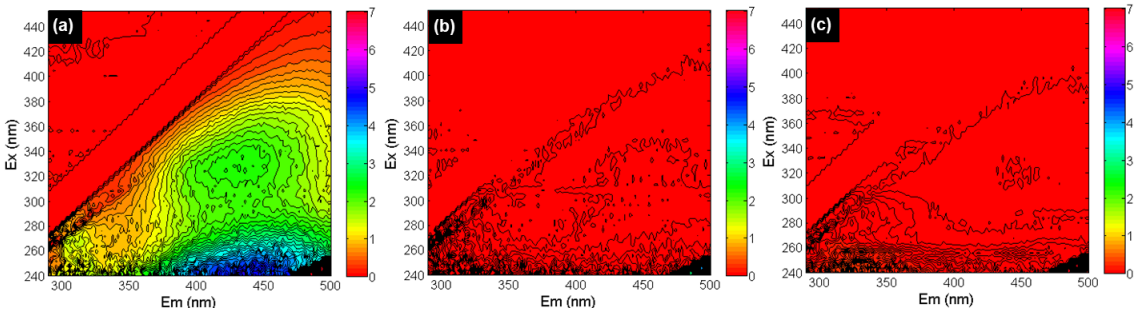

Figure 4.7 *FEEM analysis of the (a) RO concentrate at 85 % recovery, (b) 0.05 M NaOH cleaning solution, and (c) 0.05 M HCl cleaning solution (Ex and Em represent excitation and emission wavelengths)*

As illustrated in Figure 4.7a, peaks for both HA and FA (with high intensity) were observed in the RO concentrate which verifies the presence of HS in the anaerobic GW. However, HA and FA peaks were not visible in the cleaning solutions of the tail element of the 3rd stage as shown in Figure 4.7b (NaOH solution) and Figure 4.7c (HCl solution). The absence of HA and FA peaks in the HCl and NaOH solutions suggests that HS were likely not responsible for the permeability decline of the 3rd stage of the RO unit in Figure 4.3c.

4.3.3 Role of antiscalants in increasing RO recovery to 85%

In the previous section, it was found that calcium phosphate was one of the scalants leading to the permeability decline of the RO unit at 85% recovery and was limiting the RO recovery when no antiscalant was added to the RO feed. The section aimed to investigate if the permeability decline at 85% could be prevented with the addition of antiscalants.

Five different antiscalants (Table 4.2) were tested that were claimed by the antiscalant suppliers to have excellent performance in preventing calcium phosphate scaling at 85% recovery. The aim was to increase the RO recovery to 85% (and even higher) with the use of antiscalants. Therefore, the RO pilot was operated at 85% recovery (Table 4.3) with the suppliers' recommended antiscalants and antiscalant doses.

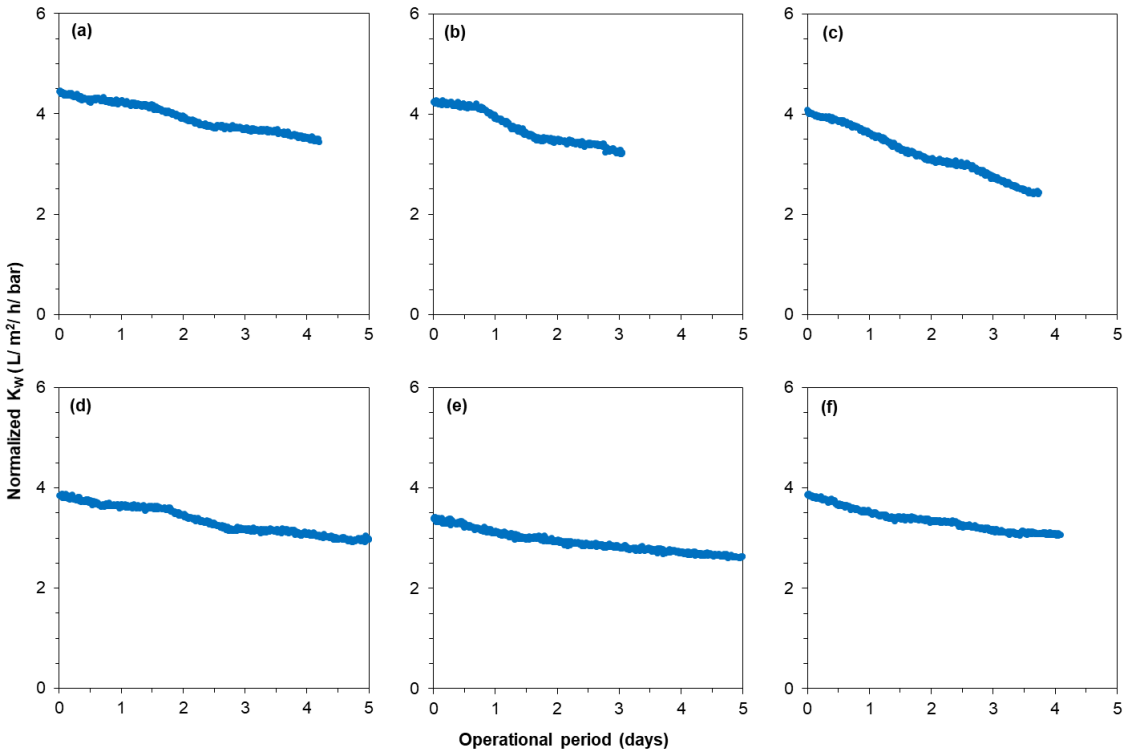

Figure 4.8 *a) Average normalized permeability of the last stage of the RO unit at 85% recovery (a) without antiscalant, (b) with 2.5 mg/L AS–1, (c) with 2.5 mg/L AS–2, (d) with 2.5 mg/L AS–3, (e) with 5 mg/L AS–4, and (f) with 5 mg/L AS–5*

Figure 4.8 shows the average normalized permeability of the 3rd stage of the RO unit at 85% recovery in the absence and presence of five tested antiscalants. As can be seen, none of the antiscalants could prevent the permeability decline of the 3rd stage. After operating the RO unit with antiscalant (AS–5), the tail element of the 3rd stage was examined with SEM-EDX, and the results were similar to those shown in Figure 4.6. It is worth mentioning that the permeability of the 3rd stage also decreased at 83% recovery

in the presence of antiscalants (Figure S4.5). The RO operation at 81% and 82% recovery was not investigated.

To summarize, calcium phosphate appeared to be one of the primary scalants precipitating in the RO unit in Kamerik, and the available antiscalants for calcium phosphate were unable to prevent calcium phosphate scaling and increase RO recovery to 85%.

Some antiscalant suppliers claim that the effectiveness of their antiscalants is reduced when iron (II) is present in the RO feed. Therefore, to understand if the tested antiscalants can prevent calcium phosphate scaling in the absence of iron (II), once-through lab-scale RO tests were performed with the synthetic concentrates of 85% recovery where calcium phosphate was the only scalant that could cause flux decline in the RO unit (Chapter 5).

4.4 CONCLUSIONS

In this study, the role of antiscalants in increasing the recovery of a future RO system of a Dutch water supply company, which will treat anaerobic groundwater in Kamerik (the Netherlands) for drinking water production, to at least 85 % and the scalants that could limit RO recovery were investigated.

The following are the main findings of this study:

- The maximum achievable recovery and the scalant limiting the RO recovery varied according to the projection programs of the different antiscalant suppliers, with some pointing to calcium carbonate and others to calcium phosphate as the limiting scaling compound. The maximum achievable recovery according to antiscalant suppliers was ranging between 77% and 89%.
- Operation of the RO at 80–85% recoveries without antiscalant:
  - The normalized permeability of the 3rd stage remained constant during a 1-month experimental period when the RO pilot was operated at 80% recovery without antiscalant, whereas the normalized permeability of the 3rd stage decreased when the RO pilot was operated at 85% recovery without antiscalant.
- Membrane autopsy of the tail element of the 3rd stage:
  - Calcium phosphate was the main scalant causing permeability decline at 85% recovery and limiting the RO recovery.
  - Calcium carbonate was not responsible for the permeability decline of the 3rd stage at 85 % recovery.
- Role of antiscalants in increasing the RO recovery to 85% (and higher):
  - In the RO pilot measurements, the tested antiscalants were found to be ineffective in increasing the RO recovery to 85% as the permeability of the 3rd stage decreased with each of the tested antiscalants.

4.5 SUPPLEMENTARY DATA

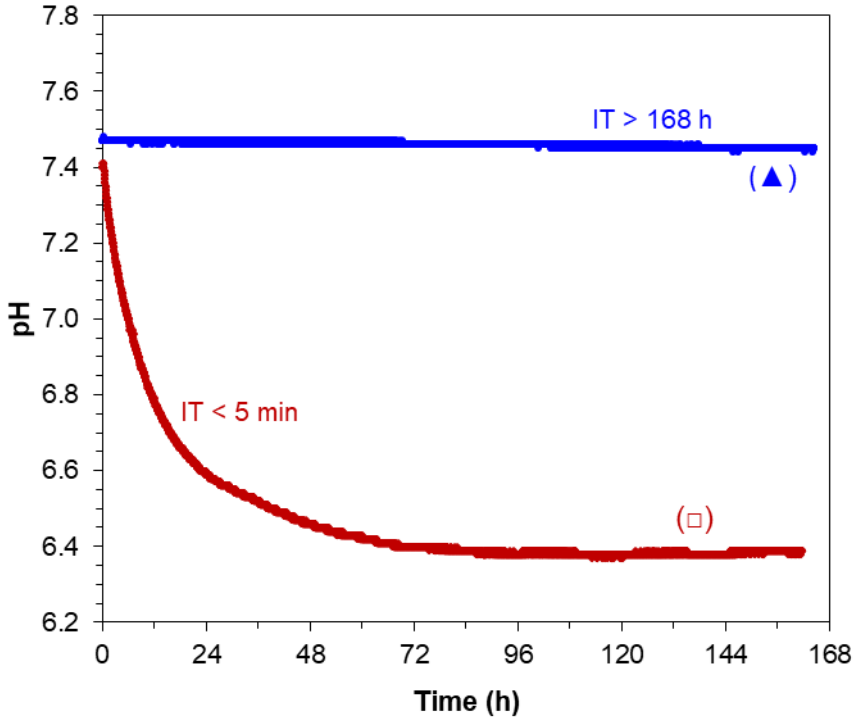

Figure S4.1 *Induction time (IT) of the (▲) real RO concentrate at 85 % recovery without antiscalant, and (□) artificial RO concentrate of 85 % recovery without antiscalant*

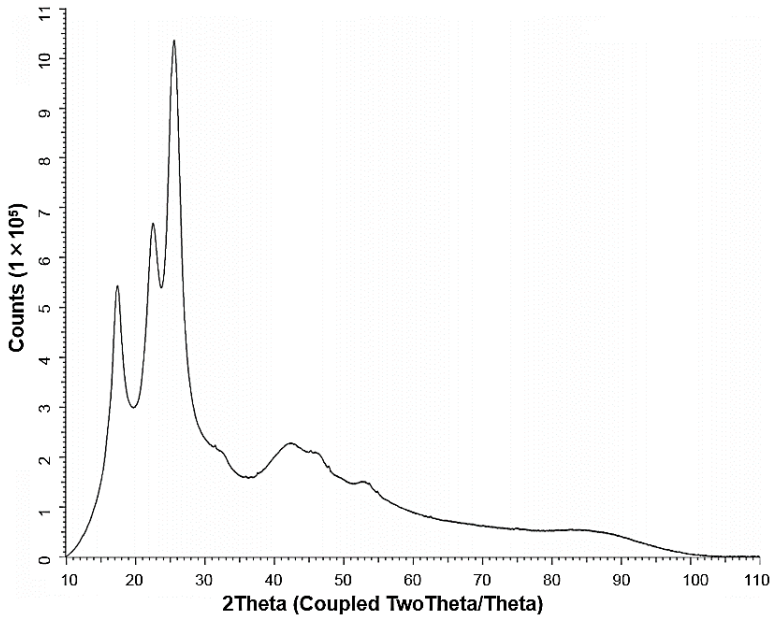

Figure S4.2 *XRD analysis of the fouled membrane (tail element) of the 3rd stage*

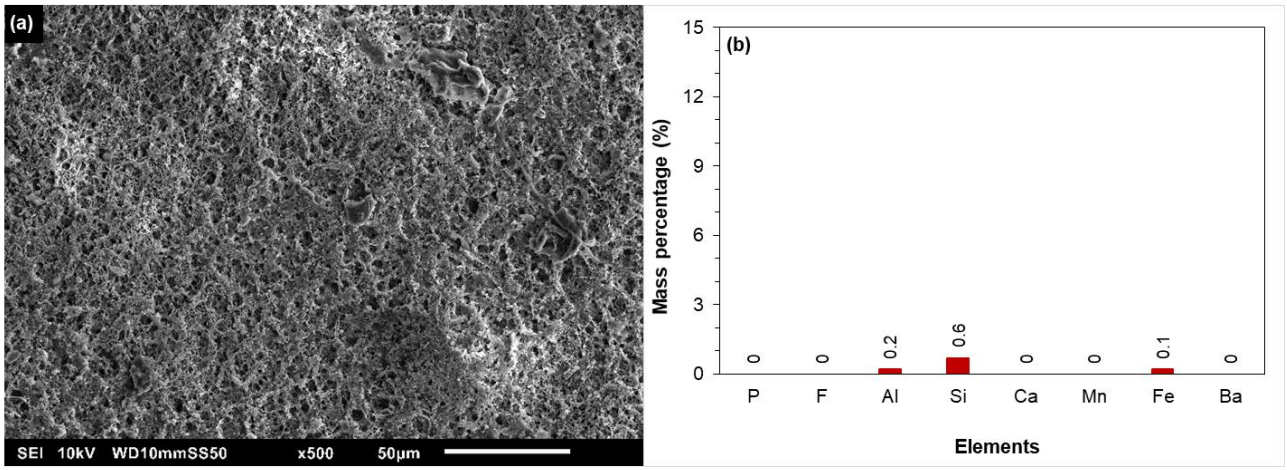

Figure S4.3 (*a) SEM image and (b) EDX analysis of the 0.45 µm filter after filtration of the 0.05 M HCl solution (of the tail element of the 3rd stage)*

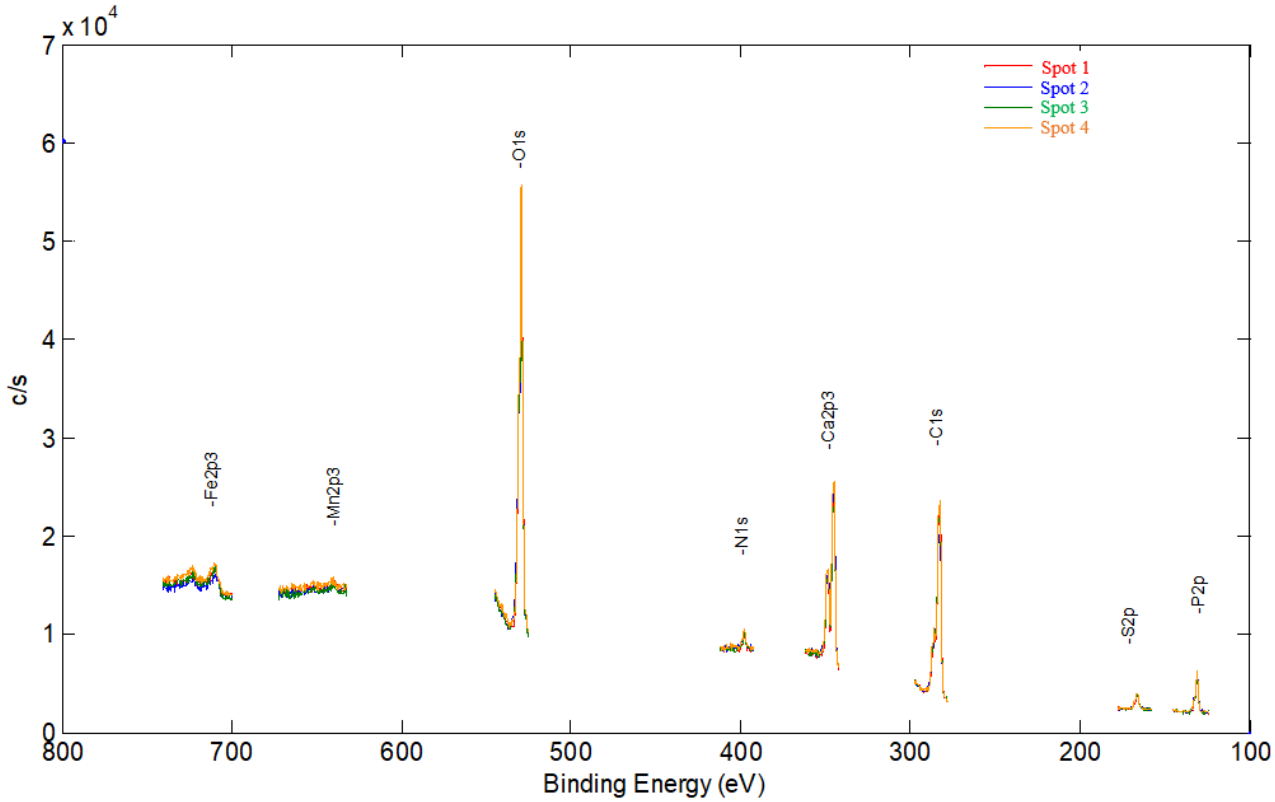

Figure S4.4 (*a) XPS analysis (from 4 different spots) of the fouled membrane (tail element) of the 3rd stage*

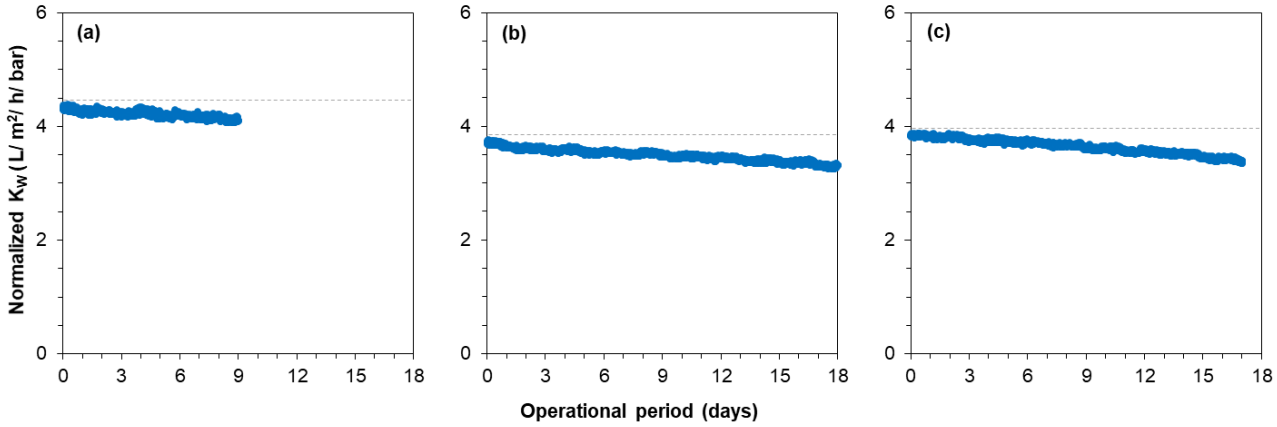

Figure S4.5 *a) Average normalized permeability of the last stage of the RO unit at 83% recovery (a) without antiscalant, (b) with 2.0 mg/L AS–1, and (c) with 2.0 mg/L AS–2*

5

EFFECTIVENESS OF ANTISCALANTS IN PREVENTING CALCIUM PHOSPHATE SCALING IN REVERSE OSMOSIS APPLICATIONS

This chapter is based on the following publication:

M.N. Mangal, S.G. Salinas-Rodriguez, J. Dusseldorp, A.J.B. Kemperman, J.C. Schippers, M.D. Kennedy, W.G.J. van der Meer, Effectiveness of antiscalants in preventing calcium phosphate scaling in reverse osmosis applications, Journal of Membrane Science, (2021) 119090. https://doi.org/10.1016/j.memsci.2021.119090

Abstract

Antiscalants are well known to prevent the precipitation of carbonate and sulphate scales of calcium in reverse osmosis (RO) applications, but according to literature their inhibitory ability against calcium phosphate is not clear. The objective of this study was to investigate if antiscalants, without acid addition, can prevent calcium phosphate scaling in RO systems. Eight calcium phosphate antiscalants from different manufacturers spanning a range of concentrations were tested in batch (in glass reactors) experiments to inhibit the formation of calcium phosphate in synthetic concentrate corresponding to 85 % recovery (Ca^{2+}=765 mg/L, PO_4^{3-}=13–15 mg/L and pH=7.6) of a groundwater RO in the Netherlands. Additionally, once-through lab-scale RO tests were conducted where an RO element was fed with synthetic concentrate and the performance of antiscalants was evaluated from the rate of flux-decline in the RO element. Without antiscalant addition, a substantial flux-decline was observed due to the deposition of amorphous calcium phosphate (ACP) on the RO membrane. The tested antiscalants were unable to inhibit the formation of ACP and were incapable of preventing the deposition of the formed ACP particles, since with each antiscalant, the flux of the RO element decreased at least 15 % in a 3-hour period. Briefly, the available antiscalants, tested in this study, did not provide acceptable inhibition of calcium phosphate scaling in RO applications.

5.1 INTRODUCTION

With the continuous development of RO technology, its application is not limited to only seawater desalination (ca. 40 Mm^3/day worldwide capacity), but RO is also increasingly applied in producing drinking water from (brackish) groundwater and surface water (ca. 28.5 Mm^3/day worldwide capacity) as well as in the treatment of secondary wastewater effluent (ca. 8 Mm^3/day worldwide capacity) (DesalData, 2020). To reduce the operational costs of RO and its impact on the environment, it is favourable to have the recovery of the RO as high as possible, since the specific energy consumption (kWh/m^3) and the production of concentrate (waste) are both low at high recoveries. However, in brackish water RO (BWRO) applications, RO recovery is generally limited due to membrane scaling. Scaling is the precipitation of sparingly soluble salts at the membrane surface which may occur when the concentration of the salts on the membrane surface exceeds their solubility limits. Depending on the feed water composition, various compounds can precipitate on the surface of RO membranes such as calcium carbonate, calcium sulphate, barium sulphate, etc. Furthermore, in the RO treatment of wastewater and groundwater containing high phosphate and calcium concentrations, calcium phosphate may also be a problematic compound limiting RO recovery. This study focuses on calcium phosphate scaling in BWRO systems.

Calcium phosphate can exist in various forms such as an amorphous phase, i.e., ACP and in crystalline phases namely, monocalcium phosphate monohydrate ($Ca(H_2PO_4)_2 \cdot H_2O$; MCPD) and its anhydrous form, dicalcium phosphate dihydrate ($CaHPO_4 \cdot 2H_2O$; DCPD) and its anhydrous form, β-tricalcium phosphate (β–$Ca_3(PO_4)_2$; β–TCP), hydroxyapatite ($Ca_5(PO_4)_3(OH)$; HA) (Dorozhkin, 2016). In RO applications, not all of the mentioned phases could be encountered. For instance, the formation of MCPD, DCPD and their anhydrous forms occur at pH values below 6.5 (Dorozhkin, 2016), and therefore their precipitation in RO applications where pH is above 7 is less likely. Additionally, the formation of β-TCP occurs at temperatures above 700 °C (Bohner et al., 1997), thus it cannot be observed in RO systems. The formation of HA, which is the most thermodynamically stable and least soluble phase of calcium phosphate, could occur in the neutral to basic pH range (Eanes, 1998). However, its formation normally is preceded by ACP (Meyer and Weatherall, 1982, Brečević and Füredi-Milhofer, 1976, Eanes and Posner, 1965, Walton et al., 1967, Termine, 1972) which suggests that HA may not be the first species responsible for flux decline in RO applications.

ACP, as generally agreed, is the first phase of calcium phosphate that forms in the nearly neutral to basic pH range when its solubility is exceeded (Amjad, 1997). Dorozhkin (2016) suggested that ACP may not occur as an individual compound of calcium phosphate, but simply as an amorphous precursor and state of other crystalline calcium phosphate species. The stability of ACP can be affected by various factors including but not limited to pH, temperature and presence of other ions (Combes and Rey, 2010). It is reported that at higher pH values until 10–10.5, the life time of ACP increases and becomes more stable, while in the acidic pH range (3–4), ACP has a shorter life time (few minutes) and is transformed to DCPD (Eanes, 1998). LeGeros et al. (2005) reported that the formation of ACP was preferred and the conversion of ACP to HA was hindered in the presence of magnesium, ferrous and carbonate. Furthermore, it is reported that in the presence of humic substances, i.e., humic acid, the transformation of ACP to other phases is hindered (Ge et al., 2019, Alvarez et al., 2004). Based on this information, one may recognise that the formation of ACP is favoured in RO concentrates when high concentrations of calcium and phosphate are present in the feed water. Therefore, the amorphous phase (and not the crystalline phases) of calcium phosphate may be the first compound that could form and cause flux decline in RO processes where pH is above 7.

It is well established that the problem with the crystalline scales, i.e., $CaCO_3$, $BaSO_4$, $CaSO_4$, etc. can be alleviated with the addition of antiscalants to the RO feed (Greenlee et al., 2010, Rahman, 2013, Salman et al., 2015). However, it is not clear if antiscalants can be effective in preventing flux decline in RO caused by the deposition of ACP particles. In general, the main mechanisms of the antiscalants in preventing scale formation are grouped into three categories: threshold inhibition, crystal distortion, and dispersion (Darton, 2000). For the antiscalants to be effective against ACP, they should

be able to either hinder the formation of ACP particles, i.e., prolonging the induction time due to their threshold inhibition mechanism and/or should not allow the deposition of the formed ACP particles on the RO membranes, i.e., by adsorbing on the particles and reducing their affinity to adhere on the membrane surface due to their dispersion capabilities.

Until now, the role of antiscalants in hindering the formation and deposition of ACP particles on the membrane surface is ambiguous. For instance, Chesters (2009) reported that an antiscalant (a blend of phosphonates and carboxylic acids) was effective in preventing calcium phosphate scaling in a waste water re-use plant at 75 % recovery with calcium and orthophosphate concentrations of 160 mg/L and 15–25 mg/L in the feed water, respectively. Furthermore, Chesters (2009) stated that a small dose (2–5 mg/l) of the mentioned antiscalant can raise the solubility of calcium phosphate 150 times which can eliminate the use of acids in wastewater RO applications (where calcium phosphate is a major challenge due to high phosphate levels in the feedwater, typically 10–30 mg/l) to control calcium phosphate scaling.

Greenberg et al. (2005), on the other hand, reported that antiscalants (including the antiscalant which was a blend of phosphonates and carboxylic acids) were not effective in preventing calcium phosphate precipitation on the RO membrane when fed with a synthetic concentrate solution (Ca^{2+} = 330 mg/L, PO_4^{3-} = 28 mg/L). In their study, however, experiments were performed using a tubular RO membrane where permeate and concentrate were recycled back to the feed tank. RO pilot studies conducted with concentrate/permeate recirculation are often a matter of debate among researchers for not being representative to the conditions of full scale RO systems because of: (*i*) the residence time in a recycled system is much longer (in the range of hours) than the residence time (< 1 min) of the concentrate in the last stage of full scale RO plants, and (*ii*) recycling of concentrate back to the feed tank may accelerate the process of scaling as micro(crystals) may be formed. Furthermore, antiscalant manufacturers emphasize that antiscalants may not be as effective in recycled systems as they should be in once-through flow systems (like RO systems) and therefore the performance of antiscalants assessed in recycled systems may not be representative.

From the available literature, one may realize that until now a study to investigate the performance of antiscalants in preventing the formation and deposition of ACP in RO systems using once-through RO experiments with synthetic solutions (where calcium and phosphate are the only precipitating ions) is not available. Additionally, as new antiscalants have been introduced to the market over the years, there is a need for a study to assess the performance of commercially available antiscalants in preventing the deposition of ACP in RO processes.

In this study, the effectiveness of eight antiscalants (dispersants), available for calcium phosphate, from seven different antiscalant manufacturers in preventing the formation and deposition of ACP particles in RO was investigated. A once-through lab-scale RO setup, without recycling the concentrate/permeate back to the feed, was developed to test the performance of the antiscalants. In this study, the following questions are addressed:

- Can ACP particles cause flux decline in RO applications?
- Can antiscalants inhibit the formation of ACP particles?
- If antiscalants are unable to inhibit the formation of ACP particles, can they prevent the deposition of the formed ACP particles in RO systems?

5.2 MATERIALS AND METHODS

5.2.1 Synthetic concentrate solutions and tested antiscalants

Experiments were performed with synthetic concentrate solutions having the same calcium and orthophosphate concentrations that were present in real RO concentrates of 80 and 85 % recoveries in an RO system treating anaerobic groundwater (Ca^{2+} = 115 mg/L, PO_4^{3-} = 2.1 mg/L and pH = 7.05) in the Netherlands. More precisely, the synthetic concentrate of 80 % recovery contained approximately 575 mg/L of Ca^{2+}, 10.5 mg/L of PO_4^{3-} and had a pH about 7.4, and the synthetic concentrate of 85 % recovery contained 767 mg/L of Ca^{2+}, 14 mg/L of PO_4^{3-}, and had a pH of 7.6. The concentration of bicarbonate in the synthetic concentrate solutions was approximately 200 mg/L for the pH adjustment. To prepare the synthetic concentrate solutions, Milli-Q water, with a conductivity < 10 µS/cm and total organic carbon (TOC) < 30 µg/L, was used. Milli-Q was obtained by treating tap water with the Elix® Advantage system (Merck Millipore). To prepare the synthetic solutions, ACS grade chemicals of $CaCl_2 \cdot 2H_2O$, $NaHCO_3$, KH_2PO_4 from Merck were employed.

The scaling tendency, i.e., saturation index (SI) of calcium phosphate in the synthetic concentrate of 80 and 85 % recoveries was calculated using Visual MINTEQ (version 3.1), Hydranautics IMS-Design (version 2.227.85) and with the projection programs of various antiscalant manufacturers.

In general, the antiscalant dose recommended by the antiscalant suppliers lies in the range between 2 to 5 mg/L in the feed water (Hydranautics., 2013). In this study, antiscalant doses of 2 mg/L and 5 mg/L in the feed water were tested which corresponded to 13.3 mg/L and 33.3 mg/L in the synthetic concentrate of 85 % recovery, respectively. The doses greater than 5 mg/L was not employed, since the maximum antiscalant dose recommended by the antiscalant suppliers was 5 mg/L. In this study, the actual names of the eight tested antiscalants (dispersant) were replaced with arbitrary names. In Table 5.1,

the arbitrary names of the tested antiscalants with some properties which were shared by the antiscalant suppliers are presented.

Table 5.1 *Properties of the tested antiscalants with their arbitrary names assigned in this study*

Antiscalants[⌂]	pH	Specific gravity	Chemical nature
AS–A	6.0–6.4	1.14–1.16	Blend of phosphonates and carboxylic acids
AS–B	4.5–6.5	1.15 ± 0.05	Proprietary acrylic polymer with chelate agent
AS–C	4.0–4.5	1.15	A group of aminophosphonate
AS–D	2.0–3.0	1.22–1.26	Phosphinocarboxylic acid
AS–E	3.0 ±	1.10 ± 0.05	Information not available
AS–F	3.5	1.16	Polycarboxylate
AS–G	4.5	1.22	Sulfonated Polycarboxylate
AS–H	4.0	1.26	A modified polycarboxylate

[⌂]The actual names of the antiscalants are replaced with the arbitrary names.

5.2.2 Experiments in the Applikon glass reactors to study the formation of ACP

To investigate the effect of antiscalants on the formation of ACP, experiments were performed with the synthetic concentrate solutions in an air-tight double wall 3 L Applikon (Delft, Netherlands) glass reactor. A schematic diagram of the experimental setup is illustrated in Figure 5.1. The internal diameter and height of the reactor were 12 cm and 24 cm, respectively. The reactor consisted of a mixing controller and a shaft to allow the solution to be stirred at a rate of 150 rpm. A thermostat was employed for maintaining a constant temperature of 20 °C during the test.

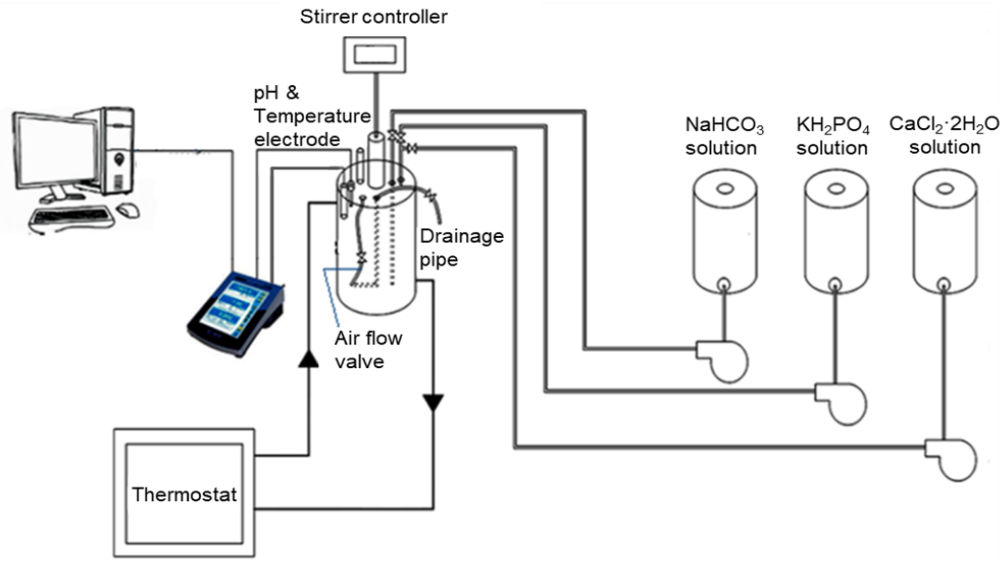

Figure 5.1 *Batch setup for calcium phosphate scale inhibition studies*

To run an experiment, the 3 L reactor was initially half-filled with $NaHCO_3$ and KH_2PO_4 solutions. Then, the pH was adjusted to the desired value (7.5–7.6) using a 0.1 M NaOH solution or 0.1 M HCl solution. Following this, antiscalant was added to the solution of $NaHCO_3$ and KH_2PO_4. Afterwards, the remaining half of the reactor was filled with the $CaCl_2 \cdot 2H_2O$ solution through the fine nozzles located 3 cm from the bottom of the reactor to maintain the uniform distribution of the solution. While adding the $CaCl_2 \cdot 2H_2O$ solution, the mixture in the reactor was stirred at 150 rpm to allow uniform mixing of the solutions and to avoid the occurrence of any local supersaturated zones.

5.2.3 Turbidity measurements

To detect the formation of calcium phosphate in the synthetic concentrate solutions, turbidity measurements were conducted using the HACH Turbidimeter (Model 2100AN, USA). The measurements were executed immediately after filling the reactor with $CaCl_2 \cdot 2H_2O$ solution, and every 15 minutes thereafter. For each turbidity measurement, approximately 30 mL of the solution was taken from the reactor. An increase in turbidity from the initial turbidity values (0.08 NTU) of the individual synthetic solutions of $CaCl_2 \cdot 2H_2O$, $NaHCO_3$ and KH_2PO_4 would indicate the formation of precipitates, i.e., calcium phosphate.

At the end of each experiment, the reactor was filled with 0.2 M HCl to dissolve any calcium phosphate particles attached to the reactor. The HCl solution was stirred at 1250 rpm for 30 min. After acid cleaning, the reactor was flushed twice with demineralized water for 10 min.

5.2.4 Dead-end filtration tests with 0.45 µm and 100 kDa membrane filters

To detect the presence of ACP in the synthetic concentrate solutions in case of no increase in turbidity, the synthetic concentrate solutions were filtered either *(i)* at constant pressure of 2 bar through 0.45 µm filters (cellulose acetate, Whatman) where the filtration volume was between 1–1.5 L, and/or *(ii)* at constant flux of 100 $L/m^2/h$ through a 100 kDa filter (Polyether sulfone, Merck) where the filtration volume was between 40–50 mL. In the former case, a decrease in flux, whereas in the latter case, an increase in pressure would indicate the presence of formed particles in the synthetic concentrate solutions since no decrease in flux (in the former case) and increase in pressure (in the latter case) would occur when the individual solutions of $CaCl_2 \cdot 2H_2O$, $NaHCO_3$ and KH_2PO_4 were filtered. The retained deposits were then examined by scanning electron microscopy (SEM) (JEOL, JSM-6010LA, Japan). Additionally, the deposits on the filter were analysed with X-ray powder diffraction (XRD) (Bruker D8 Advance) to determine the phase of precipitated calcium phosphate.

5.2.5 Particle size measurement

Furthermore, a number of measurements were performed with a Zetasizer-Nano-ZS (Malvern Panalytical) to know the effect of antiscalants on the size of ACP particles, i.e., agglomeration of ACP particles. To measure the particles size of ACP, samples of the synthetic concentrate solution from the Applikon glass reactor were taken immediately after filling the reactor with $CaCl_2 \cdot 2H_2O$ solution and directly at the end of each experiment (ca. 60 min).

5.2.6 Lab-scale RO experiments

To evaluate the performance of antiscalants in preventing ACP deposition in RO systems, a lab-scale RO setup (Figure 5.2) was used. In this setup, as illustrated, antiscalant, HCO_3^-, PO_4^{3-} and NaOH were dosed from stock solutions each at 2 L/h to a stream of demineralized-water (demi-water) with a flow rate of 37 L/h, resulting in a final flow rate of 45 L/h. The dosage of NaOH was executed from a 0.01–0.02 M stock solution to adjust the pH of the final solution to 7.6. To another stream of demi-water (with a flow rate of 43 L/h), Ca^{2+} was dosed from the stock solution at 2 L/h, also resulting in a final flow rate of 45 L/h. Both streams were then connected to a single pipe resulting in the final flow rate of 90 L/h which had nearly the same composition of the synthetic concentrate of 85 % recovery. The final solution (synthetic concentrate solution) was introduced to a 4 L reactor in which the synthetic concentrate solution was stirred at a rate of 200 rpm with a residence time shorter than 1 min. The residence time of less than 1 min was achieved by maintaining equal flow rates (90 L/h) of the synthetic concentrate solution entering and leaving the reactor and by keeping the volume of the synthetic concentrate solution in the reactor to approximately 1.5 L.

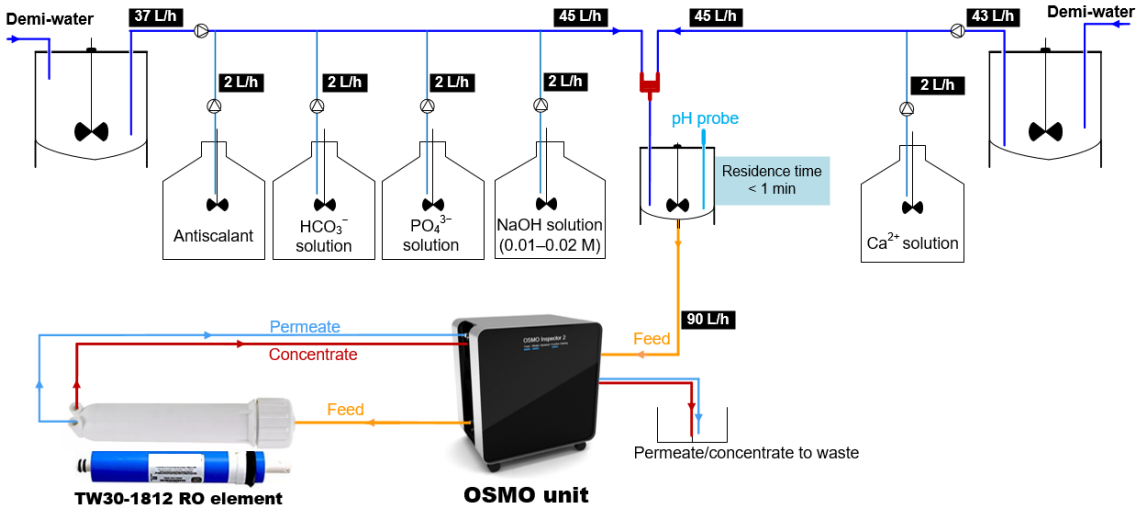

Figure 5.2 *Once-through lab-scale RO setup for calcium phosphate scale inhibition studies*

The synthetic solution was fed at a rate of 90 L/h to a TW30-1812-50 RO element (OsmoPure Water Systems) with the use of an OMSO Inspector unit (Convergence Industry B.V., Netherlands). The OSMO unit was equipped with a very sensitive flow meter (with high accuracy) which could measure the permeate flow rate of 2mL/min (0.12 L/h) to 500mL/min (30 L/h). The piping and instrumentation diagram (P&ID) of the OSMO unit is shown in Figure S1. For each experiment, a new RO element was used. In all experiments, the initial recovery of the membrane element was in the range of 5–6 % and the permeate flux was between 13–15 $L/m^2/h$. According to the membrane manufacturer, the minimum ratio of the concentrate flow to the permeate flow should not drop below 5. In this study, the concentrate flow was 18 times greater than the permeate flow. The cross-flow velocity was in the 10–12 cm/s range. Both permeate and concentrate were directed to the drain. All experiments were carried out at room temperature (20–23 °C).

5.3 RESULTS AND DISCUSSION

5.3.1 Scaling potential of calcium phosphate in the synthetic concentrates of 80 and 85 % recoveries

In Table 5.2, SI values of various phases of calcium phosphate, calculated with Visual MINTEQ, for the synthetic concentrate solutions of 80 and 85 % recoveries are presented.

Table 5.2 *SI of calcium phosphate phases for the synthetic concentrates of 80 and 85 % recoveries with Visual MINTEQ*

Compound	Formula	R = 80 %	R = 85 %
ACP	$Ca_3(PO_4)_2$	− 0.70	0.13
DCPD	$CaHPO_4{\cdot}2H_2O(s)$	− 0.23	− 0.07
β-TCP	$Ca_3(PO_4)_2$ (beta)	2.97	3.79
OCP	$Ca_4H(PO_4)_3{\cdot}3H_2O(s)$	2.16	3.15
HA	$Ca_{10}(PO_4)_6(OH)_2$	11.50	12.94

As can be seen, all crystalline phases of calcium phosphate, except DCPD, were supersaturated at both 80 and 85 % recoveries. The formation of DCPD, as discussed earlier in section 5.1, occurs in the acidic pH range and therefore its precipitation in the synthetic concentrate of 80 % (pH = 7.4) and 85 % (pH = 7.6) recoveries used in this research is not likely. Additionally, the precipitation of β-Tricalcium phosphate in the synthetic concentrate solutions is also not expected since it forms at very high temperatures as mentioned earlier in section 5.1. This means that octacalcium phosphate and hydroxyapatite are the crystalline calcium phosphate species that might precipitate in

the synthetic solutions of 80 and 85 % recoveries. Whether these compound(s) and which compound(s) exactly will cause flux-decline in RO, will be addressed shortly in the coming sections. In addition, the program suggested that ACP may form in the synthetic concentrate of 85 % recovery as SI was greater than zero, while its formation in the synthetic concentrate of 80 % is not likely since the SI value was negative.

Based on the Hydranautics IMS-Design program, calcium phosphate ($Ca_3(PO_4)_2$) was supersaturated at both 85 and 80 % recoveries and the SI values were 2.1 and 1.7, respectively which suggested that calcium phosphate scaling may occur at the aforementioned recoveries. On the other hand, from the Filmtec technical manual (Dow, 2010), in which the formula of Kubo et al. (1979) is mentioned for the determination of the saturation level of calcium phosphate, the calculated SI value of calcium phosphate ($Ca_3(PO_4)_2$) for the synthetic concentrate of 80 % recovery was −0.25 which suggested that calcium phosphate scaling at the aforementioned recovery is unlikely. Whereas, for the synthetic concentrate of 85 % recovery, the SI value with the formula proposed by Kubo et al. (1979) was 0.33 which indicated that calcium phosphate scaling may occur at 85 % recovery.

According to the projection programs of some antiscalant suppliers, calcium phosphate with the chemical formula $Ca_3(PO_4)_2$ was undersaturated at both 85 and 80 % recoveries and according to some others, the SI of calcium phosphate was considered in the safe range which meant that calcium phosphate precipitation would not occur at these recoveries. The exact reason for the discrepancies in the SI values given by the projection programs of the antiscalant suppliers is not known but it could be that every program uses a different method to determine the saturation level of calcium phosphate or perhaps the discrepancy comes from the differences in the reported values of solubility products for calcium phosphate in literature. For instance, in the case of ACP, it is challenging to precisely determine its solubility and therefore different solubility products were given by various researchers (Combes and Rey, 2010, Dorozhkin, 2012).

In brief, at this point, it is not clear whether or not the formation of calcium phosphate, or more precisely, the formation of ACP would occur in the synthetic concentrate of 85 and 80 % recoveries due to the differences in the SI levels. The formation of calcium phosphate at both 85 and 80 % will be investigated in the coming sections.

5.3.2 Formation of ACP in the synthetic concentrates of 80 and 85 % recoveries

In section 5.3.1, it became difficult to know if calcium phosphate would form in the synthetic concentrates of 80 and 85 % recoveries due to the discrepancies in the SI values. In this section, the question "*Does calcium phosphate form in the synthetic concentrate*

of 80 and 85 % recoveries, and if it does, which phase(s) of calcium phosphate would form in the synthetic concentrates?" is addressed.

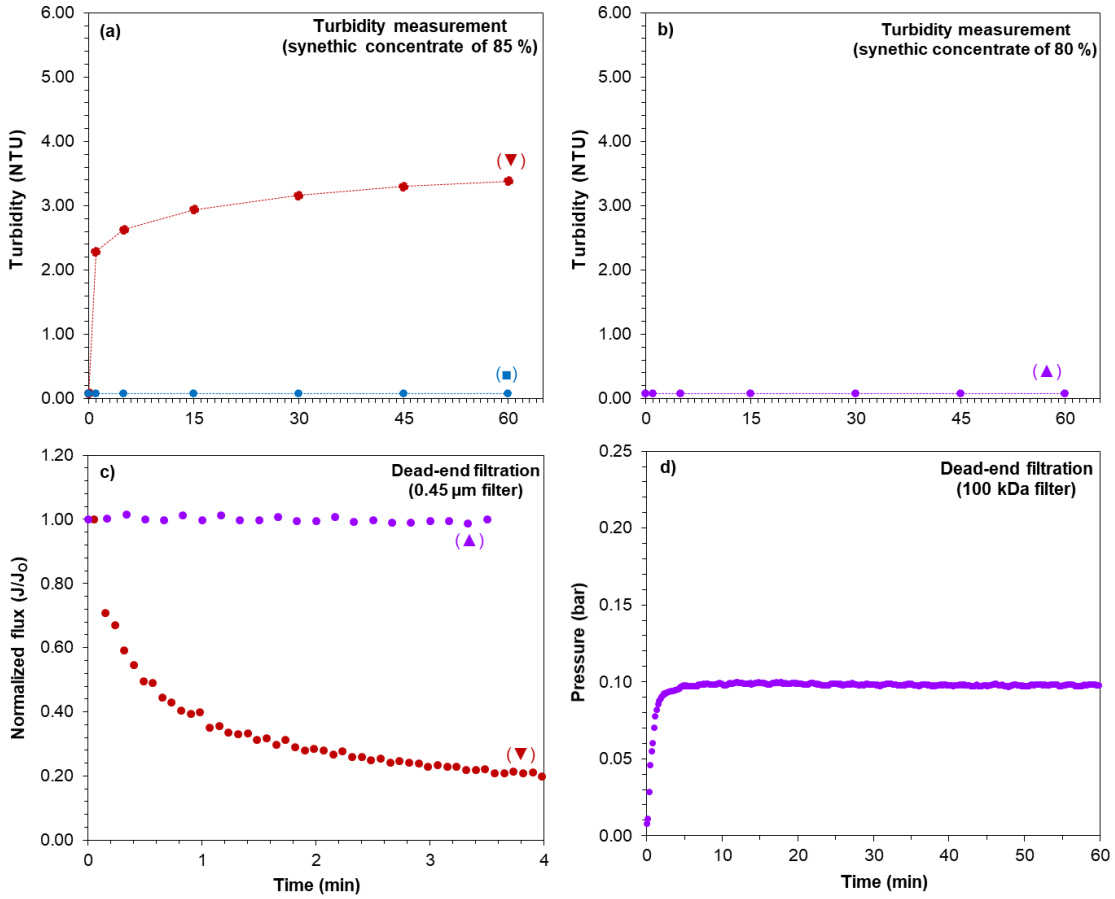

Figure 5.3 *a) Turbidity values of the (▼) synthetic concentrate of 85 %, and (■) synthetic concentrate of 85 % (without phosphate), b) turbidity values of the (▲) synthetic concentrate of 80 % , c) Normalized flux of the (▼) synthetic concentrate of 85 %, and (▲) synthetic concentrate of 80 % when each filtered through 0.45 µm filter at constant pressure of 2 bar, and (d) pressure to maintain the constant flux of 100 L/m^2/h of the synthetic concentrate of 80 % when filtered through 100 kDa filter*

In Figure 5.3a, turbidity values of the synthetic concentrate solutions of 85 % recovery are shown. As illustrated, the formation of ACP (explained later in Figure 5.4a and Figure 5.4c) in the synthetic concentrate solution of 85 % recovery was immediate. In less than 1 min, the turbidity value of the synthetic concentrate increased from 0.08 NTU to approximately 2.1 NTU which further increased to approximately 3.4 NTU after 60 min. This result showed that ACP was supersaturated at 85 % recovery and the projection programs of some antiscalant suppliers underestimated the saturation level (SI < 0) of ACP. It is worth mentioning that the observed increase in turbidity in Figure 5.3a was only due to the formation of ACP. Although $CaCO_3$ was also supersaturated (SI = 0.9) in

the synthetic concentrate of 85 %, its formation did not occur during the experiment which can be clearly seen from the turbidity values of the synthetic concentrate of 85 % recovery in the absence of phosphate (Figure 5.3a). The turbidity values of the synthetic concentrate, in the absence of phosphate, did not increase from the initial value of 0.08 NTU during the entire experiment. In addition, pH of the synthetic concentrate of 85 % was monitored and no decrease in pH was observed which confirmed that $CaCO_3$ did not precipitate in the solution and had an induction time of longer than 60 min.

In Figure 5.3b, turbidity values of the synthetic concentrate of 80 % recovery are shown. As can be seen, turbidity of the synthetic concentrate did not increase in 60 min which suggested that ACP did not form at this recovery. In Figure 5.3c, flux of the synthetic concentrate solutions of 80 and 85 % recoveries when filtered through 0.45 µm filter at constant pressure of 2 bar is shown. As can be seen, no decrease in flux was observed when 1.4 L of the synthetic concentrate of 80 % recovery was filtered which also indicated that ACP did not form in the solution, while flux decreased by about 80 % after filtering approximately 0.4 L of the synthetic concentrate of 85 % recovery. In Figure 5.4a, SEM pictures of the 0.45 µm filter after filtering the synthetic concentrate of 85 % is shown. The retained deposits on the 0.45 µm filter were amorphous since crystalline peaks, resembling with the peaks of OCA and HA, were not observed in the XRD analysis as illustrated in Figure 5.4c. This indicated that ACP formed first before the formation/precipitation of crystalline phases of calcium phosphate, i.e., octacalcium phosphate and hydroxyapatite. This observation is in agreement to the findings of some researchers (Eanes et al., 1965, Feenstra and De Bruyn, 1981) in applications other than RO.

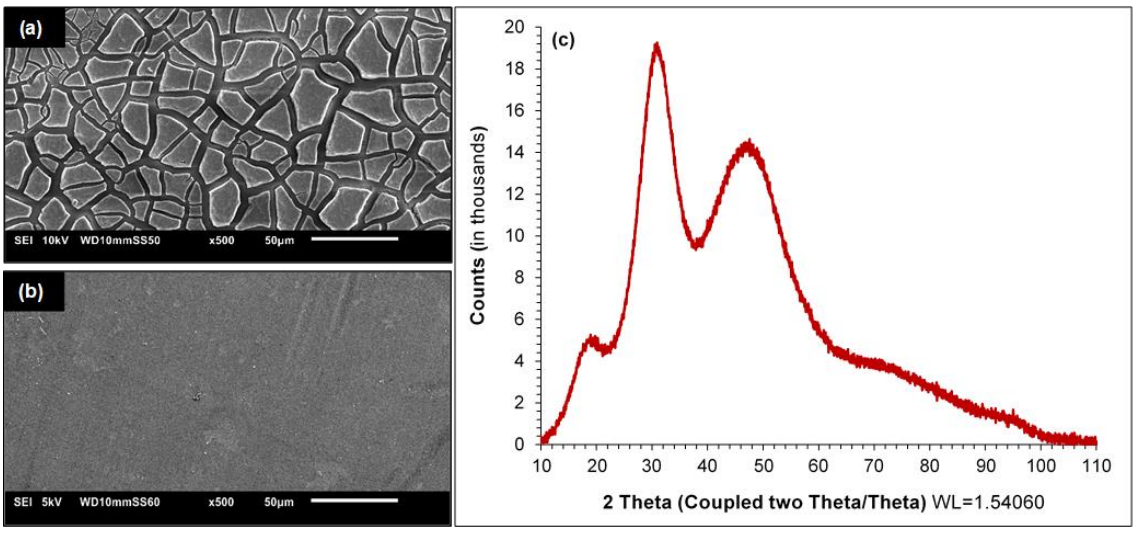

Figure 5.4 *a) SEM image (500x magnification) of the 0.45 µm after filtering the synthetic concentrate of 85 % recovery, b) SEM image (500x magnification) of the 100 kDa filter after filtering the synthetic concentrate of 80 % recovery, and c) XRD analysis of the retained deposits on the 0.45 µm filter after filtering the synthetic concentrate of 85 % recovery*

One may argue that the constant flux with the synthetic concentrate of 80 % in Figure 5.3c could be due the fact that ACP particles were much smaller than 0.45 µm which possibly were not retained on the filter. However, this was not the case since no increase in pressure was observed when the concentrate of 80 % recovery was filtered through a 100 kDa filter (with an average pore size of 10 nm) at constant flux of 100 L/m^2/h (Figure 5.3d). Furthermore, no particles were observed on the 100 kDa filter in the SEM analysis as illustrated in Figure 5.4b which revealed that ACP did not form in the synthetic concentrate of 80 % recovery.

5.3.3 Flux decline in RO applications due to the deposition of ACP particles

In the previous section, it was found that the formation of ACP occurred in the synthetic concentrate of 85 % recovery, while it did not form in the synthetic concentrate of 80 % recovery. In this section the question "*Can ACP particles, in the absence of antiscalants, deposit on the membrane surface and cause flux decline in RO applications*?" is addressed with the use of lab-scale RO.

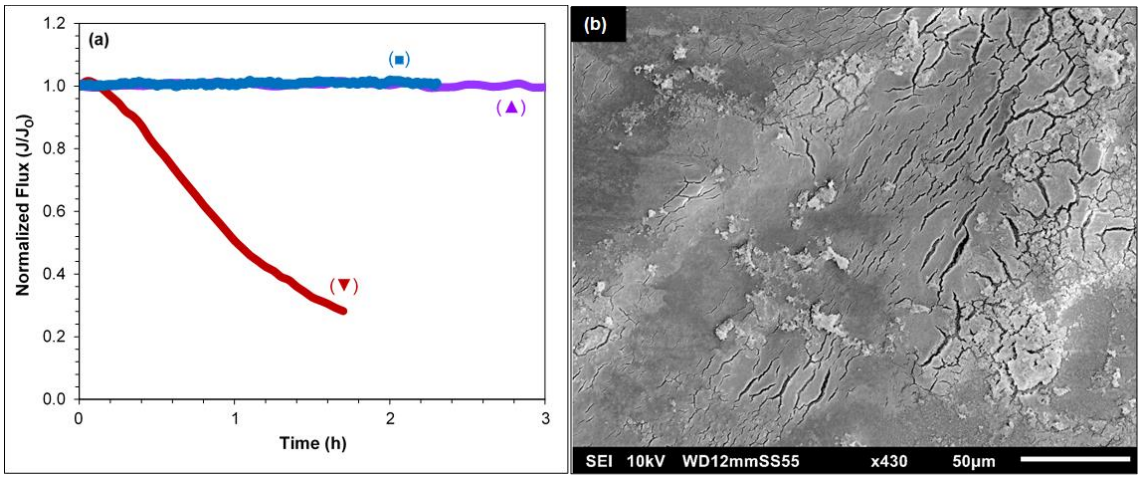

Figure 5.5 *(a) Normalized flux of the TW30-1812-50 RO element fed with (▼) synthetic concentrate of 85 % recovery (with phosphate) without antiscalant addition, (■) synthetic concentrate of 85 % recovery in the absence of phosphate and antiscalant, and (▲) synthetic concentrate of 80 % recovery (with phosphate) without antiscalant addition, (b) SEM image of the membrane surface of the RO element fouled with the synthetic concentrate of 85 % recovery (with phosphate) without antiscalant*

Figure 5.5a presents the normalized flux of the TW30-1812-50 RO element when fed *(i)* with the synthetic concentrate of 85 % recovery which contained phosphate ions but no antiscalant, *(ii)* with the synthetic concentrate of 85 % which contained neither phosphate nor antiscalant, and *(iii)* with the synthetic concentrate of 80 % recovery which contained phosphate ions but no antiscalant. As can be seen, the normalized flux decreased sharply, i.e., approximately 75 % in less than 2 h when the RO element was fed with the synthetic

concentrate of 85 % recovery which contained phosphate but no antiscalant. The sharp decrease was caused due to the deposition of ACP particles which formed a cake layer on the membrane surface as illustrate in Figure 5.5b.

On the other hand, the normalized flux remained constant when the RO element was fed with the synthetic concentrate of 85 % recovery (in the absence of phosphate) without antiscalant addition. The purpose of the second experiment (with the synthetic concentrate of 85 % in the absence of phosphate) was to verify that the flux decline in the first experiment (with the synthetic concentrate of 85 % in the presence of phosphate) was only due to ACP and that calcium carbonate formation/precipitation did not contribute to the observed flux decline. It was expected that the precipitation of calcium carbonate would not occur in the RO element since it was already known from the turbidity measurements (Figure 5.3a) and the stable pH throughout the experiment.

Furthermore, as illustrated in Figure 5.5a, the normalized flux of the RO element fed with the synthetic concentrate of 80 % recovery remained constant for an experimental period of 3 h which is in agreement with the results of the batch experiments (Figure 5.3c) where no increase in turbidity was observed. This suggested that ACP may not be an issue at 80 % recovery. It is worth mentioning that the experiment was run for a period of 3 h, but if the unit was run for a period longer than a week or even month(s), would other phases of calcium phosphate such as Hydroxyapatite (SI = 11.5) precipitate on the membrane? This is an open question which was not addressed here as it was beyond the scope of this study. It is, however, difficult to run a once-though experiment with synthetic concentrate for long periods of time since this requires the use of a massive amount of high-grade chemicals.

In brief, the results presented in Figure 5.5a revealed that ACP particles can deposit on the membrane surface and can cause noticeable flux decline in RO systems.

5.3.4 Effectiveness of antiscalants in hindering the formation of ACP particles

In this section, the question "*Can antiscalants inhibit the formation of ACP particles in RO applications*?" is addressed using the synthetic concentrate of 85 % recovery in batch experiments.

In Table 5.3, turbidity values of the synthetic concentrate of 85 % recovery without antiscalant addition and with 13.3 and 33.3 mg/L of various antiscalants are shown. As can be seen, with 13.3 mg/L of each antiscalant, the turbidity values of the synthetic concentrate increased which indicated that the tested antiscalants at the aforementioned concentration were not effective in preventing the formation of ACP. However, the tested antiscalants had an influence on the formation of ACP. For instance, when antiscalant was not present, turbidity of the synthetic concentrate increased from 0.08 NTU to more

than 3 NTU in 60 min, while with AS–H, the turbidity of the synthetic concentrate solution increased slightly and then remained constant. Actually, the AS–H was not able to inhibit the formation of the ACP particles, but was able to prevent their agglomeration which can be clearly seen from Figure 5.6. As shown, the average particle size of ACP particles, in the presence of 13.3 mg/L of AS–H, remained approximately 50 nm during the 1-hour experimental period. On the other hand, when antiscalant was not added, the average particle size of ACP reached to approximately 1.4 µm in 5 min which further increased to more than 6 µm (exceeding the range of the Zetasizer) in 60 min. This showed that ACP particles agglomerate rapidly over time.

Table 5.3 *Turbidity of the synthetic concentrate of 85 % recovery without antiscalant addition and with 13.3 and 33.3 mg/L of various antiscalants in batch (glass reactor) experiments*

Time	**Turbidity** (NTU)								
(min)	**No AS**	**AS–A**	**AS–B**	**AS–C**	**AS–D**	**AS–E**	**AS–F**	**AS–G**	**AS–H**
0	0.08	0.08	0.08	0.08	0.08	0.08	0.08	0.08	0.08*
		0.08	0.08	0.08	0.08	0.08	0.08	0.08	0.08*
1	2.29	1.13	1.53	0.33	0.25	0.34	0.27	0.57	0.12
		1.56	1.01	0.69	0.08	0.08	0.09	0.08	0.08
15	2.94	1.97	3.01	2.02	0.79	0.39	0.46	0.66	0.12
		4.61	2.57	1.62	0.08	0.08	0.12	0.08	0.08
30	3.16	2.36	3.25	3.13	0.98	0.45	0.53	0.70	0.12
		5.85	3.23	2.26	0.08	0.08	0.18	0.08	0.08
45	3.3	2.83	3.65	3.66	1.24	0.51	0.61	0.73	0.12
		7.01	3.82	2.91	0.08	0.08	0.26	0.08	0.08
60	3.38	3.25	4.06	4.23	1.43	0.55	0.66	0.75	0.12
		7.60	4.19	3.60	0.08	0.08	0.39	0.08	0.08

* A "dashed" underline represents the turbidity value for an antiscalant dose of 13.3 mg/L, while a "solid" underline denotes the turbidity value for an antiscalant dose of 33.3 mg/L.

Furthermore, the turbidity values of the synthetic concentrate with 13.3 mg/L of AS–A, AS–D, AS–E, AS–F, AS–G were also lower than those when antiscalant was not used which can be attributed to the fact that antiscalants suppressed the agglomeration of ACP particles as can be seen from the average particle size measurements presented in Figure 5.6. It is also likely that lower turbidity values in the presence of antiscalants might be due to the formation of fewer ACP particles. Surprisingly, with AS–B and AS–C, the turbidity values of the synthetic concentrate were higher than those without antiscalant. One may suggest that the mentioned two antiscalants might have favoured the agglomeration of ACP particles which, however, was not the case as shown in particle size measurements (Figure 5.6). It could be that the number of ACP particles formed with AS–B and AS–C were higher than the number formed without antiscalant. Yet, the actual reason for the high turbidity values with the mentioned antiscalants is not known and

requires further investigation. This issue was not investigated further in this study as the objective here was to investigate if (commercially) available antiscalants for calcium phosphate can inhibit the formation of ACP particles. Based on the turbidity and particle size results, it can be concluded that none of the tested antiscalants at a concentration of 13.3 mg/L could inhibit the formation of ACP.

From Figure 5.6, it can be observed that some antiscalants had better dispersion capabilities than others. For example, AS–H (a modified polycarboxylate) had the best dispersion capability among all other antiscalants, as the average size of the ACP particles with this antiscalant remained below 0.06 µm throughout the entire experimental period. On the other hand, AS–A (blend of phosphonates and carboxylic acids) and AS–B (proprietary acrylic polymer with chelate agent) exhibited the poorest dispersion capability, as the average particle size of ACP with both antiscalants exceeded 6 µm in 1-hour period.

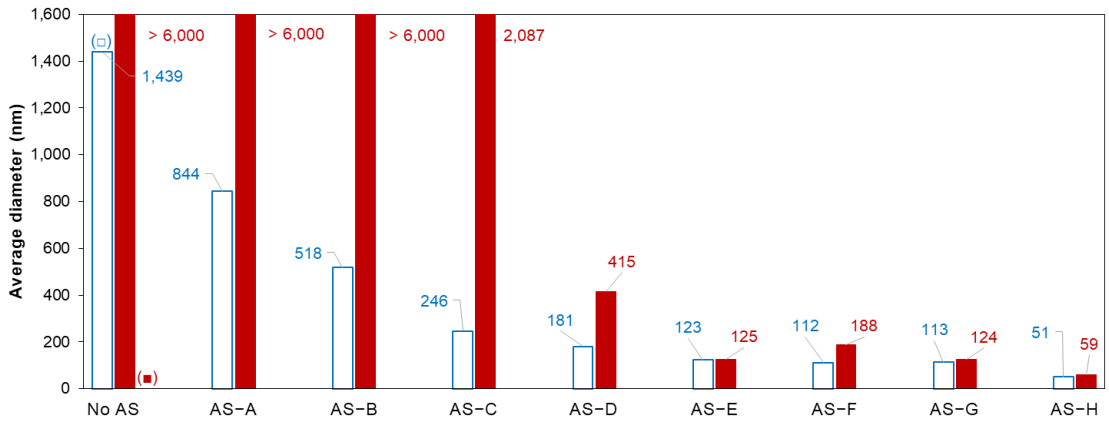

Figure 5.6 *Size measurement of the ACP particles in the synthetic concentrate of 85 % recovery without antiscalant addition and with 13.3 mg/L of various antiscalants at (□) Time < 5 min and (■) Time ≈ 60 min*

In Table 5.3, the turbidity values of the synthetic concentrate of 85 % recovery in the presence of 33.3 mg/L of various antiscalants are also presented. One can see that the formation of ACP particles was not inhibited even when a higher concentration (than 13.3 mg/L) of each AS–A, AS–B, AS–C and AS–F was used, since turbidity increased with each of the mentioned antiscalants. Interestingly, no increase in turbidity was observed in 1-hour period when 33.3 mg/L of each AS–D, AS–E, AS–G and AS–H was added. At first, this result suggested that the formation of ACP particles was inhibited in the presence of 33.3 mg/L of mentioned antiscalants. However, turbidity readings alone were not considered conclusive at this point. It was hypothesized that perhaps the formation of ACP particles occurred in the solution, but their agglomeration was inhibited in the

presence of the aforementioned antiscalants and therefore the size of the ACP particles was too small to be detected by turbidity measurements. To verify this, synthetic concentrate solutions, in the presence of antiscalants with no increase in turbidity (Table 5.3), were initially analysed with the Zetasizer to detect the presence of particles and to determine their size in case they were formed. But, it turned out that the Zetasizer could not provide reliable and conclusive information about the particle size (results not presented), since the measurements didn't meet the quality criteria of the instrument which could be due to the *(i)* presence of particles with sizes smaller than the detection limit of the Zetasizer (< 0.3 nm), *(ii)* presence of very few particles in the solution, or *(iii)* absence of particles in the solution.

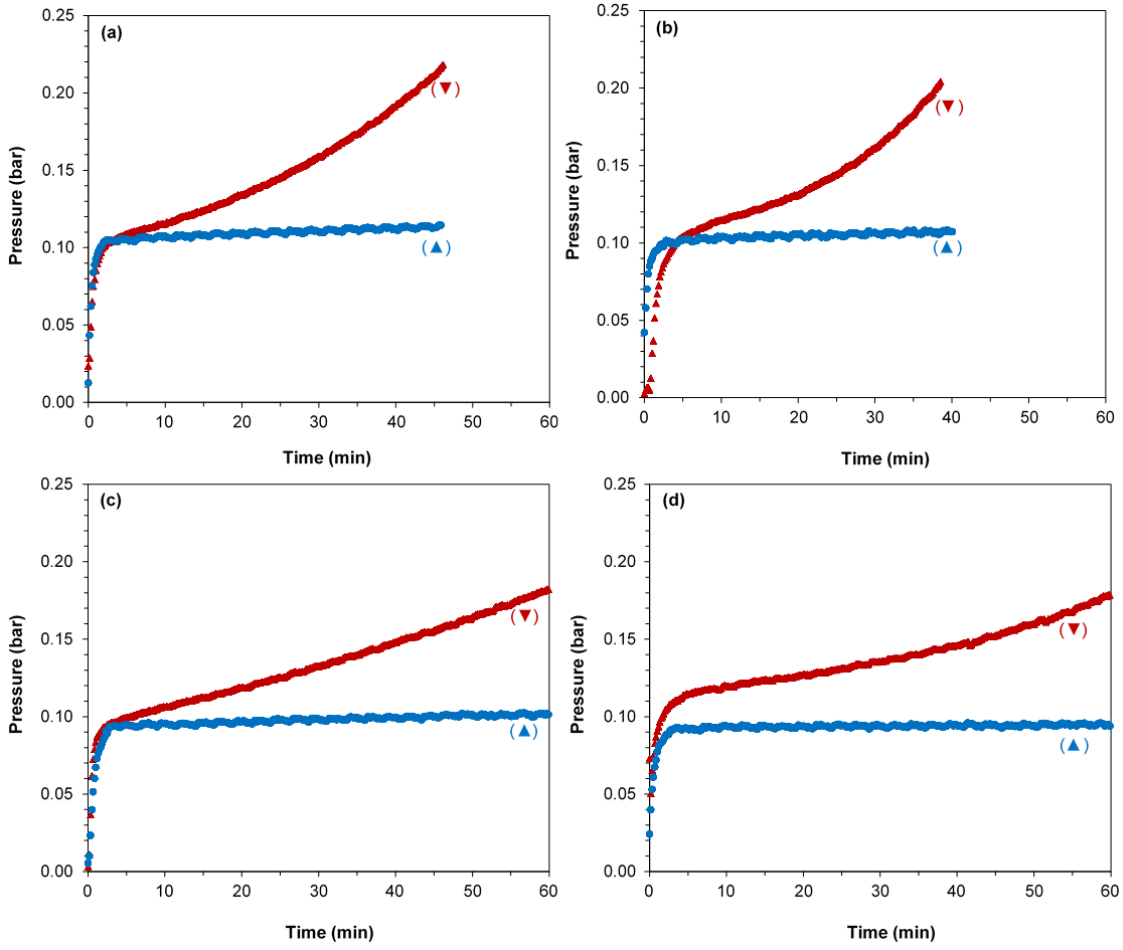

Figure 5.7 *Filtration at constant flux of 100 L/m^2/h through 100 kDa filter of the (▼) synthetic concentrate of 85 % recovery (with phosphate) in the presence of 33.3 mg/L of a) AS–D, b) AS–E, c) AS–G, and d) AS–H, and (▲) synthetic concentrate of 85 % (without phosphate) in the presence of 33.3 mg/L of a) AS–D, b) AS–E, c) AS–G, and d) AS–H*

In parallel with the size measurements, the synthetic concentrate solutions with no increase in turbidity were filtered immediately, after the first turbidity measurement, through 100 kDa filters at a constant flux of 100 L/m^2/h and the increase in pressure to maintain the constant filtration flux was recorded to detect the presence of particles. One can argue that an increase in pressure may not be necessarily attributed to the presence of ACP particles, since the increase in pressure might be caused due to particles which may possibly form from a reaction of calcium with antiscalant. For this reason, synthetic solutions (without phosphate but with the same concentrations of calcium, bicarbonate and antiscalant that were present in the synthetic concentrate of 85 % recovery with no increase in turbidity) were also filtered through 100 kDa filters at a constant flux of 100 L/m^2/h.

As illustrated in Figure 5.7a–d, an increase in pressure was observed when the synthetic concentrate solutions of 85 % recovery in the presence of 33.3 mg/L of each AS–D, AS–E, AS–G and AS–H were filtered at constant flux. On the other hand, pressure did not increase when the synthetic solutions (without phosphate) in the presence of each AS–D, AS–E, AS–G and AS–H were filtered at constant flux. This indicated that there was no formation of particles due to calcium-antiscalant reaction and the observed increase in pressure (Figure 5.7a–d) was due to ACP particles. Therefore, the mentioned antiscalants with a 33.3 mg/L concentration were unable to inhibit the formation of ACP particles in 1-hour period.

Figure 5.8 shows the SEM images of the 100 kDa filters from the filtration experiment of Figure 5.7. As can be seen, the filter surface was covered with ACP particles when the synthetic concentrate solutions of 85 % recovery in the presence of each AS–D, AS–E, AS–G and AS–H were filtered (Figure 5.8a–d), while no particles were observed on the filter surface when the synthetic solutions (without phosphate) with each of the mentioned antiscalants were filtered (Figure 5.8d–h). This revealed that the formation of ACP particles in the synthetic concentrate of 85 % recovery was not inhibited with 33.3 mg/L of AS–D, AS–E, AS–G and AS–H even when no increase in turbidity was observed. The reason for not observing an increase in the turbidity of the synthetic concentrate of 85 % recovery could be due to the formation of fewer ACP particles with very small size by the aforementioned antiscalants.

In brief, none of the tested antiscalants could inhibit the formation of ACP particles. But it may not necessarily mean that the formed ACP particles in the presence of antiscalants would deposit on the membrane surface in RO systems where the filtration mode is not dead-end but cross-flow. It could be that the adsorbed antiscalants (dispersants) on the formed ACP particles may diminish their tendency to deposit on the membrane surface in a cross-flow operation.

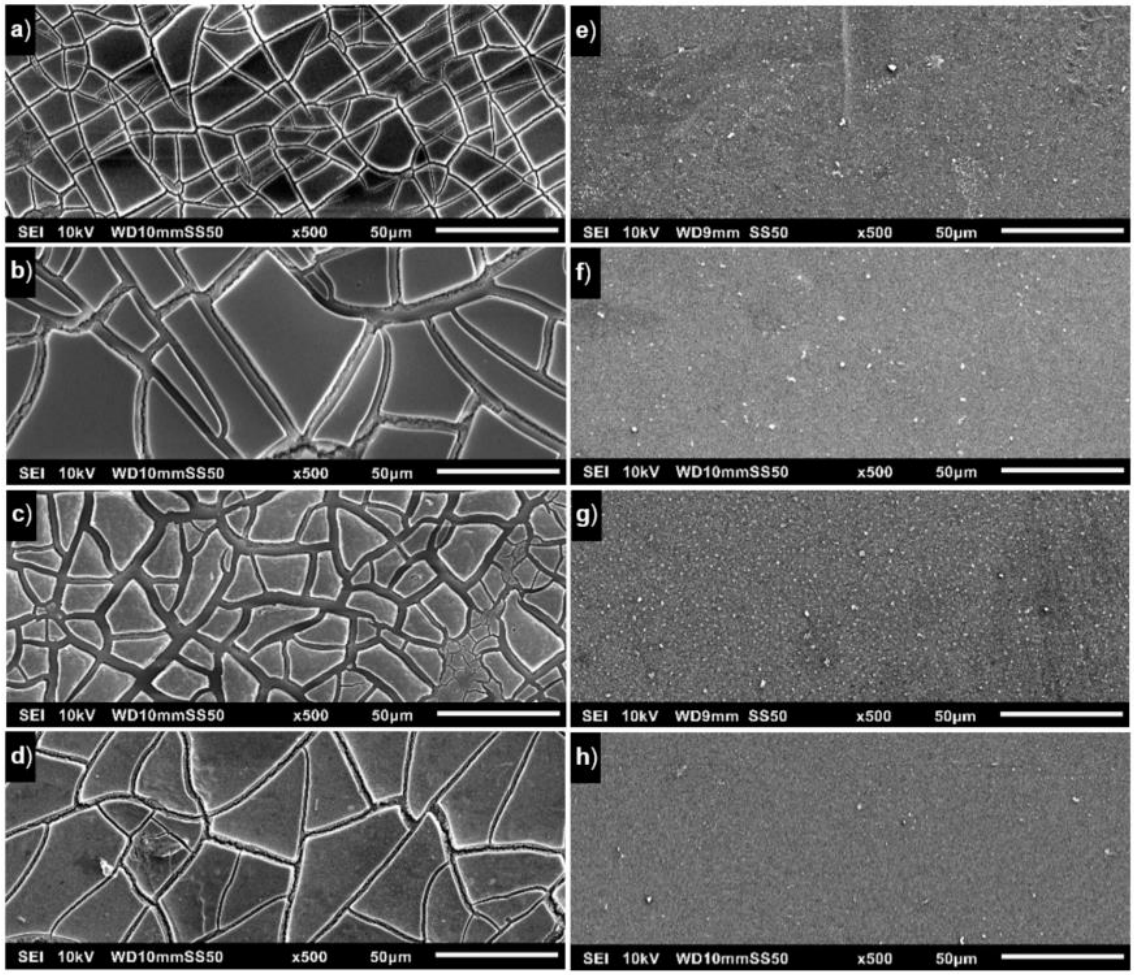

Figure 5.8 *SEM images (500x magnification) of the 100 kDa filter after filtering the synthetic concentrate of 85 % recovery (with phosphate) in the presence of 33 mg/L of a) AS–D, b) AS–E, c) AS–G, and d) AS–H, and filtering the synthetic concentrate of 85 % (without phosphate) in the presence of 33 mg/L of e) AS–D, f) AS–E, g) AS–G, and h) AS–H*

5.3.5 Effectiveness of antiscalants in preventing the deposition of ACP particles in RO applications

In this section the question "*Can antiscalants inhibit the deposition of ACP particles on the membrane surface in RO systems*?" is addressed using the synthetic concentrate of 85 % recovery with the use of the lab-scale RO unit.

In Figure 5.9, the normalized flux of the RO element when fed with synthetic concentrate of 85 % recovery without antiscalant addition and with 33.3 mg/L of various antiscalants is shown. The initial flux for each experiment is presented in Table 5.4.

Table 5.4 *Initial flux of the small RO element when fed with the synthetic concentrate of 85 % recovery without and with the addition of 33.3 mg/L of various antiscalants*

	No AS	**AS–A**	**AS–B**	**AS–C**	**AS–D**	**AS–E**	**AS–F**	**AS–G**	**AS–H**
Flux (L/m^2/h)	13.9	14.4	14.2	14.4	14.0	14.7	13.7	14.6	13.8

As can be seen from Figure 5.9, none of the antiscalants could completely prevent the deposition of ACP particles on the membrane surface since the permeate flux decreased in the presence of each antiscalant. However, it is evident that the rate of flux-decline decreased in the presence of antiscalants. Additionally, one can see that some antiscalants had better performance than others in slowing down the flux decline. For instance, the permeate flux decreased by 25 % with AS-A, approximately 17 % with each AS–B, AS–C and AS–F and about 7 % with each AS–D, AS–G and AS–H in 1.5 h, while no decrease was observed with AS–E in the same duration. However, after 3 h of operation, the permeate flux with AS–E decreased by approximately 15 %. The possible reasons for some antiscalants performing better than others might be due to *(i)* the formation of fewer particles (which needed longer time to foul the membrane) in the presence of such antiscalants, and/or *(ii)* less deposition of the formed particles due to the reduction in the deposition propensity of the particles by the antiscalants.

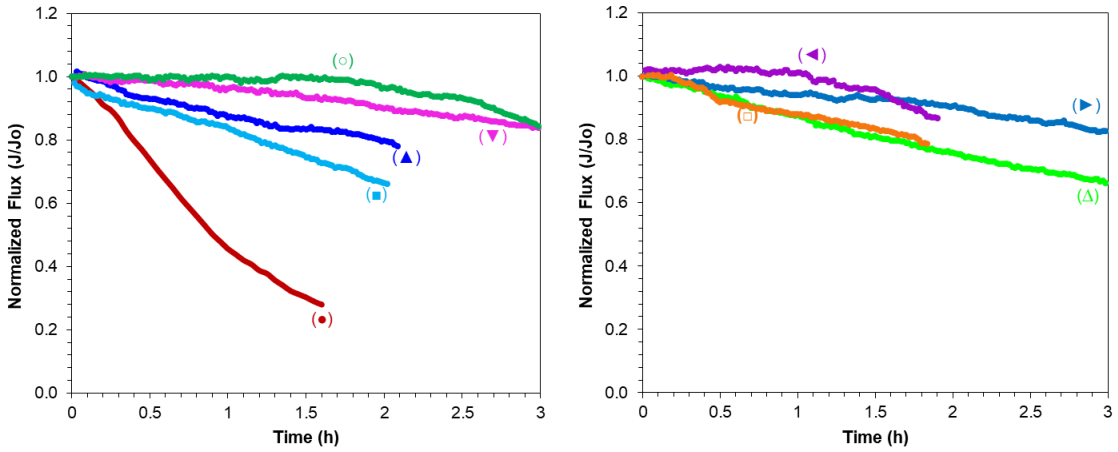

Figure 5.9 *Normalized flux of the small RO element when fed with the synthetic concentrate of 85 % recovery (●) without antiscalant addition, and with 33.3 mg/L of (■) AS–A, (▲) AS–B, (▼) AS–D, (○) AS–E, (□) AS–F, (Δ) AS–C, (►) AS–G, and (◄) AS–H*

In brief, the tested antiscalants were not effective in preventing the flux decline caused due to the formation and deposition of ACP particles in RO systems. These results suggest that the formation/deposition of ACP could be a major concern in the application of RO purification of secondary treated wastewater and RO treatment of groundwater at higher recoveries when the solubility of ACP is exceeded and possibly could be the main factor limiting the recovery of the RO. As antiscalants appeared to be ineffective, other measures

(e.g., lowering the saturation level) could be implemented to prevent calcium phosphate scaling in RO systems.

5.4 CONCLUSIONS

In this study, the performance of eight antiscalants, without acid addition, in preventing calcium phosphate scaling in RO applications was investigated. The major findings of this study can be summarized as follows:

- The determination of the scaling tendency of calcium phosphate with the use of projection programs was contradictory, since at the same conditions (e.g., temperature, pH, concentrations of calcium and phosphate, etc.), some programs predict high potential of calcium phosphate scaling, while some other predict no scaling tendency at all.
- The amorphous phase and not the crystalline phases of calcium phosphate was responsible for the sharp flux-decline when the RO element was fed with the synthetic concentrate of 85 % recovery (Ca^{2+} = 767 mg/L, PO_4^{3-} = 13–15 mg/L and pH = 7.6).
- A concentration of 13.3 mg/L and 33.3 mg/L of 8 different antiscalants, which is equivalent to the recommended dosing rates of the antiscalant suppliers, was unable to inhibit the formation of amorphous calcium phosphate particles in synthetic RO concentrate, but some antiscalants hindered the agglomeration of the formed particles.
- None of the tested antiscalants (with a 33.3 mg/L concentration) could prevent the deposition of the amorphous calcium phosphate particles on the membrane surface of a TW30-1812-50 RO element in once-through lab-scale RO tests when the RO element (fed with the synthetic concentrate of 85 % recovery) was operated at 5–6 % recoveries and fluxes in the range of 13–15 L/m^2/h. The normalized flux of the RO element with each antiscalant decreased by more than 15 % in a 3-hour period.

In brief, the (commercially) available antiscalants for calcium phosphate (tested in this study) may not provide acceptable inhibition of calcium phosphate scaling in RO systems.

6

CONCLUSIONS AND FUTURE OUTLOOK

6.1 CONCLUSIONS

This study was carried out in the context of developing an approach to minimize antiscalant consumption in RO processes and to investigate the performance of antiscalants in preventing calcium phosphate scaling in RO systems.

The proof of principle, validity and application of a dosing algorithm (for optimizing antiscalant dose) was investigated using pilot-scale RO operation, lab-scale RO operation and controlled precipitation (induction time) experiments. In addition, the effect of antiscalant overdose/underdose on the operation of RO and the role of phosphate and humic substances in reducing antiscalant dose were also studied.

Furthermore, the effectiveness of several commercial antiscalants (from different suppliers) in preventing calcium phosphate scaling were evaluated using a once-through lab-scale RO setup which was developed in this research study. The performance of antiscalants were also assessed using pilot-scale RO measurements as well as in batch (glass reactor) induction time experiments.

The major conclusions of this research study are summarized in section 6.1.1 and 6.1.2, and recommendations for future research are presented in section 6.1.3.

6.1.1 Optimizing antiscalant dose in RO processes

- In the presence of high calcium concentrations, an antiscalant overdose to prevent calcium carbonate scaling could be harmful to RO operation. In this study, an overdose of phosphonate antiscalant prevented calcium carbonate scaling, but resulted in permeability decline due to calcium phosphonate precipitation (Chapter 2). An antiscalant underdose, defined as a dose less than the optimum dose, is also detrimental to the RO operation as it will lead to scaling, i.e. calcium carbonate scaling. As a result, a safe range of antiscalant dose exists while preventing calcium carbonate scaling; the lower limit of the antiscalant safe range is governed by calcium carbonate scaling potential (precipitation kinetics), and the upper limit is governed by the scaling potential (precipitation kinetics) of calcium-antiscalant/phosphonate compounds.
- The dosing algorithm temporarily underdoses the antiscalant while establishing the optimum dose which can cause scaling in RO. Nevertheless, the accumulation of scale due to under-dosing of antiscalant can be stopped as the algorithm increases the antiscalant dose to the optimum level (Chapter 2).
- The dosing algorithm is a useful tool that considers the variation in RO feedwater quality and identifies real-time optimum antiscalant doses necessary to prevent scaling for a given recovery in RO. For two RO pilot units in this study, the algorithm reduced antiscalant dose by more than 85% compared to the suppliers' recommended

dose. This showed that the suppliers' recommended doses are far greater than the actual (optimum) dose required to control scaling (Chapter 2).

- The required antiscalant dose for inhibiting calcium carbonate scaling is significantly impacted by the feedwater composition (e.g., the presence of phosphate and humic substances) and currently these factors are not taken into account when antiscalant dosing is recommended by the suppliers. For the RO pilot unit in the Netherlands, both phosphate and HS considerably hinder the formation of calcium carbonate scaling in the RO unit which made it possible to operate the RO unit at 80% recovery without dosing any antiscalant to the feedwater (Chapter 3).

6.1.2 Antiscalants and calcium phosphate scaling

- The determination of the scaling tendency of calcium phosphate with the use of projection programs of the antiscalant suppliers was contradictory, since at the same conditions (e.g., temperature, pH, concentrations of calcium and phosphate, etc.), some programs predict high potential of calcium phosphate scaling, while some others predict no scaling tendency at all (Chapter 5). For instance, for the RO pilot unit in the Netherlands, the scalant limiting the RO recovery varied according to the projection programs of the different antiscalant suppliers, with some pointing to calcium carbonate and others to calcium phosphate as the limiting scaling compound (Chapter 4). The membrane autopsy of the RO pilot unit in the Netherlands indicated that calcium phosphate was the precipitating compound, which implied that the projection programs of antiscalant suppliers can be misleading in identifying the problematic scalant and choosing a proper antiscalant (Chapter 4).
- In RO systems, the amorphous phase of calcium phosphate (and not the crystalline phases) is responsible for the flux decline. The available calcium phosphate antiscalants (tested in this study) are unable to inhibit the formation of amorphous calcium phosphate particles. Some antiscalants hindered the agglomeration of the formed calcium phosphate particles which indicated that they had better dispersant capability than the others. However, none of the antiscalants could prevent the deposition of formed calcium phosphate particles on the membrane surface which was observed in once-through lab-scale RO measurements (Chapter 5). In addition, all antiscalants, tested in this study, were unable to prevent calcium phosphate scaling in the RO pilot unit in the Netherlands (Chapter 4). This study showed that the available antiscalants for calcium phosphate may not provide acceptable inhibition of calcium phosphate scaling in RO systems (Chapter 4 and 5).

6.2 FUTURE PERSPECTIVE

This research primarily focused on the use of antiscalants in RO processes in terms of minimizing their consumption and evaluating their ability to control scaling, particularly calcium phosphate scaling. Furthermore, this study touched on a number of additional issues that emerged during the course of the research and require further investigation, as summarized below:

- It was demonstrated that an overdose of a commercial phosphonate antiscalant resulted in a decrease in RO membrane permeability due to calcium phosphonate precipitation. It is important to understand when and under what conditions an antiscalant (e.g., a phosphonate antiscalant) in the presence of calcium can precipitate on the membrane surface. This necessitates additional research into the solubility and precipitation kinetics of the calcium antiscalant/phosphonate compound and the development of clear guidelines to avoid the precipitation of such compound(s) in RO installations.
- In this study, the algorithm's proof of principle was executed for calcium carbonate, and the algorithm was applied in RO units where calcium carbonate was the precipitating compound. The algorithm should be able to identify the optimum dose of antiscalant for any scaling compound (e.g., calcium carbonate, calcium sulphate, barium sulphate, etc.) as long as the following two conditions are met: i) antiscalant is effective in preventing the precipitation of the scaling compound, and ii) the accumulation of scale due to under-dosing of antiscalant can be stopped by increasing the antiscalant dose to the optimum level. Nonetheless, it is recommended that the algorithm's proof of principle be carried out for all compounds that are commonly encountered as scalants in RO processes.
- The current methods (e.g., projection programs of antiscalant suppliers, etc.) for determining the scaling tendency of calcium phosphate make it difficult to predict whether calcium phosphate is supersaturated and whether it will precipitate in the RO unit. Therefore, additional in-depth research into methods to determine the scaling tendency of calcium phosphate in RO systems is required.
- The antiscalants tested in this study were ineffective against calcium phosphate scaling. It is thus recommended that additional research be carried out in collaboration with antiscalant suppliers to further investigate and develop antiscalants that could prevent amorphous calcium phosphate scaling in RO systems.

REFERENCES

AHMED, S. B., TLILI, M. M. & AMOR, M. B. 2008. Influence of a polyacrylate antiscalant on gypsum nucleation and growth. *Crystal Research and Technology***,** NA-NA.

ALVAREZ, R., EVANS, L., MILHAM, P. & WILSON, M. 2004. Effects of humic material on the precipitation of calcium phosphate. *Geoderma,* 118**,** 245-260.

AMJAD, Z. 1996. Scale inhibition in desalination applications—an overview. *Proceedings of the Corrosion '96, NACE Conference, Paper 230*

AMJAD, Z. 1997. Inhibition of the amorphous calcium phosphate phase transformation reaction by polymeric and non-polymeric inhibitors. *Phosphorus Research Bulletin,* 7**,** 45-54.

AMJAD, Z., PUGH, J. & REDDY, M. 1998. Kinetic inhibition of calcium carbonate crystal growth in the presence of natural and synthetic organic inhibitors. *Water Soluble Polymers: Solution Properties and Application.* New York: Plenum Press.

ANTONY, A., LOW, J. H., GRAY, S., CHILDRESS, A. E., LE-CLECH, P. & LESLIE, G. 2011. Scale formation and control in high pressure membrane water treatment systems: a review. *Journal of Membrane Science,* 383**,** 1-16.

ARMBRUSTER, D., MÜLLER, U. & HAPPEL, O. 2019. Characterization of phosphonate-based antiscalants used in drinking water treatment plants by anion-exchange chromatography coupled to electrospray ionization time-of-flight mass spectrometry and inductively coupled plasma mass spectrometry. *Journal of Chromatography A,* 1601**,** 189-204.

ARMBRUSTER, D., ROTT, E., MINKE, R. & HAPPEL, O. 2020. Trace-level determination of phosphonates in liquid and solid phase of wastewater and environmental samples by IC-ESI-MS/MS. *Analytical and Bioanalytical Chemistry,* 412**,** 4807-4825.

BERNER, R. A. 1975. The role of magnesium in the crystal growth of calcite and aragonite from sea water. *Geochimica et Cosmochimica Acta,* 39**,** 489-504.

BEYER, F., RIETMAN, B. M., ZWIJNENBURG, A., VAN DEN BRINK, P., VROUWENVELDER, J. S., JARZEMBOWSKA, M., LAURINONYTE, J., STAMS, A. J. M. & PLUGGE, C. M. 2014. Long-term performance and fouling analysis of full-scale direct nanofiltration (NF) installations treating anoxic groundwater. *Journal of Membrane Science,* 468**,** 339-348.

BISCHOFF, J. L. 1968. Kinetics of calcite nucleation: Magnesium ion inhibition and ionic strength catalysis. *Journal of Geophysical Research (1896-1977),* 73**,** 3315-3322.

BLANKERT, B., BETLEM, B. H. L. & ROFFEL, B. 2007. Development of a control system for in-line coagulation in an ultrafiltration process. *Journal of Membrane Science,* 301**,** 39-45.

BOELS, L. & WITKAMP, G.-J. 2011. Carboxymethyl Inulin Biopolymers: A Green Alternative for Phosphonate Calcium Carbonate Growth Inhibitors. *Crystal Growth & Design,* 11**,** 4155-4165.

BOERLAGE, Ś. F. E., KENNEDY, M. D., BREMERE, I., WITKAMP, G. J., VAN DER HOEK, J. P. & SCHIPPERS, J. C. 2000. Stable barium sulphate supersaturation in reverse osmosis. *Journal of Membrane Science,* 179**,** 53-68.

BOHNER, M., LEMAîTRE, J. & RING, T. A. 1997. Kinetics of dissolution of β-tricalcium phosphate. *Journal of Colloid and Interface Science,* 190**,** 37-48.

BREČEVIĆ, L. J. & FÜREDI-MILHOFER, H. 1976. The transformation of amorphous calcium phosphate into crystalline hydroxyapatite. *In:* MULLIN, J. W. (ed.) *Industrial Crystallization.* Boston, MA: Springer US.

BURTON, E. A. & WALTER, L. M. 1990. The role of pH in phosphate inhibition of calcite and aragonite precipitation rates in seawater. *Geochimica et Cosmochimica Acta,* 54**,** 797-808.

CHEN, T., NEVILLE, A. & YUAN, M. 2005. Assessing the effect of Mg^{2+} on $CaCO_3$ scale formation–bulk precipitation and surface deposition. *Journal of Crystal Growth,* 275**,** e1341-e1347.

CHEN, W., WESTERHOFF, P., LEENHEER, J. A. & BOOKSH, K. 2003. Fluorescence excitation−emission matrix regional integration to quantify spectra for dissolved organic matter. *Environmental Science & Technology,* 37**,** 5701-5710.

CHESTERS, S. P. 2009. Innovations in the inhibition and cleaning of reverse osmosis membrane scaling and fouling. *Desalination,* 238**,** 22-29.

CHOPPIN, G. R. & SHANBHAG, P. M. 1981. Binding of calcium by humic acid. *Journal of Inorganic and Nuclear Chemistry,* 43**,** 921-922.

COMBES, C. & REY, C. 2010. Amorphous calcium phosphates: Synthesis, properties and uses in biomaterials. *Acta Biomaterialia,* 6**,** 3362-3378.

COOPER, K. G., HANLON, L. G., SMART, G. M. & TALBOT, R. E. 1979. The threshold scale inhibition phenomenon. *Desalination,* 31**,** 257-266.

DARTON, E. 2000. Membrane chemical research: centuries apart. *Desalination,* 132**,** 121-131.

DE VET, W., GENUCHTEN, C., VAN LOOSDRECHT, M. & DIJK, J. 2009. Water quality and treatment of river bank filtrate. *Drinking Water Engineering and Science Discussions,* 3**,** 79-90.

DESALDATA 2020. Worldwide desalination inventory (MS Excel format), Available from: www.DesalData.com.

DOROZHKIN, S. 2012. Amorphous calcium orthophosphates: Nature, chemistry and biomedical applications. *International Journal of Materials and Chemistry,* 2**,** 19-46.

DOROZHKIN, S. V. 2016. Calcium orthophosphates (CaPO4): occurrence and properties. *Progress in Biomaterials,* 5**,** 9-70.

DOVE, P. M. & HOCHELLA, M. F. 1993. Calcite precipitation mechanisms and inhibition by orthophosphate: In situ observations by scanning force microscopy. *Geochimica et Cosmochimica Acta,* 57**,** 705-714.

DOW, W. S. 2010. FILMTEC™ reverse osmosis membranes - technical manual. *Technical Manual, Form***,** 1-180.

DRAK, A., GLUCINA, K., BUSCH, M., HASSON, D., LAÎNE, J.-M. & SEMIAT, R. 2000. Laboratory technique for predicting the scaling propensity of RO feed waters. *Desalination,* 132**,** 233-242.

EANES, E. D. 1998. Amorphous calcium phosphate: Thermodynamic and kinetic considerations. *In:* AMJAD, Z. (ed.) *Calcium Phosphates in Biological and Industrial Systems.* Boston, MA: Springer US.

EANES, E. D., GILLESSEN, I. H. & POSNER, A. S. 1965. Intermediate states in the precipitation of hydroxyapatite. *Nature,* 208**,** 365-367.

EANES, E. D. & POSNER, A. S. 1965. Division of biophysics: kinetics and mechanism of conversion of noncrystalline calcium phosphate to crystalline hydroxyapatite. *Transactions of the New York Academy of Sciences,* 28**,** 233-241.

EL-SHALL, H., RASHAD, M. & ABDEL-AAL, E. 2002. Effect of phosphonate additive on crystallization of gypsum in phosphoric and sulfuric acid medium. *Crystal Research and Technology,* 37**,** 1264-1273.

FANE, T. 2016. Inorganic Scaling. *In:* DRIOLI, E. & GIORNO, L. (eds.) *Encyclopedia of Membranes.* Berlin, Heidelberg: Springer Berlin Heidelberg.

FEENSTRA, T. P. & DE BRUYN, P. L. 1981. The ostwald rule of stages in precipitation from highly supersaturated solutions: A model and its application to the formation of the nonstoichiometric amorphous calcium phosphate precursor phase. *Journal of Colloid and Interface Science,* 84**,** 66-72.

FINK, J. 2021. Chapter 7 - Scale inhibitors. *In:* FINK, J. (ed.) *Petroleum Engineer's Guide to Oil Field Chemicals and Fluids (Third Edition).* Gulf Professional Publishing.

FLEMMING, H.-C. 1997. Reverse osmosis membrane biofouling. *Experimental Thermal and Fluid Science,* 14**,** 382-391.

FLEMMING, H. C. 1993. Mechanistic aspects of reverse osmosis membrane biofouling and prevention. *Reverse Osmosis***,** 163-209.

FRIDJONSSON, E. O., VOGT, S. J., VROUWENVELDER, J. S. & JOHNS, M. L. 2015. Early non-destructive biofouling detection in spiral wound RO membranes using a mobile earth′s field NMR. *Journal of Membrane Science,* 489**,** 227-236.

GALLEGO, S., VIGO, F. D., CHESTERS, S. & BUÑUEL, P. L. Practical experience with high silica concentration in RO waters. WIM International Congress, July 9-11 2008 Santiago, Chile.

GE, X., WANG, L., ZHANG, W. & PUTNIS, C. V. 2019. Molecular understanding of humic acid-Limited phosphate precipitation and transformation. *Environ Sci Technol,* 54**,** 207-215.

GIANNIMARAS, E. K. & KOUTSOUKOS, P. G. 1987. The crystallization of calcite in the presence of orthophosphate. *Journal of Colloid And Interface Science,* 116**,** 423-430.

GREENBERG, G., HASSON, D. & SEMIAT, R. 2005. Limits of RO recovery imposed by calcium phosphate precipitation. *Desalination,* 183**,** 273-288.

GREENLEE, L. F., TESTA, F., LAWLER, D. F., FREEMAN, B. D. & MOULIN, P. 2010. The effect of antiscalant addition on calcium carbonate precipitation for a simplified synthetic brackish water reverse osmosis concentrate. *Water Research,* 44**,** 2957-2969.

GRIFFIN, R. & JURINAK, J. 1973. The interaction of phosphate with calcite. *Soil Science Society of America Journal,* 37**,** 847-850.

HIEMSTRA, P., KOLPA, R., EEKHOUT, J. M. J. M., KESSEL, T., ADAMSE, E. & PAASSEN, J. 2003. 'Natural' recharge of groundwater: Bank infiltration in the Netherlands. *Journal of Water Supply: Research and Technology - AQUA,* 52**,** 37-47.

HIEMSTRA, P., VAN PAASSEN, J., RIETMAN, B. & VERDOUW, J. Aerobic versus anaerobic nanofiltration: fouling of membranes. AWWA Membrane Conference, Long Beach, CA, 28 February-3 March 1999.

HOCH, A. R., REDDY, M. M. & AIKEN, G. R. 2000. Calcite crystal growth inhibition by humic substances with emphasis on hydrophobic acids from the Florida Everglades. *Geochimica et Cosmochimica Acta,* 64**,** 61-72.

HYDRANAUTICS. 2013. Chemical treatment for RO and NF, Technical application bulletin no. 111. Available: http://www.membranes.com/docs/tab/TAB111.pdf.

INSKEEP, W. P. & BLOOM, P. R. 1986. Kinetics of calcite precipitation in the presence of water-soluble organic ligands. *Soil Science Society of America Journal,* 50**,** 1167-1172.

ISMAIL, A. F., KHULBE, K. C. & MATSUURA, T. 2019. Chapter 8 - RO Membrane Fouling. *In:* ISMAIL, A. F., KHULBE, K. C. & MATSUURA, T. (eds.) *Reverse Osmosis.* Elsevier.

KLEPETSANIS, P. G., KLADI, A., OSTVOLD, T., KONTOYIANNIS, C. G., KOUTSOUKOS, P. G., AMJAD, Z. & REDDY, M. M. 2002. The inhibition of calcium carbonate formation in aqueous supersaturated solutions, spontaneous precipitation and seeded crystal growth. *In:* AMJAD, Z. (ed.) *Advances in Crystal Growth Inhibition Technologies.* Boston, MA: Springer US.

KOSTOGLOU, M. & KARABELAS, A. J. 2011. On modeling incipient crystallization of sparingly soluble salts in frontal membrane filtration. *Journal of Colloid and Interface Science,* 362**,** 202-214.

KOUTSOUKOS, P. 2010. Calcium carbonate scale control in industrial water systems. *the science and technology of industrial water treatment.* Boca Raton, FL: CRC Press.

KUBO, S., TAKAHASHI, T., MORINAGA, H. & UEKI, H. 1979. Inhibition of calcium phosphate scale on heat exchanger: The relation between laboratory test results and tests on heat transfer surfaces. *Corrosion'79***,** 1979.

KUCERA, J. 2010. Reverse Osmosis Membrane Fouling Control. *The science and technology of industrial water treatment.* Boca Raton, FL: CRC Press.

LANGERAK, E. P. A. V., BEEKMANS, M. M. H., BEUN, J. J., HAMELERS, H. V. M. & LETTINGA, G. 1999. Influence of phosphate and iron on the extent of calcium carbonate precipitation during anaerobic digestion. *Journal of Chemical Technology & Biotechnology,* 74**,** 1030-1036.

LEE, S., KIM, J. & LEE, C.-H. 1999. Analysis of CaSO4 scale formation mechanism in various nanofiltration modules. *Journal of Membrane Science,* 163**,** 63-74.

LEE, S. & LEE, C. H. 2005. Scale formation in NF/RO: mechanism and control. *Water Science and Technology,* 51**,** 267-275.

LEGEROS, R. Z., MIJARES, D. Q., PARK, J., CHANG, X. F., KHAIROUN, I., KIJKOWSKA, R., DIAS, R. & LEGEROS, J. P. 2005. Amorphous calcium phosphates (ACP): Formation and stability. *Key Engineering Materials,* 284-286**,** 7-10.

LUO, M. & WANG, Z. 2001. Complex fouling and cleaning-in-place of a reverse osmosis desalination system. *Desalination,* 141**,** 15-22.

MANGAL, M. N., SALINAS-RODRIGUEZ, S. G., BLANKERT, B., YANGALI-QUINTANILLA, V. A., SCHIPPERS, J. C., VAN DER MEER, W. G. J. & KENNEDY, M. D. 2021a. Role of phosphate and humic substances in controlling calcium carbonate scaling in a groundwater reverse osmosis system. *Journal of Environmental Chemical Engineering,* 9**,** 105651.

MANGAL, M. N., SALINAS-RODRIGUEZ, S. G., DUSSELDORP, J., BLANKERT, B., YANGALI-QUINTANILLA, V. A., KEMPERMAN, A. J. B., SCHIPPERS, J. C., VAN DER MEER, W. G. J. & KENNEDY, M. D. 2022. Foulant identification and performance evaluation of antiscalants in increasing the recovery of a reverse osmosis system treating anaerobic groundwater. *Membranes,* 12**,** 290.

MANGAL, M. N., SALINAS-RODRIGUEZ, S. G., DUSSELDORP, J., KEMPERMAN, A. J. B., SCHIPPERS, J. C., KENNEDY, M. D. & VAN DER MEER, W. G. J. 2021b. Effectiveness of antiscalants in preventing calcium phosphate scaling in reverse osmosis applications. *Journal of Membrane Science***,** 119090.

MANGAL, M. N., SALINAS-RODRIGUEZ, S. G., YANGALI-QUINTANILLA, V. A., KENNEDY, M. D. & SCHIPPERS, J. C. 2021c. Scaling. *Seawater Reverse Osmosis Desalination: Assessment and Pre-treatment of Fouling and Scaling.* IWA Publishing.

MARTÍNEZ, C., GÓMEZ, V., POCURULL, E. & BORRULL, F. 2014. Characterization of organic fouling in reverse osmosis membranes by headspace solid phase microextraction and gas chromatography–mass spectrometry. *Water Science and Technology,* 71**,** 117-125.

MEYER, J. L. & WEATHERALL, C. C. 1982. Amorphous to crystalline calcium phosphate phase transformation at elevated pH. *Journal of Colloid and Interface Science,* 89**,** 257-267.

NEOFOTISTOU, E. & DEMADIS, K. D. 2004. Use of antiscalants for mitigation of silica (SiO2) fouling and deposition: fundamentals and applications in desalination systems. *Desalination,* 167**,** 257-272.

NIELSEN, M. R., SAND, K. K., RODRIGUEZ-BLANCO, J. D., BOVET, N., GENEROSI, J., DALBY, K. N. & STIPP, S. L. S. 2016. Inhibition of calcite

growth: combined effects of Mg^{2+} and SO_4^{2-}. *Crystal Growth & Design,* 16**,** 6199-6207.

NIST X-ray photoelectron spectroscopy database, NIST standard reference database number 20, National Institute of Standards and Technology, Gaithersburg MD, 20899 (2000), doi:10.18434/T4T88K, retrieved [30-11-2020].

OKAMOTO, Y. & LIENHARD, J. H. 2019. How RO membrane permeability and other performance factors affect process cost and energy use: A review. *Desalination,* 470**,** 114064.

PANDEY, S. R., JEGATHEESAN, V., BASKARAN, K. & SHU, L. 2012. Fouling in reverse osmosis (RO) membrane in water recovery from secondary effluent: a review. *Reviews in Environmental Science and Bio/Technology,* 11**,** 125-145.

PAXÉUS, N. & WEDBORG, M. Calcium binding to an aquatic fulvic acid. 1991 Berlin, Heidelberg. Springer Berlin Heidelberg, 287-296.

PEÑA, N., GALLEGO, S., DEL VIGO, F. & CHESTERS, S. P. 2013. Evaluating impact of fouling on reverse osmosis membranes performance. *Desalination and Water Treatment,* 51**,** 958-968.

PERVOV, A. G. 1991. Scale formation prognosis and cleaning procedure schedules in reverse osmosis systems operation. *Desalination,* 83**,** 77-118.

POTTS, D. E., AHLERT, R. C. & WANG, S. S. 1981. A critical review of fouling of reverse osmosis membranes. *Desalination,* 36**,** 235-264.

PRISCIANDARO, M., OLIVIERI, E., LANCIA, A. & MUSMARRA, D. 2006. Gypsum precipitation from an aqueous solution in the presence of nitrilotrimethylenephosphonic acid. *Industrial & Engineering Chemistry Research,* 45**,** 2070-2076.

PYTKOWICZ, R. 1973. Calcium carbonate retention in supersaturated seawater. *American Journal of Science,* 273**,** 515-522.

RAHMAN, F. 2013. Calcium sulfate precipitation studies with scale inhibitors for reverse osmosis desalination. *Desalination,* 319**,** 79-84.

REDDY, M. M. 1977. Crystallization of calcium carbonate in the presence of trace concentrations of phosphorus-containing anions: I. Inhibition by phosphate and glycerophosphate ions at pH 8.8 and 25°C. *Journal of Crystal Growth,* 41**,** 287-295.

SALINAS-RODRIGUEZ, S. G. 2011. *Particulate and organic matter fouling of seawater reverse osmosis systems: characterization, modelling and applications. UNESCO-IHE PhD Thesis,* Delft, CRC Press/Balkema.

SALMAN, M. A., AL-NUWAIBIT, G., SAFAR, M. & AL-MESRI, A. 2015. Performance of physical treatment method and different commercial antiscalants to control scaling deposition in desalination plant. *Desalination,* 369**,** 18-25.

SIMKISS, K. 1964. Phosphates as crystal poisons of calcification. *Biological Reviews,* 39**,** 487-504.

SINGH, R. 2005. Chapter 2 - Water and membrane treatment. *In:* SINGH, R. (ed.) *Hybrid Membrane Systems for Water Purification.* Amsterdam: Elsevier Science.

SÖHNEL, O. & MULLIN, J. W. 1988. Interpretation of crystallization induction periods. *Journal of Colloid and Interface Science,* 123**,** 43-50.

TANAKA, R., SAMU, Y., SUZUKI, T., NIINAE, M., LIN, L., LUH, J. & CORONELL, O. 2016. The effects of humic acid fouling on the performane of polyamide composite reverse osmosis membranes. *Journal of MMIJ,* 132**,** 123-128.

TANG, C., KWON, Y.-N. & LECKIE, J. 2007a. Characterization of humic acid fouled reverse osmosis and nanofiltration membranes by transmission electron microscopy and streaming potential measurements. *Environmental science & technology,* 41**,** 942-9.

TANG, C. Y., CHONG, T. H. & FANE, A. G. 2011. Colloidal interactions and fouling of NF and RO membranes: a review. *Advances in Colloid and Interface Science,* 164**,** 126-143.

TANG, C. Y., KWON, Y.-N. & LECKIE, J. O. 2007b. Fouling of reverse osmosis and nanofiltration membranes by humic acid—effects of solution composition and hydrodynamic conditions. *Journal of Membrane Science,* 290**,** 86-94.

TERMINE, J. D. 1972. Mineral chemistry and skeletal biology. *Clinical Orthopaedics and Related Research®,* 85**,** 207-241.

TZOTZI, C., PAHIADAKI, T., YIANTSIOS, S. G., KARABELAS, A. J. & ANDRITSOS, N. 2007. A study of CaCO3 scale formation and inhibition in RO and NF membrane processes. *Journal of Membrane Science,* 296**,** 171-184.

VAN DE LISDONK, C. A. C., VAN PAASSEN, J. A. M. & SCHIPPERS, J. C. 2000. Monitoring scaling in nanofiltration and reverse osmosis membrane systems. *Desalination,* 132**,** 101-108.

VAN ENGELEN, G. & NOLLES, R. 2013. A sustainable antiscalant for RO processes. *Desalination and Water Treatment,* 51**,** 921-923.

VROUWENVELDER, H. S., VAN PAASSEN, J. A. M., FOLMER, H. C., HOFMAN, J. A. M. H., NEDERLOF, M. M. & VAN DER KOOIJ, D. 1998. Biofouling of membranes for drinking water production. *Desalination,* 118**,** 157-166.

VROUWENVELDER, J. S., GRAF VON DER SCHULENBURG, D. A., KRUITHOF, J. C., JOHNS, M. L. & VAN LOOSDRECHT, M. C. M. 2009. Biofouling of spiral-wound nanofiltration and reverse osmosis membranes: a feed spacer problem. *Water Research,* 43**,** 583-594.

WALTON, A. G., BODIN, W. J., FUREDI, H. & SCHWARTZ, A. 1967. Nucleation of calcium phosphate from solution. *Canadian Journal of Chemistry,* 45**,** 2695-2701.

WALY, T. 2011. *Minimizing the use of chemicals to control scaling in sea water reverse osmosis: Improved prediction of the scaling potential of calcium carbonate,* CRC Press/Balkema. Leiden. Netherlands.

WALY, T., KENNEDY, M. D., WITKAMP, G.-J., AMY, G. & SCHIPPERS, J. C. 2012. The role of inorganic ions in the calcium carbonate scaling of seawater reverse osmosis systems. *Desalination,* 284**,** 279-287.

WALY, T., MUNOZ, R., KENNEDY, M. D., WITKAMP, G. J., AMY, G. & SCHIPPERS, J. C. 2010. Effect of particles on the induction time of calcium carbonate in synthetic SWRO concentrate. *Desalination and Water Treatment,* 18**,** 103-111.

XU, P., DREWES, J. E., KIM, T.-U., BELLONA, C. & AMY, G. 2006. Effect of membrane fouling on transport of organic contaminants in NF/RO membrane applications. *Journal of Membrane Science,* 279**,** 165-175.

YANGALI-QUINTANILLA, V. A., DOMINIAK, D. M. & VAN DE VEN, W. J. C. 2019. *A dosing pump for dosing antiscalant into a membrane-based water treatment system*. United States patent application 16157591.

YU, W., SONG, D. & CHEN, W. 2020. Antiscalants in RO membrane scaling control. *Water Research,* 183**,** 115985.

ZAIDI, S. J. & SALEEM, H. 2022. Chapter 5 - Pretreatment: Fouling and Scaling Control. *In:* ZAIDI, S. J. & SALEEM, H. (eds.) *Reverse Osmosis Systems.* Elsevier.

ZHAO, X., WU, Y., ZHANG, X., TONG, X., YU, T., WANG, Y., IKUNO, N., ISHII, K. & HU, H. 2019. Ozonation as an efficient pretreatment method to alleviate reverse osmosis membrane fouling caused by complexes of humic acid and calcium ion. *Frontiers of Environmental Science & Engineering,* 13**,** 55.

ZUDDAS, P., PACHANA, K. & FAIVRE, D. 2003. The influence of dissolved humic acids on the kinetics of calcite precipitation from seawater solutions. *Chemical Geology,* 201**,** 91-101.

LIST OF ACRONYMS

ACP	Amorphous calcium phosphate
BWRO	Brackish water RO
CDOC	Chromatographic dissolved organic carbon
DCPD	Dicalcium phosphate dihydrate
DOC	Dissolved organic carbon
ESI-TOF	Electrospray-ionization time-of-flight mass spectrometry
FA	Fulvic acid
FEEM	Fluorescence excitation–emission matrix
GW	Groundwater
HA	Humic acid
HOC	Hydrophobic organic carbon
HS	Humic substances
ICP-MS	Inductively coupled plasma mass spectrometry
IHSS	International Humic Substances Society
IT	Induction time
LC-OCD	Liquid chromatography–organic carbon detection
LMW	Low molecular weight
LSI	Langelier Saturation Index
MCPD	Monocalcium phosphate monohydrate
NDP	Net driving pressure
OMP	Organic micropollutants
P&ID	Piping and instrumentation diagram
ppb-C	Parts per billion carbon
RO	Reverse osmosis
SEM-EDX	Scanning electron microscopy with energy dispersive X-ray
SI	Saturation index
Sr	Saturation ratio
TCF	Temperature correction factor
TCP	Tricalcium phosphate
TDS	Total dissolved solids
XPS	X-ray photoelectron spectroscopy
XRD	X-ray powder diffraction

ABOUT THE AUTHOR

Nasir Mangal was born on August 1, 1989, in Paktia, Afghanistan. He received his BSc degree in Civil Engineering from the Engineering Faculty of Kabul University in 2011. After completing his undergraduate studies, he worked as a Project Manger and Civil Engineer in construction projects for three years. He was awarded the Rotary International scholarship to pursue his graduate studies in The Netherlands. He completed with distinction his master's degree in Urban Water and Sanitation with specialization in Water Supply Engineering in 2016 at IHE- Delft. His Master's thesis focused on developing adenosine triphosphate (ATP) method for saline water to monitor biofouling in seawater reverse osmosis (SWRO) applications. From August 2016, he started his PhD studies at IHE- Delft and University of Twente which was funded by Oasen Drinking Water Company and Grundfos. His PhD research focused on minimizing antiscalant consumption and controlling (calcium phosphate) scaling in RO processes.

Journals publications

Mangal M.N., V.A. Yangali-Quintanilla, S.G. Salinas-Rodriguez, J. Dusseldorp, B. Blankert, A.J.B. Kemperman, J.C. Schippers, M.D. Kennedy, W.G.J. van der Meer, (2022). Application of a smart dosing pump algorithm in identifying real-time optimum dose of antiscalant in reverse osmosis systems, Journal of Membrane Science, 658, 120717.

Mangal M.N., Salinas-Rodriguez S.G., Blankert B., Yangali-Quintanilla V.A., Schippers J., Kemperman A.J.B., van der Meer W.G.J., Kennedy M.D. (2022). Foulant identification and performance evaluation of antiscalants in increasing the recovery of a reverse osmosis system treating anaerobic groundwater. Membranes, 12, 290.

Mangal M.N., Salinas-Rodriguez S.G., Dusseldorp J., Kemperman A.J.B., Schippers J., Kennedy M.D., van der Meer W.G.J. (2021). Effectiveness of antiscalants in preventing calcium phosphate scaling in reverse osmosis applications. Journal of Membrane Science, 623, 1-11.

Mangal M.N., Salinas-Rodriguez S.G., Blankert B., Yangali-Quintanilla V.A., Schippers J., van der Meer W.G.J., Kennedy M.D. (2021). Role of phosphate and humic substances in controlling calcium carbonate scaling in an anaerobic groundwater reverse osmosis system. Journal of Environmental Chemical Engineering, 9, 105651.

Abushaban, A., **Mangal, M.N.**, Salinas-Rodriguez, S.G., Nnebuo, C., Mondal, S., Goueli, S.A., Kennedy, M.D. (2017). Direct measurement of ATP in seawater and application of ATP to monitor bacterial growth potential in SWRO pre-treatment systems. Desalination and Water Treatment, 99, 91-101.

Abushaban A, Salinas-Rodriguez SG, **Mangal M.N.**, Mondal S., Goueli S.A., Knezev A., Vrouwenvelder J.S., Schippers J.C., Kennedy M.D. (2019) ATP measurement in seawater reverse osmosis systems: Eliminating seawater matrix effects using a filtration-based method. Desalination 453: 1-9.

Book chapters

Mangal, M.N., Salinas-Rodriguez S.G., Yangali-Quintanilla V.A., Kennedy, M.D., Schippers, J.C., (2021). Chapter 8: Scaling. In, Seawater Reverse Osmosis Desalination: Assessment & Pre-treatment of Fouling and Scaling. IWA Publishing, London. ISBN:9781780409856

Salinas-Rodriguez S.G., **Mangal, M.N.**, Villacorte L., Abushaban, A., (2021). Chapter 3: Methods for assessing fouling and scaling in brackish and seawater desalination. In,

Removal of pollutants from saline water: Treatment technologies, CRC press. ISBN: 9781032028354

Dhakal, N., Abushaban, A., **Mangal, M.N.**, Abunada, M., Schippers, J.C., Kennedy, M.D., (2020). Chapter 12: Membrane fouling and scaling in Reverse Osmosis. In, Membrane Desalination: from nanoscale to real world applications, CRC press. ISBN:9780367030797

Conference presentations

European Desalination Society (EDS) international conference: Desalination for the Environment: Clean Water and Energy, Athens, Greece, 3–6 September, 2018.

> Oral presentation: Inhibition of calcium carbonate scaling by phosphate and humic substances in a reverse osmosis system treating anaerobic groundwater

10th International Desalination Workshop (IDW): Water desalination, water treatment and reuse, Busan, South Korea, 22–25 November, 2017.

> Oral presentation: Role of humic substances in the inhibition of calcium carbonate scaling in a reverse osmosis system treating anaerobic groundwater

Netherlands Research School for the
Socio-Economic and Natural Sciences of the Environment

D I P L O M A

for specialised PhD training

The Netherlands research school for the
Socio-Economic and Natural Sciences of the Environment
(SENSE) declares that

Muhammad Nasir Mangal

born on 1st August 1989 in Paktia, Afghanistan

has successfully fulfilled all requirements of the
educational PhD programme of SENSE.

Enschede, 19 April 2023

Chair of the SENSE board

Prof. dr. Martin Wassen

The SENSE Director

Prof. Philipp Pattberg

The SENSE Research School has been accredited by the Royal Netherlands Academy of Arts and Sciences (KNAW)

KONINKLIJKE NEDERLANDSE
AKADEMIE VAN WETENSCHAPPEN

The SENSE Research School declares that **Muhammad Nasir Mangal** has successfully fulfilled all requirements of the educational PhD programme of SENSE with a work load of 35.0 EC, including the following activities:

SENSE PhD Courses

- Environmental research in context (2017)
- Speciation and Bioavailability of Metals, Organics and Nanoparticle, University of Antwerp and SENSE (2017)
- Research in context activity: 'Create Wikipedia page "Membrane Scaling" (2022)

Other PhD and Advanced MSc Courses

- TGS PhD introduction workshop, University of Twente (2017)
- Crystallization, International school of crystallization Spain (2018)

External training at a foreign research institute

- Data Visualization in Python Masterclass, Udemy online (2020)
- Presentation Skills Masterclass, Udemy online (2020)

Management and Didactic Skills Training

- Supervising two MSc students with thesis entitled 'Optimization of antiscalant dose in the brackish water reverse osmosis (BWRO) plant at Kamerik' (2018) and 'Controlling scaling in brackish water reverse osmosis applications' (2020)
- Teaching workshop on "calculating saturation indices to predict scaling in RO systems and the use of projection programs to design an RO process " to MSc students (2018)

Oral Presentations

- *Role of ferrous and humic substances in the inhibition of calcium carbonate scaling in reverse osmosis applications*. The 10th International Desalination Workshop, 22-25 November 2017, Busan, South Korea
- *Inhibition of CaCO3 scaling by humic substances in a reverse osmosis system treating anaerobic groundwater*. Desalination for the Environment: Clean Water and Energy Conference, 3-6 September 2018, Athens, Greece
- *Effect of Humic substances on calcium carbonate scaling*. IHE Delft PhD Symposium, 1-2 October 2018, Delft, The Netherlands

SENSE coordinator PhD education

Dr. ir. Peter Vermeulen

IHE DELFT
Institute for Water Education
under the auspices of UNESCO

UNIVERSITY OF TWENTE.

Antiscalants are well known for preventing the precipitation of sparingly soluble compounds such as calcium carbonate in reverse osmosis (RO) applications, but it is unclear whether they can also inhibit calcium phosphate scaling. Furthermore, a reliable method to determine the optimum antiscalant dose in RO is currently not available. The main objectives of this study were: i) to optimize the dosing of antiscalants and minimize antiscalant consumption in RO systems, and ii) to investigate the performance of antiscalants in preventing calcium phosphate scaling in RO processes. A dosing algorithm was investigated to minimize antiscalant consumption for calcium carbonate in different RO plants. Furthermore, the effectiveness of several commercial antiscalants (from different suppliers) in preventing calcium phosphate scaling was evaluated using pilot scale RO measurements and using a once-through laboratory scale RO system, which was developed in this research study.

The dosing algorithm proved to be a useful tool in identifying real-time optimum antiscalant doses required to prevent scaling for a given RO recovery. With the implementation of the dosing algorithm, the consumption of antiscalant in the RO plants was reduced by 85-90%. It was revealed that the feedwater chemistry, specifically the presence of phosphate and humic substances, plays a significant role in antiscalant dose reduction. For example, antiscalant was not required at all for a RO plant in the Netherlands as calcium carbonate scaling was prevented by the phosphate and humic substances naturally present in the RO feed. Furthermore, the amorphous phase of calcium phosphate was found to be responsible for flux decline in RO, for which the tested antiscalants were unable to provide acceptable inhibition, as flux decreased by at least 15% in less than 24 hours with each antiscalant. Consequently, further research is required, in collaboration with antiscalant suppliers, to develop and test antiscalants that are capable of preventing amorphous calcium phosphate scaling in RO systems.

This book is printed on paper from sustainably managed forests and controlled sources